DEVELOPMENT AND CHARACTERIZATION OF WHEY BASED ALPHA-LACTALBUMIN PROTEIN NANOTUBES FOR FOOD APPLICATIONS

A Thesis Submitted to
the Graduate School of Engineering and Sciences of
İzmir Institute of Technology
in Partial Fulfillment of the Requirements for the Degree of

DOCTOR OF PHILOSOPHY

in Food Engineering

by
Özgür TARHAN

June 2013
İZMİR

We approve the thesis of **Özgür TARHAN**

Examining Committee Members:

Prof. Dr. H. Şebnem HARSA
Department of Food Engineering, İzmir Institute of Technology

Assoc. Prof. Dr. F. Banu ÖZEN
Department of Food Engineering, İzmir Institute of Technology

Assoc. Prof. Dr. Yusuf SELAMET
Department of Physics, İzmir Institute of Technology

Prof. Dr. Salih OKUR
Department of Material Science and Engineering, İzmir Katip Çelebi University

Assoc. Prof. Dr. Sevcan ÜNLÜTÜRK
Department of Food Engineering, İzmir Institute of Technology

11 June 2013

Prof. Dr. H. Şebnem HARSA
Supervisor,
Department of Food Engineering
İzmir Institute of Technology

Prof. Dr. Vural GÖKMEN
Co-supervisor,
Department of Food Engineering
Hacettepe University

Prof. Dr. Ahmet YEMENİCİOĞLU
Head of Department of Food Engineering
İzmir Institute of Technology

Prof. Dr. R. Tuğrul SENGER
Dean of the Graduate School of
Engineering and Sciences

ACKNOWLEDGEMENTS

I would like to express my sincere gratitude and appreciation to Professor Şebnem Harsa for her supervision, guidance, support, encouragement, and confidence in me during my PhD research. I also would like to thank Profesor Vural Gökmen for his guidance and help especially in MS and encapsulation studies. I am grateful to Professor Canan Tarı, Associate Professor Yusuf Selamet, and Associate Professor Banu Özen for their valuable contributions and suggessions during sthe progression of this research.

I am very much thankful to Specialists Yekta Günay Oğuz and Dane Rusçuklu, and also Özgür Yılmazer, and Evrim Balcı, from Biotechnology and Bioengineering Central Research Laboratory, for their help and support, especially for protein purification studies and for many other experimental works.

I am equally grateful to Specialists Mine Bahçeci for AFM analyses, Duygu Oğuz and Gökhan Erdoğan for STEM analyses, Z. Sinem Hortooğlu for TGA analyses, and Technician Canan Güney for XRF analyses, from the Center for Material Research.

I also thank Specialist Tuba Endoğan from METU-Central Research Laboratory for TEM analysis.

I would like to express my sincere gratitude to Associate Professor M. Mustafa Demir and Research Assistant Özge Tunusoğlu for their help during DLS analyses; Professor Talat Yalçın, Research Assistant Ahmet Emin Atik and Specialist Dr. Filiz Yeşilırmak for their contributions in MS analyses; Professor Metin Tanoğlu, Research Assistants Taner Erdoğan, Oylum Çolpankan and Sema Yıldız for their help in rheological studies; and Associate Professor Banu Özen for her guidance in FT-IR analyses.

I appreciate to Specialist Dr. Ebru Kuzgunkaya from Geothermal Energy Research and Application Center and Specialist Dr. Filiz Özmıhçı for DSC analyses.

I would like to thank Specialist İlknur Şen for her help in HPLC analysis; and also Tecnician Sibel Basut for her help in SDS-PAGE analysis carried out during my pregnancy, especially.

I also thank Assistant Professor A. Oğuz Büyükkileci and Research Assistant Merve Şamlı for providing hemicellulose to use in rheological studies.

I would like to express great appreciation to my dear husband Assistant

Professor Enver Tarhan for his help in Raman analyses, and also for his collaboration and valuable contributions in optical characterization.

Special thanks are extended to my colleagues Mert Sudağıdan, Çelenk Molva, Murat Molva, Nihan Göğüş, Mehmet Reşat Atılgan, Hande Demir, Bengi Hakgüder Taze, and Hatice Yavuzdurmaz for their help, support and friendship during my research.

And finally, I would like to express my endless indebtedness and appreciation to my father Gürses Apaydın who inspired and encouraged me for an academic carier at Izmir Insitute of Technology, to my mother Nuray Apaydın, and my sister Sinem Apaydın Şentürk who always provided endless love and support with their full confidence in me. I am deeply grateful to my beloved husband Enver Tarhan for his understanding, patience, support, and love, in addition to his scientific contributions. Very special thanks go to my lovely son Mustafa Emir Tarhan for being a part of our lifes bringing an endless joy and happiness.

Lastly, I thank everyone who helped and supported me during this thesis research and my whole education life.

The work presented in this thesis was supported financially by the The Scientific and Technological Research Council of Turkey (project no: 109O866, 2010-2011) and İzmir Institute of Technology, Scientific Research Projects (project no: İYTE03, 2009-2011).

ABSTRACT

DEVELOPMENT AND CHARACTERIZATION OF WHEY BASED ALPHA-LACTALBUMIN PROTEIN NANOTUBES FOR FOOD APPLICATIONS

Alpha-lactalbumin (α-La) is one of the major proteins in whey. When partially hydrolyzed with protease, it produces nanotubular structures by self-assembly process. The aim of this PhD thesis is to develop and characterize whey based α-La nanotubes. In this study, purification of α-La from whey using ultrafiltration and chromatography, development of protein nanotubes with standard and purified α-La fractions, their characterization by microscopic, optical and spectrophotometric methods, analysis of hydrolysis process, and investigation of these nanotubes in relation to food applications were presented. Lactose was eliminated and proteins were concentrated in whey powder by diafiltration assisted ultrafiltration prior to chromatography. α-La and besides β-lactoglobulin were purified individually from whey protein concentrate with high purity (95–99 %). The obtained protein nanotubes were longer than 100 nm up to few microns with ~20 nm width in bundled, rod and chain-like fashions. Remarkable conformational changes occurred in the protein secondary structure during nanotube formation. Calcium to protein ratio critically affected nanotube formation and stability. Both hydrolysis and nanotube growth triggered gelation, but stiffer gel network was obtained with nanotubes. Viscoelasticity and stiffness were improved by blending with cellulose. As the calcium content increased the transparent appearance of the gels got turbid due to aggregation. α-La nanotubes were stable up to ~ 60 °C. The nanotubular gels entrapped a coloring agent by enhancing transparency. Binding of catechin to nanotubes was occured as reversible with low stability. α-La nanotubes and gels can be used as functional ingredients in food processing involving low and moderate heat treatments.

ÖZET

GIDA UYGULAMALARI İÇİN PEYNİRALTI SUYU KAYNAKLI ALFA-LAKTALBUMİN PROTEİN NANOTÜPLERİNİN ÜRETİMİ ve KARAKTERİZASYONU

Alfa-laktalbumin (α-La) peyniraltı suyundaki (PAS) temel proteinlerden birisidir. Bu protein proteazla kısmi hidrolizinin ardından, kendiliğinden dizilim yöntemiyle nanotubik yapılar oluşturabilmektedir. Bu doktora tezinin amacı, PAS tabanlı α-La nanotüplerinin geliştirilmesi ve karakterizasyonudur. Çalışmada, ultrafiltrasyon ve kromatografik tekniklerle PAS'dan α-La saflaştırılması, standart ve saflaştırılan a-La fraksiyonlarından protein nanotüp oluşturulması ve bunların mikroskobik, optik ve spektrofotometrik metodlarla karakterizasyonu, protein hidroliz işlemi ve bu nanotüplerin gıda uygulamalarına ilişkin araştırmalar sunulmuştur. Diyafiltrasyon destekli ultrafiltrasyon ile, kolon kromatografi öncesi PAS tozundaki laktoz uzaklaştırılmış ve proteinler konsantre edilmiştir. α-La'nın yanısıra β-laktoglobulin de PAS konsantratından yüksek saflıkla (95-97 %) ayrı ayrı saflaştırılmıştır. Elde edilen α-La nanotüplerinin uzunlukları 100 nm'den bir kaç mikrona kadar olup, ~20 nm genişlikte çubuk şeklinde demet ve zincir gibi yapıdadır. Nanotüp oluşumu sırasında proteinin ikincil yapısında dikkat çekici konformasyonal değişiklikler olmuştur. Kalsiyum ve protein oranı nanotüp oluşumunu ve stabilitesini önemli ölçüde etkilemiştir. Hidroliz ve nanotüp oluşumu jelleşmeyi tetiklemiş fakat, nanotüpler daha kuvvetli bir jel ağı oluşturmuştur. Viskoelastisite fiberlerle harmanlanarak geliştirilmiştir. Kalsiyum miktarı arttıkça jellerin geçirgen görünümü agregasyondan dolayı bulanıklaşmıştır. α-La nanotüpleri ~ 60 °C kadar ısıya dayanmıştır. Nanotüp jelleri şeffaflığı artırarak renk maddesini hapsetmiştir. Kateşinin nanotüplere bağlanması düşük stabilitede tersinir olmuştur. α-La nanotüpleri ve jelleri düşük ve orta ısıl işlem içeren gıda proseslerinde fonksiyonel ajan olarak kullanılabilirler.

This work is dedicated to my family;
Mustafa Emir, Enver, Gürses, Nuray, and Sinem

TABLE OF CONTENTS

LIST OF FIGURES

LIST OF TABLES

LIST OF SYMBOLS AND ABBREVIATIONS

AEC	Anion Exchange Chromatography
AFM	Atomic Force Microscopy
α-La	Alpha-Lactalbumin
α-LaNTs	Alpha-Lactalbumin Nanotubes
β-Lg	Beta-Lactoglobulin
BLP	*Bacillus licheniformis* Protease
BSA	Bovine Serum Albumin
C-α-La	WPC Based Alpha-Lactalbumin
C-α-LaNTs	Nanotubes Constructed from WPC Based Alpha-Lactalbumin
DLS	Dynamic Light Scattering
DSC	Differential Scanning Calorimetry
FT-IR	Fourier Transform Infrared Spectroscopy
HPLC	High Pressure Liquid Chromatography
I-α-La	WPI Based Alpha-Lactalbumin
I-α-LaNTs	Nanotubes Constructed from WPI Based Alpha-Lactalbumin
MALDI-TOF MS	Matrix Assisted Laser Induced Time of Flight Mass Spectrometry
S-α-La	Commercial Standard of Alpha-Lactalbumin
S-α-LaNTs	Nanotubes Constructed from Commercial Standard of Alpha-Lactalbumin
SEC	Size Exclusion Chromatography
STEM	Scanning Transmission Electron Microscopy
TEM	Transmission Electron Microscopy
TGA	Thermogravimetric Analysis
WP	Whey Powder
WPC	Whey Protein Concentrate
WPI	Whey Protein Isolate
WPS	Whey Powder Solution
XRF	X-Ray Flourescence Spectrometry

CHAPTER 1

INTRODUCTION

Food proteins are widely used in processed foods because they have high nutritional value. They are generally recognized as safe (GRAS) and have different functional properties, such as emulsification, gelation, foaming and water binding capacity (Bryant and McClement, 1998; Dickinson, 2001; Foegeding et al., 2002). In addition, recently they have been researched for their potential as novel nutraceutical delivery systems. These systems could be produced generated by decreasing the matrix size from micrometers to nanometers for better incorporation of nutrients through newly developed protein and peptide vehicles (Chen et al., 2006). This capability is one of the most important aspects of nanotechnology in food and bio applications including development of smart foods and beverages, encapsulation and delivery of nutrients, improvement of textural properties, detection of pathogens, and controlled release in drug delivery.

Food grade nanoscale structures such as protein and peptide nanotubes can be produced by breaking up the bulk materials and building up the novel supramolecular structure from molecules through self-assembly. These nano structures may have unique properties providing potential applications in food technology. Enzymatic hydrolysis leads to breakdown of the proteins through smaller protein/peptide fragments depending on the degree of hydrolysis. Then, naturally occurring self-assembly, which may be identified by the spontaneous diffusion and specific association of molecules through non-covalent interactions, gives rise to the fabrication of novel structures from these fragments (Rajagopal and Schneider, 2004). Self-assembly is a ‘bottom up’ approach for the production of nano structures.

Whey proteins, extracted from an industrial waste, whey, were selected as the model proteins to fabricate nanotubes in this study. Whey is the most important by-product of cheese production and is rich in its protein content. These proteins are used to improve technological properties in processed foods, and also consumed as dietary support due to high nutritional value. Beta-lactoglobulin (β-Lg) and alpha-lactalbumin (α-La) are the major proteins in whey. Partial hydrolysis leads to formation of fibrillar

aggregates for β-Lg and nanotubular structures for α-La, through self-assembly. These nano structures are predicted to have an important potential for various food applications. Furthermore, bioactive peptides of these proteins may have contributions in the production of multifunctional nanotubes by adding high value through introducing different manipulations.

This PhD research study targets development and characterization of protein / peptide nanotubes from whey-based α-La proteins and examination of the constructed nanostructures for a few food applications. α-La and besides β-Lg were purified from whey protein isolate (WPI) and whey powder (WP) by ultrafiltration and chromatographic techniques. The purified fractions were characterized in terms of protein profiling, purity, isoelectric pH, molecular weight, and protein structure. Protein nanotubes were developed from both commercial and purified α-La through self-assembly after partial enzymatic hydrolysis. Microscopic characterization of nanotubes was performed by transmission electron microscopy (TEM), scanning transmission electron microscopy (STEM), and atomic force microscopy (AFM). Nanotube growth analysis was carried out by dynamic light scattering (DLS) and UV-spectrophotometry. Protein hydrolysis was investigated through high performance liquid chromatography (HPLC) and matrix assisted mass spectrometry (MALDI-TOF MS) analyses. Optical characterization was performed by Raman and Fourier transform infrared (FT-IR) spectroscopy. In relation to food applications, rheological characteristics of protein nanotubes were evaluated by means of gelation properties, and thermal stabilities were investigated by differential scanning calorimetry (DSC) and thermogravimetric analysis (TGA). Additionally, encapsulation of a bioactive ingredient (phenolics of green tea) and dye binding capacities by the constructed nanotubes were examined.

This study is expected to provide novel technological and scientific information for the new nano-food technology area especially in our country, besides contributing to the solution of environmental pollution problems caused by whey disposal.

CHAPTER 2

WHEY AND WHEY PROTEINS

2.1. Whey

Whey is the most important by-product of cheese and casein manufacture. It is the liquid part remaining after milk has been curdled by acid or rennet and strained. When the milk is directly acidified, as in cottage cheese, acid whey is obtained with the pH equal or smaller than 5.1. If it is coagulated by rennet, as in most cheese making process, sweet whey is obtained with the pH equal or higher than 5.6 (Pintado et al., 2001). Generally, whey contains carbohydrates (~5%, lactose), proteins (~1%), minerals (~0.5%), vitamins and fat. The actual concentrations of whey ingredients depend on different parameters, such as the type of whey, the source of milk, and process quality.

Whey production increases in parallel with increasing cheese consumption within time in our country and in the world. When 100 kg milk is processed, the amount of whey obtained is 80-90 kg besides 10-20 kg of cheese (Cheryan, 1998). If this by-product is drained through sewage instead of collection and processing, it causes a serious environmental pollution due to its high biological oxygen demand (BOD) which is 32-60 g/l (Cheryan, 1998). Evaluation of whey, through preparation of whey protein concentrates with high nutritional value, use of the high value products produced by lactose fermentation, and searching out of novel applications by various modifications will provide benefits on behalf of environment and economy. Different studies are present in current literature related to the evaluation of whey. Some researchers carry out studies on production of biogas from whey by fermentation in large reactors (Sözer and Yıldız, 2006; Kavacık and Topaloğlu, 2007). Also, lactose in whey content can be evaluated in biotechnological manufacturings, and the remaining minerals are used to enrich growth media for some microorganisms (Ferrari et al., 2001).

Whey is an important raw material, especially due to its proteins. In this study, extracted and purified whey proteins are planned to be used as starting material for further manipulations. The main target is construction of nanotubes from purified α-La protein.

2.2. Whey Proteins

Whey is regarded as a valuable source due to its proteins. β-Lg and α-La constitutes the main part of proteins in whey, whereas immunoglobulins, bovine serum albumin, lactoferrin and lactoperoxidase are found in the remaining part (Table 2.1). Whey proteins are globular molecules with the main content of α-helices, in which the acidic/basic and hydrophobic/hydrophilic amino acids are distributed in balance through the polypeptide chains (Evans, 1982; Madureira et al., 2007).

Table 2.1. Whey proteins and their basic properties*

Protein	Concentration (g/l)	Molecular weight (kDa)	Isoelectric pH
β-Lactoglobulin	2.7	18,362	5.2
α-Lactalbumin	1.2	14,147	4.5 – 4.8
Immunoglobulins	0.65	15,000-1.000,000	5.5 – 8.3
Bovine serum albumin	0.4	69,000	4.7 – 4.9
Lactoferrin	0.1	78,000	9.0
Lactoperoxidase	0.02	89,000	9.5
Glycomacropeptide		7,000	

* Wong et al., 1996; Cayot and Lorient, 1997; Zydney, 1998

Whey is an important raw material having various applications in food industry, especially due to its protein content. Whey protein concentrates (WPC) or whey protein isolates (WPI) are used in baby foods, diets of athletes, and diets requiring high protein content. Besides providing nutritive nitrogen and amino acids, the presence of antimicrobial properties, positive effects on immune system, antioxidant and anticarcinogenic activities of these proteins have been discovered and currently investigated (McIntosh et al., 1998; Madureira et al., 2007). Some of the main biological activities of whey proteins are given in Table 2.2.

Whey proteins are used for various applications in the food industry due to their functional properties such as gelation, foam formation, and emulsification (Foegeding et al., 2002). Enrichment of the protein content of diet foods, bakery products, fizzy beverages, athlete diets, and dairy products; providing water absorption in sausage and

salami; viscosifying in ready soup and tomato paste; emulsification in ice cream, meat products and mayonnaise; gelation in bakery products, desserts, meat, and dairy products are some of the industrial applications that making use of whey protein functionalities (Barth and Behnke, 1997; Demirci et al., 2000).

Table 2.2. Some biological functions of whey proteins

Protein	Biological function	References
Whole whey proteins	prevention of cancer (breast, intestine)	MacIntosch et al., 1995 Gill and Cross, 2000 Badger et al., 2001
	antimicrobial activities	Clare et al., 2003
β-Lactoglobulin	transporter of retinol, palmitate, fatty acids, vitamin D and cholesterol	Puyol et al., 1991 Wang et al., 1997 Wu et al., 1999
α-Lactalbumin	prevention of cancer and lactose synthesis	de Wit, 1998 Markus et al., 2002
Bovine serum albumin	anti-mutagenic function and immunomodulation	Bosselaers et al., 1994 Ormrod and Miller, 1991

Since the context of the first part of this research is mainly focused on the purification of two major whey protein (α-La and β-Lg), their structural properties enabling manupulations, are required to be considered firstly.

β-Lg is the most abundant whey protein constituting nearly 60% (~3g/l). It is synthesized in mammary gland of ruminants and has several genetic variants of which β-Lg A is the most common. It is mainly composed of β-sheet structures (Figure 2.1) and has 162 amino acid residues in the peptide chain with the molecular weight of 18,277 kDa (Eigel et.al., 1984). The pH of the medium is highly effective on its quaternary structure. It presents as a dimmer (36,700 kDa) at pH values between 7.0 and 5.2; octamer (140,000 kDa) at pH values between 5.2 and 3.5; and monomer (18,277 kDa) at pH equal to 3.0 and above 8.0 (de Wit, 1989).

Figure 2.1. 3D structure of β-Lg
(Source: http://en.wikipedia.org/wiki/Beta-lactoglobulin)

Alpha-Lactalbumin is the second most abundant whey protein with approximately 20%. It is synthesized in mammary gland and is the principle protein in human milk (Brew and Grobler, 1992). It has three genetic variant identified as A, B, C (Fox, 1989). Native α-La consists of two domains: a large α-helix and a small β-sheet domain, and are connected by a calcium binding loop (Figure 2.2). It contains 123 amino acid residues and has the molecular weight of 14,175 kDa (Brew et al., 1970). It is a compact globular protein and the structural stabilization is provided by disulphide bonds at pH between 5.4 and 9.0 (Evans, 1982).

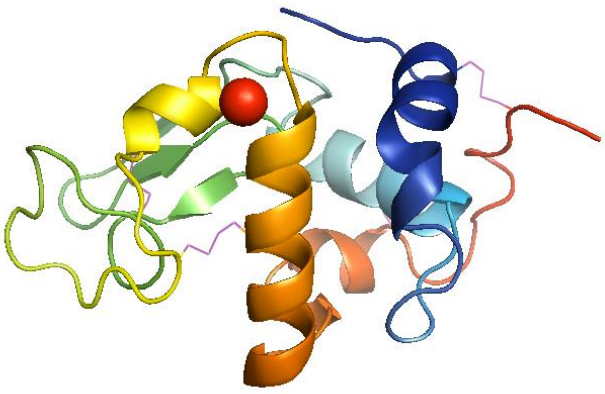

Figure 2.2. 3D structure of α-La
(Source: Graveland-Bikker, 2005)

Various methodologies have been reported in literature for the analysis and/or purification of the whey proteins. These include; salting-out (Aschaffenburg and

Drewry, 1957; Mailliart and Ribadeau-Dumas, 1988), selective precipitation (Bramaud et al., 1997; Lucena et al., 2007; Fernández et al., 2011), membrane filtration (Zydney, 1998; Cheang and Zydney, 2004; Konrad and Kleinschmidth, 2008), and chromatographic methods (Kristiansen et al., 1998; Ye et al., 2000; Neyestani et al., 2003; Doultani et al., 2004). Most of them can provide effective purification in the laboratory scale; however, some limitations can also be encountered such as low purity or recovery of the proteins. Preperative scale purification of whey proteins through membrane filtration and ion-exchange chromatography was also be described to extract proteins with high purity for production at large scale (Kristiansen et al., 1998; Gerberding and Byers, 1998). Separation by ion-exchange chromatography includes the selective reversible adsorption of charged protein molecules through a matrix and stepwise elution through salt and/or pH gradients.

In the presented thesis study, the target whey protein α-La was purified by membrane filtration and anion exchange chromatography based on elution by pH gradient. Commercial whey protein isolate (WPI) and whey powder (WP), kindly supplied by a company, were used as raw materials. Purified α-La fractions were then used for protein nanotube formation.

CHAPTER 3

PROTEIN AND PEPTIDE NANOTUBES

Macromolecules such as proteins, lipids and carbohydrates can be used for the formation of various novel nano structures having different food applications. Nanoliposomes based on lipids, nanocapsules based on natural carbohydrate polymers (alginate, chitosan), and proteins (albumin, gelatin) are the examples of food-grade nanostructures. Among these, proteins and their building blocks, peptides have a special importance due to their ability for formation of supramolecular structures naturally by self-assembly. Self-assembly is identified by the spontaneous and reversible aggregation due to polymerization of molecules by non-covalent intermolecular interactions such as hydrogen bonding, electrostatic, hydrophobic and Van der Waals interactions (Rajagapol and Schneider, 2004). It is a 'bottom up' approach in which proteins and peptides are used as monomeric building blocks for the development of higher order structures.

In literature, various recent studies emphasize that protein and peptide based nanotubes have a great significance related to their unique structural and functional properties (Hou et al., 2005; Rajagopal and Schneider, 2004; Scanlon and Aggeli, 2008). Hartgerink et al. (1996) reported the general design criteria and synthesis approaches of peptide-based, solid, tubular nanostructures. They have identified the peptide nanotubes as the extended tubular β-sheet-like structures constructed by self-assembly of flat, ring-shaped peptide subunits consisting of alternating D- and L- amino acid residues. These researchers have emphasized that peptide self-assembly is directed by intermolecular hydrogen bondings and the structure is stabilized by hydrophobic interactions providing good mechanical and thermal stability against long periods of exposure to water and some common organic solvents (DMSO). Yu et al. (2005) have developed peptide nanotubes by self-assembly and examined these nanostructures for encapsulation of a microbial lipase; then, they have noticed that the enzyme activity have been increased significantly. In another study, avidin and albumin (bovine) have been immobilized on self-assembled peptide nanotubes and the availability of these nanotubes as templates for fabrication of protein nanotubes have been investigated; then

these protein nanotubes have been suggested as basic tools for production of protein biosensors and various microelectronic devices (Douberly Jr. et al., 2001).

Some researchers developed protein nanotubes from whey protein, α-La, by self-assembly (Ipsen and Otte, 2001; Graveland-Bikker et al., 2004). The mechanism for this technique consists of three stages arranged as; conformational destabilization, nucleation and nanotube elongation. In the first stage, monomeric peptides, formed by conformational change of α-La native structure through enzymatic hydrolysis, assemble into dimers through β-sheet stacking. In the next stage, when the dimeric units reach the saturation concentration a critical nucleus is formed containing about five building blocks. This nucleus is able to extend with time and stabilized with calcium ions acting as salt bridges between building blocks. In the last stage, the structure elongates by binding of other dimers, in the presence of calcium ions, and the nanotube is formed (Ipsen and Otte, 2007).

Besides self-assembly, protein and peptide nanotubes can be developed with more controlled dimensions by template-sythesized layer by layer assembly (Hou et al., 2005; Tian et al., 2006). Layer by layer assembly is based on the alternate adsorption of oppositely charged molecules on a support surface, thus, multilayer ultra-thin films are developed on the solid surfaces (Decher, 1997). In this method, nanotubes are developed in the pores of nanoporous templates that are mostly alumina. These templates are alternately immersed into protein/peptide solutions for few times, attachment of molecules to inner surface forms first layer, than they attach to each other to form the following layers. In this way, after separation of templates from the thin film structure, layer by layer assembled protein/peptide nanotubes are obtained (Hou et al., 2005). In addition, in the pressure-filter-template technique, using layer by layer deposition strategy as well, protein/peptide solutions are passed a few times under pressure through the templates, stabilized with two stainless steel filters at its both ends. Then, the nanotubes developed in the pores of alumina templates are obtained after separating templates by washing concentrated sodium hydroxide solutions (Ai et al., 2003). These are ‘bottom-up’ approaches for development of nanostructures from monomeric units, by self assembling.

Besides construction of protein and peptide nanotubes, characterization by different techniques have great significance for identification of these materials according to size, structural, mechanical, and optical properties in relation with application purposes. Current literature have various studies related to development and

characterization of protein and peptide nanotubes from different sources. Lu et al. (2005) obtained protein nanotubes from human serum albumin and phospholipids by using pressure filter technique (PFT) through layer by layer assembly within the pores of an alumina template. Microscopic (SEM) and spectrophotometric (CD, UV-VIS) characterization indicated regularly distributed nanotubes with standard dimensions, approximately 30 nm thick, 60 μm long and these nanotubes have been suggested to be used as biological sensors by the researchers. Similarly, another research group constructed protein nanotubes through PFT-layer by layer assembly with an alumina template by binding synthetic hem group (FeP) to human serum albumin (Lu et al., 2007). X- ray spectroscopy, TEM and SEM analysis, and UV-VIS absorption spectroscopy determined the elemantal analysis, diameters and oxygen binding capacity of nanotubes, respectively. Hemoprotein nanotubes have been reported with uniform dimensions, approximately 400 nm in diameter, 60 μm in length and 100 nm in wall thickness, and they enabled the reversible binding of dioxygen, leading to developments of novel performances in electronic, photonic and magnetic fields. In another study, using the same technique and the same template, protein nanotubes were developed from cytochrome C with gluteraldehyde and polysodium styrenesulfonate, and characterized by SEM, TEM and EDAX (energy dispersive X-ray spectra); then they were suggested to be the carriers for biocatalysts (Tian et al., 2006).

In this thesis study, protein/peptide nanotubes were constructed using commercial and purified whey-based alpha-lactalbumin. There is a lack of information in the literature related to whey protein based nanotubes. α-La nanotube studies have been reported by two research groups and given as follows. Ipsen and coworkers first reported self-assembly of partially hydrolysed α-La resulting in strong gels with novel microstructures. (Ipsen et al., 2001). Ipsen and Otte (2003) produced α-La nanotubes by self-assembly of peptites after partial hydrolysis of α-La extracted from whey obtained by acidification of milk. They have also investigated gelation properties of these nanotubes at different pH values. Up to date, the most detailed research related to α-La protein nanotubes was reported by Graveland-Bikker and co-workers. These researchers produced nanotubes by molecular self-assembling process from partially hydrolyzed α-La extracted from milk (Graveland-Bikker et el., 2004, 2005, 2006a, 2006b, 2009). Detailed characterization of α-La nanotubes were achieved by microscopic (SEM, TEM); spectrophotometric (DLS, SLS, SAXS, CD) and chromatographic (LC-MS, RP-HPLC) methods. Also, rheological characteristics of gels made by these nanotubes were

determined. Kinetic studies were performed for nanotube growth and the related model showed that α-La nanotubes were approximately 20 nm in diameter, having 8nm of cavity diameter and 10 nm per minute elongation rate. Additionally, some potential food applications were suggested, such as viscosifying, gelation and encapsulation (Graveland-Bikker and de Kruif, 2006).

3.1. Protein Self-assembly

Proteins and their building blocks, peptides, have a special importance due to their ability for formation of supramolecular structures naturally by self-assembly. Self-assembly is identified by the spontaneous and reversible aggregation due to polymerization of molecules by non-covalent intermolecular interactions such as hydrogen bonding, electrostatic, hydrophobic and Van der Waals interactions, as well as kinetically labile metal coordination (Rajagapol and Schneider, 2004). It is a 'bottom up' approach in which proteins and peptides are used as monomeric building blocks for the development of homogeneously ordered structures. Self-assembly differs from aggregation which can be defined as self-association of molecules, usually irreversibly, involving both covalent and non-covalent interactions leading to formation of heterogenous structures (Kentsis and Borden, 2004; Graveland-Bikker and de Kruif, 2006a). The non-covalent interactions involved in self assembly may be considered as weak and small in magnitude individually, but it results in a significant strength in the final structure with large number of interactions (Rajagapol and Schneider, 2004). The enthalpy gained from these weak interactions offsets slightly the large entropic cost of ordering molecules and this emphasizes the thermodynamic equilibration of the self-assembly system.

Self-assembled protein architectures such as nanotubes and monolayers with a nanoscale order offer different structural motifs including particles, fibers, ribbons and sheets (Santoso et al., 2002). Generally, assemblies with β-sheets in the secondary structure are the most common ones, however, helical-based ones are less common (Rajagapol and Schneider, 2004). Peptide and protein-based tubular structures, such as tobacco mosaic virus, microtubules, and bacterial pili, already exist in nature (Hartgerink et al., 1996). Besides them, synthetic nanotubes have been constructed in laboratory conditions. Artificial peptide nanotubes are synthesized with controlled

dimensions by stacking carefully designed short peptides through specific interactions between amino acids (eg. hydrophilic/hydrophobic interactions, β-sheet/helical or aromatic stacking) (Zhang, 2003; Graveland-Bikker and de Kruif, 2006).

3.2. Structure of Alpha-Lactalbumin

Alpha-Lactalbumin is an acidic calcium-binding globular protein found in bovine and human milk. Bovine α-La comprises 20-25% of whey protein and human milk α-La is the dominant protein having 74% conserved amino acid sequence homology with bovine α-La (Kamau et al., 2010). α-La is a member of the lysozyme family of proteins and it has a high homology with the C-type lysozyme (Sugai and Ikeguchi, 1994). It is made up of 123 amino acids with NH_2 -terminal glutamic acid and COOH-terminal leucine (Figure 3.1).

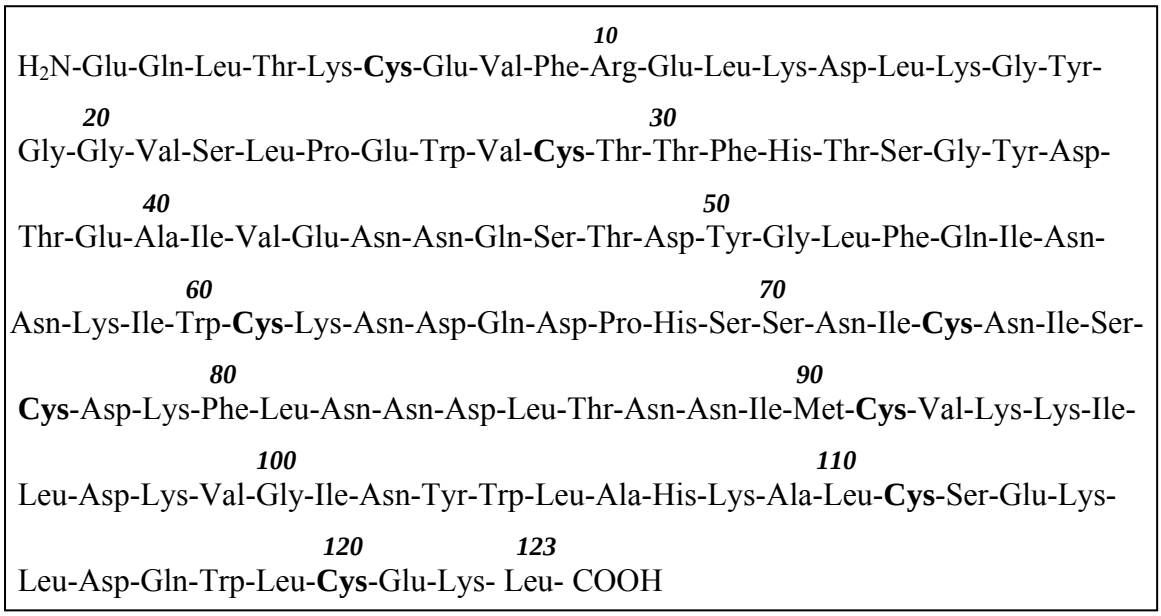

Figure 3.1. The complete amino acid sequence of α-Lactalbumin (from Brew et al., 1970)

α-La is a compact globular protein with the dimensions of 2.5nm X 3.7nm X 3.2nm (Graveland-Bikker, 2005). The native structure of α-La consists of two domains; a large α-helical domain (residues 1-34 and 86-123 at amino- and carboxyl- terminals of polypeptide chain) and a small β-sheet domain (residues 35-85 at the central part of polypeptide chain), connected with a calcium binding loop (Figure 2.2). The structure is

cross-linked and stabilized by four disulfite bridges: residues 6-120, 61-77, 73-91, and 28-111. The cystine bridge between residues 73 and 91 holds two domains by forming a loop and enclosing calcium (Ca^{2+}-binding loop). Also, the sulfide bridge between the residues 61 and 77 connects α-helical and β-sheet domains as well (Acharya et al., 1991; Anderson et al., 1997). The α-helical domain consist of four major α-helices (residues 5-11, 23-24, 86-98 and 105-110) and two short 3_{10} helices (residues 18-20 and 115-118). Smaller β-sheet domain consist of a small three-stranded antiparallel β-sheet (residues 41-44, 47-50, 55-56), a short 3_{10} helix (residues77-80) and some irregular structure (Chrysina et al., 2000; Goers et al., 2002). The high affinity Ca^{2+}-binding loop is located at the junctions of subdomains and contains a portion of 3_{10}-helix of β-subdomain and H3-helix of α-helical subdomain. Ca^{2+} is coordinated by seven oxygen atoms supplied by main chain (Lys79 and Asp84) carbonyl groups, side chain (Asp82, 87, and 88) carbonyl groups, and two water molecules (Stuart et al., 1986; Acharya et al., 1989; Pike et al., 1996). In addition, a second Ca^{2+}-binding site located near the surface of the α-La molecule was reported with lower affinity (Chandra et al., 1998).

The binding of Ca^{2+} to α-La causes changes mostly in tertiary structure and function, not in secondary structure (Anderson et al., 1997). Besides Ca^{2+}, α-La can bind other significant cations such as Mg^{2+}, Mn^{2+}, Na^{+}, and K^{+} which can compete with Ca^{2+} for the same binding site (Permeyakov et al., 1981 and 1985; Ostrovsky et al., 1988; Anderson et al., 1997). The binding affinities of Mg^{2+}, Na^{+}, and K^{+} were reported to be lower than Ca^{2+}, but their concentrations in the medium may trigger competition for binding (Permeyakov et al., 2000). Cation binding increases the stability of α-La. However, the binding of Zn^{2+} to Ca^{2+} loaded α-La decreases thermal stability, causing aggregation, and increases susceptibility to protease digestion (Permeyakov et al., 1991). At low pH values, protons may compete with Ca^{2+} ions causing displacements at carboxylates. At this pH, α-La is present in the molten globule state in which it retains a globular but swollen shape (highly dehydrated). α-La also interacts with the low molecular weight organic compounds and these interactions are modulated by cation binding processes (Permeyakov et al., 2000). The denaturation temperature for holo- α-La (Ca^{2+}-loaded) is 63 ºC, and for apo- α-La (Ca^{2+}-depleted) is 27 ºC.

3.3. *Bacillus Licheniformis* Protease

Bacillus lichenformis protease (BLP) is an extracellular protease produced by *B.lichenformis*. It is a glutamyl endopeptidase (EC 3.4.21.19) belonging to the group of serine endopeptidases and specific to peptide bonds containing aspartic (Asp) and glutamic acid (Glu) at the carbxyl moiety (Svendsen and Breddam, 1992; Graveland-Bikker, 2005). The enzyme is supplied by Novozymes (Novo Nordisc) and expected to have the GRAS status. BLP has 222 amino acid residues in a single peptide chain and has a molecular weight of 23.6 kDa (Kakudo et al., 1992). It has optimum activity at 50ºC, with an optimum pH of 7.5 and 8.0 (Birktroft and Breddam, 1994). BLP exhibits an increase in the viscosity and enhances gel strength depending on hydrolysis of whey proteins (Otte et al., 1997; Graveland-Bikker 2005; Creusot and Gruppen, 2007).

CHAPTER 4

FOOD NANOTECHNOLOGY

Nanotechnology is a rapidly developing science and technology. It can be defined as the characterization, fabrication, and manipulation of structures smaller than 100 nm. It enhances or bring in completely novel physical, chemical or biological features to materials at atomic or molecular levels. At this scale, the surface area of the structures become larger compared to their volume with unique and novel functional properties rendering them more suitable for various potential applications. Nanotechnology offers great potential benefits for many fields such as electronics and computer, material science, textile, energy, medicine, agriculture, and food industry. In some of these industries, commercial nano products are already being manufactured. Developments in these industries are driven by fundamental and applied research in physics, chemistry, biology, engineering, and materials science (Weiss et al., 2006). When compared with the others, applications of nanotechnology in the food industry are rather limited. Nevertheless, recent improvements and discoveries have a great potential to impact many aspects of food and associated industries.

4.1. Potential Applications of Nanotechnology in Foods

Applications of nanotechnology in food concept include food processing, safety, and packaging categories through various food based nano vehicles such as nanoemulsions, nanotubes, nanocapsules, and nanosensors. Various examples can be given related to these applications such as; production of novel food materials with desired functionalities; improvement of sensorial and textural properties of foods with the addition of color, flavor and nutrients; encapsulation and delivery of nutraceuticals; detection of pathogens in food products; and enhancement of packaging to extend the shelf life of products. Worldwide, many researchers and companies focuse on these potential nanofood applications summarized in Table 3.1 (Sanguansri and Augustin, 2006; Chau et al., 2007). Additionally, some other research studies are summarized as follows: Semo et al. (2007) reported encapsulation of vitamin D2 into casein micelle

nanostructures and concluded that these nano structures can be used for transportation of hydrophobic molecules and may have potential applications such as enhancement of low-fat and non-fat food products. Kaittanis et al. (2007) have expressed that superparamagnetic iron oxide nanoparticles can be used for detection of bacteria in complex media such as milk and blood through magnetic relaxation. They have claimed that these nanoprobes are highly sensitive and fast for making microbial detection in a broad range of fields including clinical, environmental, agricultural, and food sectors.

It is expected that nanoproducts in the market will increase substantıally in the near future. According to analysts, nanofood market comprised 7.0 billion US dollars in 2005 and expected to be 20.4 billion US dollars in 2010 (Allianz and OECD, 2005). In 2015, market share is expected to be more than 26.0 billion US dolars (BCC Research, NANO31D, 2010).

Table 3.1. Some recent examples of nanotechnology applications in food industry

Category	Examples	References
Food processing	Smart foods and beverages give desired flavors and colors by the addition of nanocapsules which burst at different microwave frequencies.	ETC Group, 2005
	Development of nano-scale formulations of different traditional herbal plants.	ElAmin, 2005
	Development of nanoceramic frying oil refining catalytic device to inhibit thermal polymerization of frying oil and reduce off-odors.	OilFresh, 2005
	Production of milk protein based nanotubes having potential to be used for viscosifying, gelation and nanoencapsulation.	Graveland-Bikker and de Kruif, 2006
	Fortified flavoured waters and milk with vitamin, mineral and other functional ingredients through nanoemulsion for incorporation and controlled release of bioactives.	Decker, 2003 Hazen, 2003
Nutraceutical delivery	Rendering hydrophilic substances fat soluble and lipophilic ones water soluble, allowing nanoparticles of some functional ingredients (carotenoids, phytosterols, and antioxidants) to be dispersed in water or fruit drinks to improve their bioavailability.	Chen et al.,2006 IFTS, 2006
	Use of nanocapsules as carriers for essential oils, flavor, antioxidant, coenzyme Q10, and vitamins, minerals, and phytochemicals to improve their bioavailability.	El Amin, 2006 Fletcher, 2006

(**cont. on next page)**

Table 3.1. (cont.)

	Solid nanospheres composed of hydrophobic materials encapsulated in moisture-sensitive or pH-sensitive adhesive microspheres to enable controlled release of active ingredients.	Shefer and Shefer, 2003
	Encapsulating the nanoparticles of active ingredients to protect them from oxidation and getting to the taste receptor site, thus to reduce their undesirable offtastes in the finished application.	Heller, 2006
Food safety	Development of synthetic tree-shaped DNA being tagged with color-coded probes, as a nanobarcode device, enables the identification of food pathogens	Li et al., 2004
	Protein-coated nanocantilever, naturally vibrating at specific frequency, for the quick detection of pathogens	ElAmin, 2006
	Incorporation of silver nanoparticles into different products for suppressing the spread of bacteria and other microbes.	Nanosilver, 2004
	Nanoemulsion of vegetable oil, surfactant surrounded by trace amounts of alcohol suspended in water with properties to kill bacteria.	Newman, 2002 Hamouda and Baker, 2000
Food packaging	Packaging with nanosensors indicating when a product is not safe for consumption.	Gardner, 2003
	Adding nanocomposites or nanoparticles(silver, titanium, dioxide, silicon dioxide, and nano-clay) into packaging materials for better protection of foods by modifying the permeation behavior of foils, deodorizing, increasing barrier properties, blocking ultraviolet light, improving mechanical and heat-resistance properties, and developing antimicrobial and antifungal surfaces.	ElAmin, 2005 Fletcher, 2006 IFTS, 2006 Roach, 2006

Two basic approaches are used to create nanomaterials. In the 'bottom-up' approach, complex nanostructures are fabricated from individual molecules whereas, in 'top-down' approach greater materials are transformed into smaller ones. The choice of a particular approach for a nanomaterial development may be related to the material structure and purpose of the utilization of the nanoproduct (Nickols-Richardson, 2007). In the development of nanofood materials, main focus is the self-assembly process which is thermodynamically driven due to molecular interactions, as a 'bottom-up' approach. Various food-grade nanostructures, such as micelles, liposomes, and nanoemulsions are created by self-assembly processes.

In this study, protein nanotubes will be developed by self-assembling of α-La peptide molecules. The such obtained nanotubes will also be tested in relation with food

applications including the determination of gelation and dye-binding properties, and ability to encapsulate bioactive components.

4.2. Safety and Regulations of Nanofood Products

The application of nanotechnology in food systems is growing rapidly. The potential benefits of these novel food products are widely emphasized. Hovewer, very little is known on the safety of these products. Some researchers have recently been started to investigate the potential toxicological effects of nanotechnology on biological systems (Oberdorster et al., 2005; Nel et al., 2006). Different nanoparticles, integrated into packaging materials of foods, such as silicate, silver, magnesium, and zinc-oxide may migrate through a food material if directly contacted, and may cause serious health risks when consumed. In addition, peptide, carbohydrate, and lipid based delivery systems for food additives or dietary supplements may lead to unexpected high consumer exposure of the enclosed material (Bouwmeester et al., 2009). Many products, named as 'ultrafine food' and 'nanofood', have been found in Taiwan market, without labelling, and the producers have been fined by authorities (Chau et al., 2007). Although the risks caused by exposure to nanoparticles are not completely understood yet, the presence of nanofood products in markets without labelling, safety assesments and proper regulations may repress their beneficial effects. Currently, there are some definitions and regulations for nanotechnology in some countries, whereas, there is still no known requirement to label food products containing nanoparticles and no regulatory system for production of nanofoods. Some various criteria are recommended to consider for development of standards, control measure and regulatory aspects such as: particle size range and measurements for true identification of nano products; physical and chemical properties; processing methods for preparation of nano materials; and safety considerations for potential health and environmental impacts of nano products (Chau et al., 2007). Nowadays, some works on the regulations or policy for nanofoods become highlighted. According to OECD reports on safety of nanofoods (2008-2011), the most active reporting countries were Canada, followed by Australia/New Zeland, Austria, Czech Republic, Finland, Germany, Slovac Republic. They generate research and development programs/projects related to the safety of nanofoods such as, health and environmental risks of nanoparticles, opportunities and risks of nanomaterials, and

human toxicity of nanoparticles. In summary, the development of regulations is an urgent issue for managing the potential adverse effects of food nanotechnology for protecting public health.

CHAPTER 5

PURIFICATION OF ALPHA-LACTALBUMIN FROM WHEY

5.1. Introduction

Whey proteins have high nutritional value providing use in dietary purposes and improvement of technological properties in processed foods. Various researches on the separation and purification of whey proteins have been carried out for a long time. Different methodologies have been reported in literature for the analysis and/or purification of them. Selective precipitation by salts, membrane filtration based on size and charge, and selective adsorption and elution by means of binding to a matrix, and stepwise elution through salt and/or pH gradient are the main categories among these procedures. Some limitations can be encountered during these processes, such as; low purity or low recovery of proteins, totally or individually. In order to achieve a better separation, researchers investigate different combinations of the mentioned techniques as reported below.

Neyestani and coworkers precipitated the whey proteins by salts, then collected α-La, β-Lg and BSA protein fractions by anion exchange and gel filtration chromatography, and they analyzed protein fractions by HPLC and SDS-PAGE (Neyestani et al., 2003). They reported that protein fractions, analyzed with HPLC and SDS-PAGE, were obtained with high purity by fast and economical methods. Yoshida (1990) also fractionated α-La and β-Lg from acid whey by gel filtration and anion exchange chromatography and identified protein bands with SDS-PAGE. Konrad and Kleinschmidth (2008) isolated α-La, with 90-95 % purity and 15% recovery, from sweet whey, using ultrafiltration and trypsin hydrolysis techniques together. In another study, whey protein fractions were obtained by the adsorption of α-La and β-Lg onto anion exchange matrix, and lactoperoxidase (LPOD) and lactoferrin (LF) onto cation exchange matrix; then the protein bands were identified by SDS-PAGE analysis (Ye et al., 2000). Reverse phase-HPLC is also identified as a routine analysis for quick separation of whey proteins (Jung et al., 2003). Kristiansen et al. (1998) used

ultrafiltration and ion exchange chromatography to extract β-Lg with high purity for production at large scale. They identified the isolated β-Lg by mass spectrometry and isoelectric focusing in more detailed. Gerberding and Byers, 1998 described another methodology for the separation of major proteins and lactose from sweet dairy whey. They used preparative ion-exchange chromatography with simultaneous step elution of salt and pH gradient.

Ultrafiltration (UF) is a membrane process in which hydrostatic pressure forces a liquid against a semipermeable membrane. The solvent and the suspended small solute molecules pass through the membrane and collected as permeate, whereas larger solute molecules do not pass through the membrane and recovered in a concentrated solution as retentate. This separation process is used in industry and research for purifying and concentrating macromolecular (with molecular weights between 1-10^4 kDa) solutions, especially protein solutions. These macromolecules can be separated, purified or concentrated in either retentate or permeate fraction due to molecular weight cut-off (MWCO) of the membrane used. The MWCO of the membrane is defined as the molecular weight of globular proteins which are 90% retained by the membrane (Geankoplis, 1993). In addition to MWCO size, shape and flexibility are also important parameters. For a given molecular weight, flexible molecules can better pass the membrane than the rigid ones. Ionic strength and pH often help to determine the shape and rigidness of large molecules (Cheremisinoff, 2002). The membranes for UF are made from synthetic polymers such as polycarbonate, cellulose acetate, polysulfone and aromatic polyamides. The major limitation related with UF systems is the formation of a fouling layer on the membrane surface. This layer may alter membrane selectivity and reduce throughput. Mid-run washings or diafiltration which is water feeding to membrane during process may help to eliminate the fouling layer and increase filtration efficiency. UF process is used for various food applications, such as concentration purposes of milk products, juices and beverages, vegetable extracts, single-cell proteins and enzymes. One of the largest applications of UF is the recovery of proteins in whey. Liquid whey can be ultrafiltered to produce whey protein concentrate (WPC), then this product can be fractionated into individual whey proteins by various UF membranes or other chromatographic techniques. In this study, WPC was obtained from whey powder solution by 10 kDa UF membrane prior to chromatographic separation.

Chromatography is the term used to describe a separation technique in which a mobile phase carrying a mixture passes through a stationary phase and the molecules in

the mixture are seperated due to different strategies. Analytical chromatography is used for the analysis of the molecules with smaller quantities, whereas preparative chromatography is used to seperate molecules in larger quantities for further applications. Ion exchange is probably the most frequently used high resolution chromatographic technique for the separation and purification of proteins. Ion exchangers consists of an insoluble matrix to which charged functional groups (exchange groups) have been covalently bound. Separation in ion exchange chromatography (IEC) occurs due to reversible adsorption of charged solute molecules to oppositely charged exchange groups on ion exchange matrix and desorption of them from matrix by continuous elution with a salt gradient or by changing the charges of the exchange groups with pH adjustment. Ion exchangers are either cation exchangers having negatively charged functional groups and exchange positively charged ions (cations), or anion exchangers having positively charged functional groups and exchange negatively charged ions (anions). The ion exchange matrix may be based on inorganic compounds, synthetic resins or polysaccharides. The most common ones are DEAE (diethylaminoethyl)-Sepharose and QAE (quaternaryaminoethyl)-Sephadex as anion exchangers, CM (carboxymethyl)-Sepharose and SP (sulphonopropyl)-Sephadex as cation exchangers. The ion exchange matrix is choosen due to ionic characteristic of the protein molecule to be seperated from a mixture. As it is known, pH of the medium have great effect on the charge of protein. At pH below pI, proteins are positively charged while at pH above pI, they are negatively charged. Therefore, pH of the protein mixture and buffers related to choosen matrix is an important parameter for the analysis in IEC.

Size exclusion chromatography (SEC) is also known as gel permeation chromatography or gel filtration chromatography and separates molecules in aqueous solutions according to their sizes or molecular hydrodynamic volume as they passes through a porous matrix. It is generally used to separate biopolymers such as proteins and to determine their molecular weights. In SEC, biopolymer dissolved in an appropriate solvent (same with the mobile phase) feed into a column packed with a porous matrix with well-defined pore size. Larger molecules unable to enter the pores of matrix are eluted faster and left the column first, whereas smaller molecules able to enter the pores take longer to elute and left the column last. In this manner, high molecular weight compounds are eluted first and followed by low molecular weight compounds. SEC, especially the preperative one, is also used for cleaning purpose (e.g.

low molecular components such as pesticides and pollutants) and for desalting commonly. It may also be termed as a polishing step for purification of proteins. Sephadex is a beaded gel prepared by crosslinking dextran with epichlorohydrin is used widely as gel filtration matrix. It has different types due to its fractionation range. In the presented study, Sephadex-G75, with the fractionation range of 3-80 kDa, was used for final purification of whey proteins, α-La (14 kDa) and β-Lg (18 kDa).

In recents years, proteomic analyses by two dimensional isoelectric focusing (2D-IEF) have made substantial contributions in identification and characterization of dairy based peptides and proteins (Galvani et al., 2001; Fong et al., 2008; Ounis et al., 2008; Alonso-Fauste et al., 2012). This approach can provide rapid visualization of protein distributions and qualitative assesment of the proteins in whey (Fong et al., 2008). The 2D-IEF is an electrophoretic method including separation of proteins according to their isoelectric points along a pH gradient by IEF in the first dimension, and according to molecular weight by SDS-PAGE in the second dimension (Ong and Pandey, 2001; Garfin, 2003; Lindmark-Mansson et al., 2005).

Protein native structure is prone to the risk of denaturation during the purification processes (Liang et al., 2006; Santos et al., 2012). Raman and FT-IR spectroscopies can be quite useful for the structural analysis of protein molecules. Amide I, amide II, amide III and backbone skeletal streching modes of the peptides, observed in the Raman and FT-IR spectra provide valuable information about conformational changes in protein secondary structure (Tu, 1986; Liang et al., 2006).

The objective of this study is to obtain highly pure α-La to use in the development of protein nanotubes for food industry. Within this context, this study includes the extraction of α-La mainly from whey products, whey protein isolate (WPI), and whey powder (WP) using membrane filtration and chromatographic techniques (anion exchange chromatography, AEC and size exclusion chromatography, SEC), and characterization of purified fractions in terms of protein profiling, purity, isoelectric pH, molecular weight, and protein structure. Then, the purified α-La protein was used to construct nanotubes by self-assembly, after partial enzymatic hydrolysis.

5.2. Experimental

5.2.1. Materials

Most of the chemicals and standards were purchased from Sigma Chemicals Co. (St. Louis, MO). Anion exchanger matrix (Q-sepharose) and 2D-IEF strips and chemicals were purchased from Bio-Rad Laboratories Inc. (Hercules, CA, USA). Whey powder (WP) was kindly supplied by a commercial plant (Pınar A.Ş., İzmir, Turkey) and commercial whey protein isolate (WPI), BIPRO, was obtained from Davisco Foods Int. Inc (Eden Prairie, MN, USA). Compositions of WPI and WP were given in table 1. Ultrafiltration membranes and HPLC columns were purchased from Sartorius Stedim Biotech S.A. (Goettingen, Germany) and Agilent Technologies Inc. (Santa Clara, USA), respectively. BLP was kindly provided by Novozymes A/S (Bagsvaerd, Denmark).

Table 5.1. Compositions of whey protein isolate (WPI) and whey powder (WP)

	WPI (BIPRO)[a]	WP[b]
Lactose	1%	65-75%
Total protein	95%	10-12%
Fat	1%	0.8-1%
Moisture	5%	2.5-3%
Ash	3%	7.3-9.6%

[a]taken from specification sheet, [b]taken from Polat 2010

5.2.2. Methods

Whey proteins were purified by ultrafiltration (10 kDa membrane) assisted with diafiltration, and column chromatography. Q-Sepharose and Sephadex G-75 were used as anion exchanger and gel filtration matrices, respectively. Protein quantification was achieved by UV spectrophotometry at 280 nm. HPLC, SDS-PAGE, 2D-IEF, and MALDI-TOF MS techniques were used for the analysis of proteins purified.

5.2.2.1 Sample preparation from whey preparats

WPI was dissolved in 0.05 M Tris-HCl buffer, pH 6.0 as 1 and 2 %; whey powder (WP) was dissolved in distilled water as 2.5 and 10 %. The pH value of the WP solution (WPS) was 6.33. WPI solutions were directly fed to anion exchange chromatography for protein fractionation. However, WP solutions were first introduced to ultrafiltration to eliminate other macromolecules, such as lactose, and also small peptides and protein units, such as glycomacropeptides. Then, the resultant retentate fraction containing protein concentrate (WPC) was fed to anion exchange chromatography for further fractionation.

5.2.2.2. Ultrafiltration

Hundred ml of WPS was passed through 10 kDa membrane to obtain whey protein concentrate (WPC). The peristaltic pump was worked at 75 rpm and the solution was passed under 1.5-2 bar pressure. To prevent the formation of fouling layer above the membrane and improve the separation efficiency, diafiltration (DF) was carried out by five to ten volume of distilled water, during the process. The retentate fed to membrane continuously for about 50 minute by the help of diafiltration. Then the retentates and permeates were analyzed by SDS-PAGE after protein quantification in nanodrop. Also these fractions were analyzed by HPLC for lactose determination. The last retentate fraction, collected as 50 ml, which was WPC, was then fed to anion exchange chromatography to separate proteins individually.

5.2.2.3. HPLC Analysis for Lactose Determination

HPLC analysis was performed by using Perkin-Elmer Series 200 HPLC (USA) system with Aminex HPX-87 H colunm with dimensions 300x7.8 mm. All the standard solutions and sample dilutions were prepared by 5 mM H_2SO_4 which was the mobile phase used. The column temperature was maintained at 45°C and the injection volume was 20 µl. The isocratic elution was carried out at a flow rate of 0.6 ml/min.

5.2.2.4. Anion-exchange Chromatography (AEC)

Q-Sepharose, a strong anion exchanger matrix, was packed into a glass column with 50 cm length and 2.5 cm internal diameter. It was equilibrated with 0.05 M Tris-HCl buffer, pH 6.0. Twenty five millilitters of WPI solution was loaded to Q-Sepharose column and the column was washed with 0.05 M Tris-HCl, pH 6.0, to elute unbound proteins. The flow rates was about 0.25-1.5 ml/min. Proteins, reversibly adsorbed onto the matrix, were eluted by changing pH of the buffers. Firstly, 0.05 M Tris-HCl, pH 5.0 was used to elute β-Lg, then, 0.05 M Tris-HCl, pH 4.0 was used to elute α-La. All fractions were collected by a fraction collector according to changes in the absorbance monitored at 280 nm. Similarly, WPC sample (25 ml) was also loaded to Q-Sepharose column, elution was performed under the same conditions. The high volume fractions were concentrated by 10 kDa UF membrane and 5 kDa centrifugal membranes. All the fractions collected were analyzed by SDS-PAGE. The amounts of proteins in the fractions were quantified by UV-absorbance measurements at 280 nm. The protein quantity was determined by using the standard curve constructed previously. The main fractions collected during elution steps of AEC analysis of WPI and WPC samples were fed to Sephadex-G75 column, respectively, for further purification.

5.2.2.5. Size Exclusion Chromatography (SEC)

Sephadex-G75 gel solution, prepared by swelling of powdered product in 0.05 M Tris-HCl (pH 6.0), was packed into the glass column with 50 cm length and 2,5 cm diameter. The matrix was equilibrated with 0.05 M Tris-HCl, pH 6.0. The main fractions collected from equilibration (washing of unbound proteins) and elution (washing of adsorbed proteins) steps, during AEC analysis of WPI and WPC samples, were fed to Sephadex-G75 column, respectively, for further purification. The loaded sample volumes were changed between 15 and 50 ml for each fraction, the buffer used for elution was 0.05 M Tris-HCl, pH 6.0, and the flow rate was about 1.5-2 ml/min. New fractions were collected through a fraction collector and the high volume fractions were concentrated by 10 kDa UF membrane and 5 kDa centrifugal filter units. Then, the proteins in the collected fractions were quantified and analyzed by SDS-PAGE. Also, target proteins were analyzed by HPLC and 2D-IEF.

5.2.2.6. Protein Determination

The amount of protein in the fractions collected through chromatography was quantified by UV-absorbance measurements in the nanodrop instrument. The measurement was done by dropping 2 µl of sample through channel on the instrument and the absorbance was obtained at 280 nm. Then the protein quantity was determined by using the standard curve (A1) constructed previously.

5.2.2.7. SDS-PAGE Analysis

Proteins in the fractions were analyzed by SDS-PAGE according to Laemmli (1970). Samples were mixed with sample buffer (1:1 to 1:3) and boiled for 5 min to denaturate proteins. Electrophoresis was run with a 4% stacking gel and 12% separating gel at 100 V for 100 min. The amount of protein sample loaded to each well was 20 µl. Protein staining was performed by Coomassie Brilliant Blue R250 for 30 min and destaining was carried out for a few hours. At the end, protein bands were examined by gel documentation system (VersaDoc).

5.2.2.8. HPLC Analysis of Whey Proteins

HPLC analysis was performed by using Perkin-Elmer Series 200 HPLC (USA) system with Agilent ACE C18 colunm with dimensions 150x4.6 mm. All the standard solutions and sample dilutions were prepared by 0.1% TFA (v/v, in water) which was the mobile phase used in the HPLC. The mobile phases are buffer A 0.1% TFA (v/v) in water, and buffer B 0.09% TFA (v/v) in acetonitrile-water (80:20) (v/v). Elution was carried out by the linear gradient program from 0 to 100 % B in 40 minutes and then returned to starting conditions in 5 minutes. The column temperature was maintained at 40°C and the flow rate was 1 ml/min with the injection volume of 20 µl.

5.2.2.9. 2-D Isoelectric Focusing

Isoelectric focusing (IEF) was carried out using a Protean IEF Cell (Biorad Laboratories Inc., USA). One hundred milliliters of protein samples were mixed with

500 µl IEF rehydration buffer (8 M urea, 2% CHAPS, 50 mM DTT and 0.2 % pH 4-7 Bio-Lytes) to obtain a final protein concentration of 2 mg/ml approximately. Samples (600 µl) were loaded on to IPG strips (pH 4-7, 17 cm, Biorad Laboratories Inc.) and rehydrated passively overnight at 20 ºC in IPG sample tray. Then the strips were focused at 20 ºC in IEF Cell, considering the conditions reported by Fong et al. (2008) as follows: gradient to 200 V (30 min), gradient to 500 V (30 min), gradient to 1000 V (30 min), gradient to 3000 V (1 h), gradient to 8000 V (1 h). Focusing was continued at 8000 V for approximately 8 h with overnight focusing at 1500–3000 V to achieve a total of 100000 Vh. SDS-PAGE was achieved with a 4 % stacking gel and 12 % separating gel using a Protean II maxi gel electrophoresis system (Biorad Laboratories Inc., USA). Focused IPG strips were equilibrated with buffer I (6 M urea, 2 % SDS, 2% DTT and 20% glycerol in 0.375 M Tris HCl (pH 8.8)) and buffer II (buffer I containing 2.5 % iodoacetamide instead of DTT) for 20 minutes, respectively, prior to electrophoresis. The equilibrated strips were then embedded onto the SDS gels in 0.5 % overlay agarose solution. Electrophoresis were carried out at 16 mA/gel for the first 40 min and then at 25 mA/gel for about 5 hours, by cooling the electrophoresis unit using circulating water through entire electrophoresis. Following this, silver staining procedure was carried out, and then the protein spots on the gels were visualized and identified by a VersaDoc gel documentation system (Biorad Laboratories Inc., USA).

5.2.2.10. MALDI-TOF Mass Spectrometry

MS spectra of the samples were taken by a Bruker MALDI-TOF MS system (Germany). One µl of protein sample (1 %) was mixed with a 5 µl of matrix solution, DHB (2-, 5- dihydro benzoic acid) and CHCA (alpha-cyano hydroxy cinnamic acid) (3:2), and 2 µl of the mixture was spotted on the MALDI plate to dry for analysis. Masses were detected with the linear mode in the ranges between 5000- 20000 Da.

5.2.2.11. X-Ray Flourescence (XRF) Analysis

The elemental compositions of the standard and purified α-La protein farctions were determined by XRF, Spectro IQ II (Spectro Analytical Instruments, Germany).

5.2.3. Results and Discussion

5.2.3.1. Membrane Process

As seen in the table 5.1, protein concentrations are 95 % in WPI and 10-12 % in WP. Because of this, concentrations of the solutions prepared for the chromatography were different. WPS was prepared as 10 % and WPI solution was prepared as 2.5 % at most. In order to concentrate proteins and remove lactose prior to chromatography, WPS solution was passed through a 10 kDa UF membrane. Diafiltration facilitated membrane process by retarding fouling layer formation. It may also be considered as a washing step for proteins in whey powder. Figure 5.1 shows protein profiles of WPI (lane 1), WPS (lane 2), and permeate (lane 3) and retentate (lane 4) fractions obtained by UF process. Protein bands of commercial standards of major whey proteins (lane: 5-7) were also given for comparison. The appearance of the protein bands in WPI and WPS seemed different in lane 1 and 2. Those in WPI are alike with the commercial standards. This may arise from the running response of these two whey products on the gel due to their compositional difference.

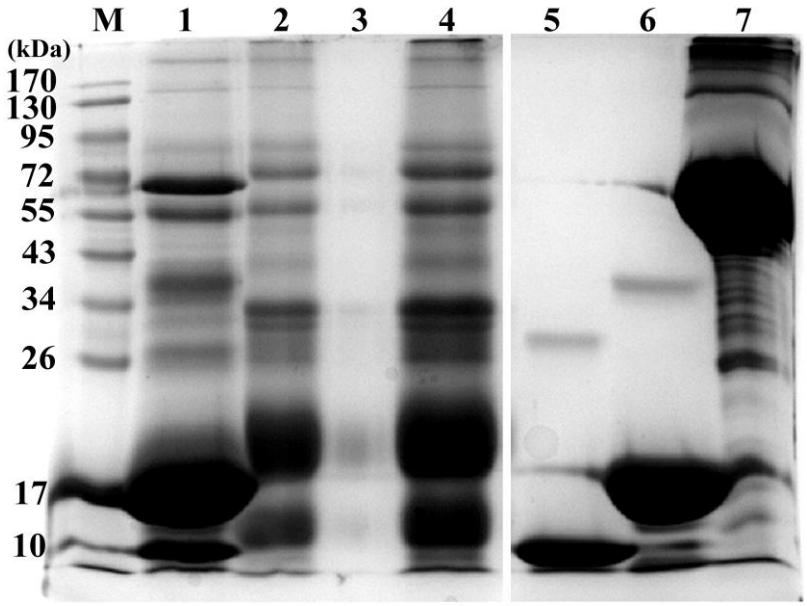

Figure 5.1. Concentration of whey proteins by UF process. Lane M: protein ladder, lane 1: WPI, lane 2: WPS, lane 3 and 4: permeate and retentate fractions of UF process, respectively, lane 5, 6 and 7: commercial standards of α-La, β-Lg and BSA.

As the molecular weights of whey proteins (given in Table 2.1) are greater than the molecular cut-off value of UF membrane (10 kDa), they could not pass the membrane and were concentrated in the retentate fraction (figure 1, lane 4). Small peptides/proteins such as glycomacropeptides were expected to pass through the permeate fraction. Since they were much diluted, no protein bands representing them were observed in lane 3, but some amount of protein was detected by UV measurements in permeate fraction. Retentate fraction, called whey protein concentrate, WPC, contained target protein α-La to fed anion exchange chromatography.

Table 5.2 and 5.3 indicate feed volumes, diafiltration volumes, and protein concentrations of WPS fractions during membrane process representatively. Totally, 100 ml WPS was washed with about 750 ml of water and five fractions of permeate and retentate were collected. Protein amounts (non-target) were decreased through following permeates and concentrated in retentates. In one batch given below, total 449 mg protein was fed to UF membrane and 155.93 mg protein (non-target) was collected in permeate fractions and 267.22 mg protein was collected in retentate fraction. Protein recovery was determined as about 94% during this membrane process. And one batch of UF process takes approximately 47.5 minutes.

Table 5.2. Fractions of WPS collected by 10kDa-UF membrane

Process no	**Feed**		**Water**	**Permeate**		**Retentate**		**time**
	ID	volume (ml)	volume (ml)	ID	volume (ml)	ID	volume (ml)	(min)
1	WPS	100	-	P1	62	R1	25	5.5
2	R1	25	200	P2	177	R2	22	10
3	R2	22	200	P3	180	R3	22	8
4	R3	22	200	P4	180	R4	22	7.8
5	R4	22	150	P5	108	R5	62	6.5

Table 5.3. Protein concentrations of WPS fractions collected by 10kDa-UF membrane

samples	WPS	P1	R1	P2	R2	P3	R3	P4	R4	P5	R5
prtn conc. (mg/ml)	4,49	1,64	12,49	0,27	11,97	0,02	11,70	0,00	11,52	0,008	4,31
volume	100	62	25	177	22	180	22	180	22	108	62
total prtn	**449,00**	101,68	312,25	49,79	263,34	3,6	257,40	0,00	253,44	0,86	**267,22**

Protein profiles of each permeate and retentate fractions of WPS are shown in figure 5.2. Permeates contained no protein bands, as retentates contained sharp protein bands.

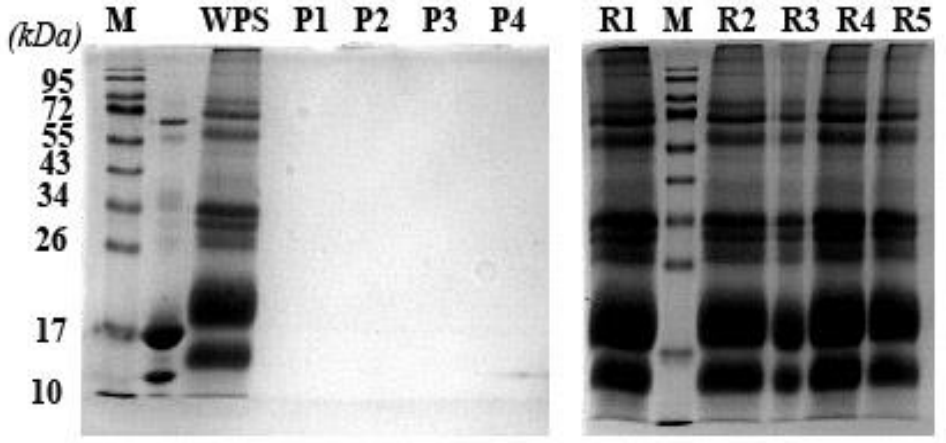

Figure 5.2. Protein profiles of WPS fractions obtained by 10kDa membrane-UF process

The main component of whey powder, lactose (65-75%) was discarded during DF assisted UF. Lactose in WPI, WPS, and UF fractions of WPS was determined by HPLC. Commercial WPI product contains only about 100 ppm lactose, whereas WPS contains 15781 ppm. After five DF runs, lactose concentration in last retentate, WPC, was reached to that in WPI. Figure 5.3 indicates clearly decrease in the lactose amounts in retentate fractions. The first permeate and retentate had 9098 ppm and 4907 ppm lactose. By the gradual decrease in lactose amount in the following fractions, the last permeate and retentate had 102 ppm and 104 ppm. Most of the lactose was removed in the first (69%) and second (26%) steps. One batch of UF-DF process took approximately 50 minutes. In overall, lactose removal was determined as 99.4% during this membrane process. This finding agreed with the literature that UF assisted with DF is a successful process for lactose removal in whey (Zydney, 1998). The initial lactose amount in WP is really high. Removal of lactose and some other non-target molecules at the beginning was expected to lead an achievement of effective protein purification in whey by chromatography. In this study, DF was carried out with 750 ml of water which corresponds to nearly eight volume of feed. However it was seen clearly that, lactose removal and concentration of target proteins were achieved in the third and/or fourth stages of this process. So, five volumes of water can be considered as sufficient for a target process. Chromatographic raw data of lactose removal was given in Appendix C.

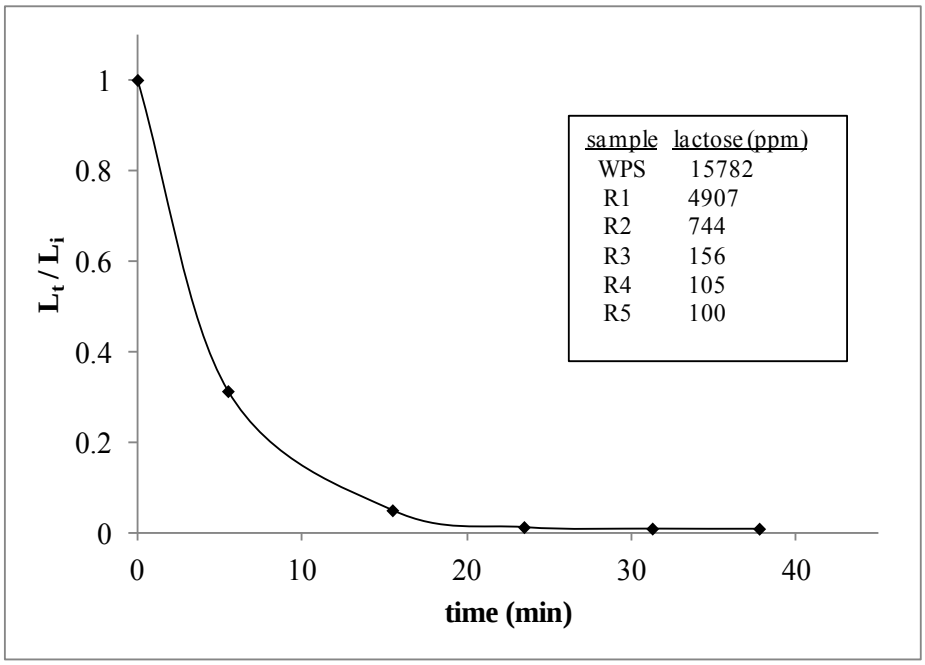

Figure 5.3. Removal of lactose in WPS retentate fractions by UF process. L_i: initial lactose amount, and L_t: lactose amounts in the following fractions. Inset table gives lactose amounts determined by HPLC in retentate fractions.

5.2.3.2. Column Chromatography

WPI and WPC (obtained by membrane process) were fed to Q-Sepharose column, respectively, to elute whey proteins. First, unbound proteins were eluted with 0.05M Tris HCl buffer, pH 6.0. Then the adsorbed ones were eluted by pH gradient in separate fractions. The anion-exchange elution approach based on the pH gradient was found to be effective in separating α-La and β-Lg fractions, even though the pI values of both proteins were close to each other. The approach is based on elution due to difference of isoelectric points of the target proteins. The isoelectric points of β-Lg and α-La are 5.2 and 4.5-4.8, respectively (Table 2.1). If the target protein has pI below than the local pH, the protein binds to an anion exchange matrix. Then, if the pH of the medium is adjusted to below the pI of the protein, the protein is desorbed from matrix (Gerberding and Byers, 1998). By considering this, protein sample was first introduced to column with Tris buffer (50 mM) of pH 6.0 to mediate binding of proteins to anionic matrix and elute unbound proteins. Then the second buffer with pH 5.0 was used to elute β-Lg, and the third buffer with pH 4.0 was used to elute α-La. A schedule was

given for a representative elution below (Table 5.4). Total volumes of buffers used and elution times were included there. In SEC assays used buffer volume and elution time changed due to protein amount in feed. In average, 200-250 ml buffer was used for one batch with 1.5 h elution time.

Table 5.4. A representative elution schedule for the AEC

Process step	Buffer volume (ml)	Flow rate (ml/min)	Elution time (min)
	WPI / WPC	WPI / WPC	WPI / WPC
Whey feed, pH 6.0	150 / 185	0.94 / 1.00	35 / 81
Tris buffer, 50 mM, pH 5.0	510 / 2000	0.27 / 1.00	1370 / 1652
Tris buffer, 50 mM, pH 4.0	150 / 2100	1.37 / 1.32	27 / 1529

Figure 5.4 shows; (a) elution chromatogram of WPI and (b) protein profiles of the fractions collected by AEC and further purified by SEC. Four peaks (1-4) were obtained by the elution with the buffer of pH 5.0 (elution 1 fractions) attributable to β-Lg rich fractions. Two peaks (5-6) corresponded to α-La rich fractions obtained by the elution with the buffer of pH 4.0 (elution 2 fractions). Further processing by SEC provided better purity for α-La (lane 8) and β-Lg (lane 10) fractions. Figure 5.5 represents separation of whey proteins from WPC by AEC. Five protein fractions were eluted. First three elution 1 fractions were β-Lg rich fractions and the last elution 1 fraction (peak 4) was rich in α-La. The fifth fraction, elution 2 fraction, was rich in β-Lg (Figure 5.5.b). Further processing by SEC provided better purity for α-La (lane 7) and β-Lg (lane 9) fractions.

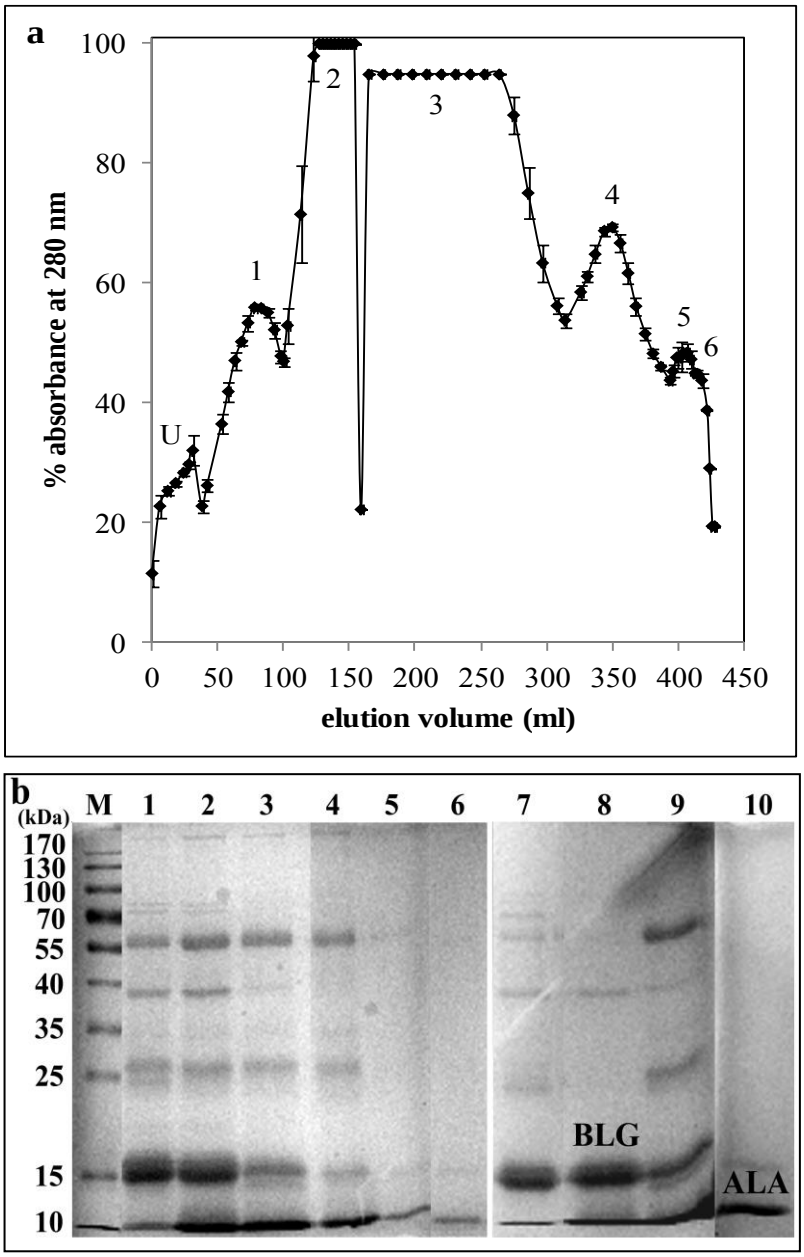

Figure 5.4. Elution of WPI proteins by AEC a) AE chromatogram of WPI. Unbound proteins (U) were eluted by 50mM Tris HCl, pH 6.0. Peak 1-4 were eluted by 50mM Tris HCl, pH 5.0 and peak 5-6 were eluted by Tris HCl, pH 4.0. Column bed volume: 10 x 2.5 cm (50 ml matrix) b) SDS-PAGE profiles of protein fractions of WPI. Lane M: protein ladder; lane 1-6: fractions eluted by AEC (corresponding to peak 1-6); lane 7-10: fractions eluted by SEC. Lane 1-4: elution 1 fractions (El1F1, El1F2, El1F3, and El1F4); lane 5-6: elution 2 fractions (El2F1, El2F2). Further purified fractions in lane 7: El1F1/F, lane 8: El1F2/F, lane 9: El1F3/F, and lane 10: El1F4/F.

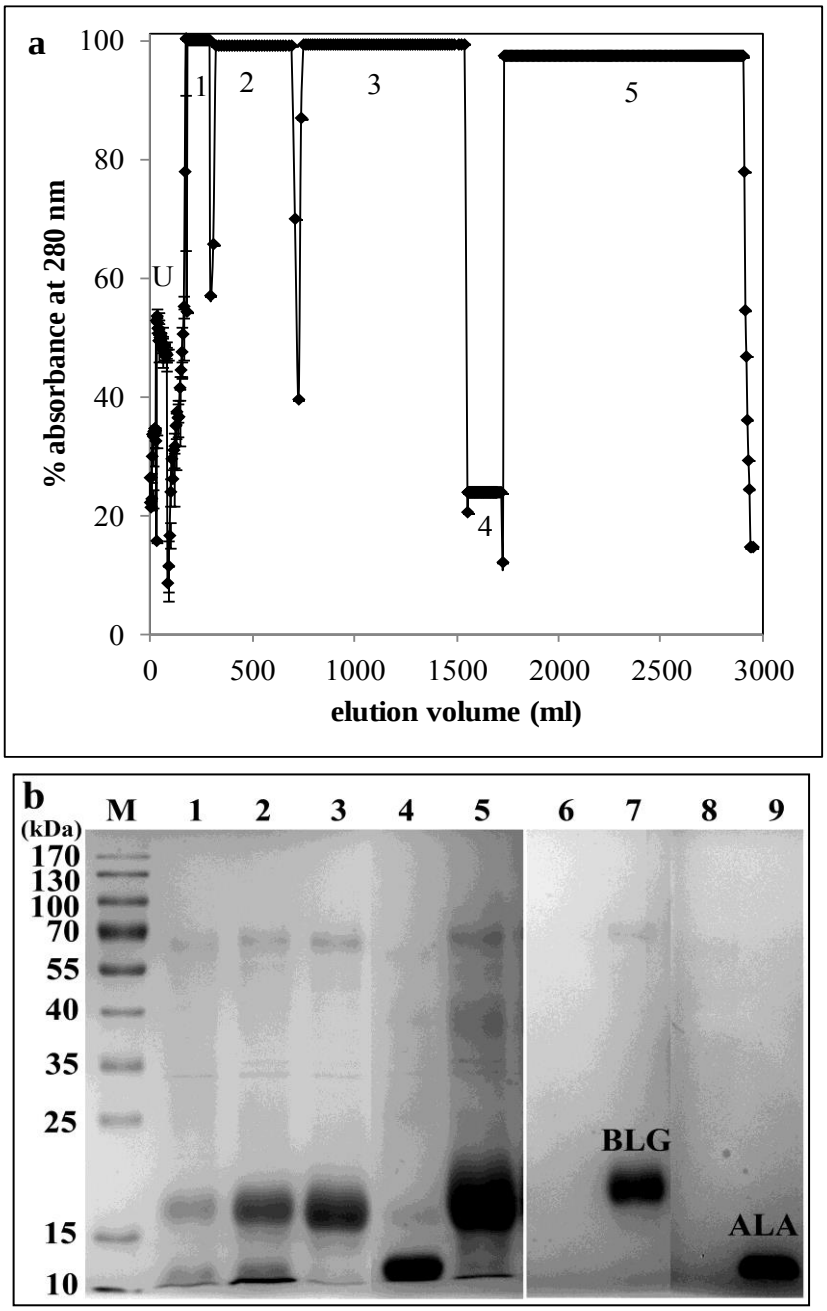

Figure 5.5. Elution of WPC proteins by AEC a) AE chromatograms of WPC. Unbound proteins (U) were eluted by 50mM Tris HCl, pH 6.0. Peak 1-4 were eluted by 50mM Tris HCl, pH 5.0 and peak 5 was eluted by Tris HCl, pH 4.0. Column bed volume: 10 x 2.5 cm (50 ml matrix) b) SDS-PAGE profiles of some protein fractions of WPC. LaneM: protein ladder, lane 1-5: fractions eluted by AEC (corresponding to peaks 1-5); lane 6-9: fractions eluted by SEC. Lane 1-4: elution 1 fractions (El1F1, El1F2, El1F3, and El1F4), lane 5: elution 2 fraction (El2F). Further purified fractions in lane 6: El1F3/F1, lane 7: El1F3/F2, lane 8: El1F4/F1, lane 9: El1F4/F2.

The elution order of α-La and β-Lg was not as expected exactly according to separation approach. In WPC, β-Lg eluted first but not completely, then α-La eluted

with the same buffer in the last fraction. And the rest of β-Lg eluted by the next buffer. The α-La should have eluted after β-Lg with the buffer of pH 4.0, instead of pH 5.0 according to its respective isoelectric points given in the literature. In WPI, some amount of α-La also eluted by the buffer with pH 5.0, and last elution 1 fraction contained more α-La besides β-Lg. Gerberding and Byers (1998) eluted α-La before β-Lg as in reversed order in comparison with the same theory considered here. They reported that the reason for this was the incomplete binding of α-La to the matrix due to competition and the greater selectivity of resin for β-Lg. Our findings also revealed that the binding of α-La to the matrix was incomplete, especially in WPC, due to competition with the other minor components. Selective binding of β-Lg to the matrix, parallel with the abundancy in whey, may also lead to this elution profile. In addition, these purified (native) α-La proteins may have pI values very close to and/or slightly above 5.0. It is clearly seen that, besides α-La (target protein), β-Lg was also extracted from whey protein products by chromatography based on elution by changing pH.

Table 5.5 summarizes protein recoveries in the WPI and WPC fractions eluted by AEC and SEC in a representative purification were batch. Total protein in WPI sample fed to AEC column was 316.3 mg and the recovered protein was 171.3 mg. Initial protein amount of WPC sample fed to column was 122.6 mg; however the recovered one was 91.1 mg. There is a great difference in protein content of feed and recovered fractions of WPI sample. The protein recovery for WPC was surprisingly lower than that of WPI. Recoveries of the proteins were 54.2 % (WPI) and 74.4 % (WPC) for AEC, and 71.4 % (WPI) and 53.6 % (WPC) for SEC, respectively. It is hard to feed the diluted protein solutions to the chromatographic columns. In order to increase the protein concentration in feed solutions, UF and centrifugal filtration techniques were used prior to the final chromatographic step (e.g. SEC). Thus, significant amount of protein may be lost during these steps. However the protein recoveries were comparable with the current literature (Gerberding and Byers, 1998; Konrad and Kleinschmidth, 2008).

Whole purified fractions obtained at the end of purification studies were presented in Appendix D. All the α-La fractions were labelled according to their source (WPI or WPC), and those purified from WPI or WPC were combined separately. One WPI-based α-La fraction, named as I-α-La, and two WPC-based α-La fractions, named as C1 and C2-α-La, were stored at -20 ºC for further studies. The purity of C1 was better than C2; therefore C1 (C) was used in nanotube formation studies.

Table 5.5. Protein recoveries in the WPI and WPC fractions eluted by AEC and SEC *

Feed		AEC fractions		Feed		SEC fractions		
name	protein amount (mg)	name	protein amount (mg)	name	protein amount (mg)	name	protein amount (mg)	recovery (%)
WPI	316	I-U	1					
		El1F1	6.5	El1F1	6.5	El1F1/F	2.4	36.9
		El1F2	42.5	El1F2	42.5	El1F2/F	23	54.1
		El1F3	110.9	El1F3	110.9	El1F3/F	92.4	83.3
		El1F4	8.5	El1F4	8.5	El1F4/F	2.4	28.2
		El1F5	1					
		El1F6	1					
						total protein fed (mg)	168.4	
	total protein recovered (mg)		171.4		total protein recovered (mg)		120.2	
	recovery (%)		54.2		recovery (%)		71.4	
WPC	122.6	C-U	0.5					
		El1F1	6.2	El1F1	6.2	El1F1/F	4.2	67.7
		El1F2	8.4	El1F2	8.4	El1F2/F	1	11.9
		El1F3	4.7	El1F3	4.7	El1F3/F2	2	42.6
		El1F4	24.1	El1F4	24.1	El1F4/F2	6.8	28.2
		El1F5	47.3	El1F5	47.3	El1F5/F	34.6	73.2
						total protein fed (mg)	90.7	
	total protein recovered (mg)		91.2		total protein recovered (mg)		48.6	
	recovery (%)		74.4		recovery (%)		53.6	

*protein amounts given were determined by nanodrop after concentration of each fraction by UF (10 kDa) and centrifugal filters (5 kDa)

5.2.3.3. Purity Control of Target Fractions

In addition to SDS-PAGE, HPLC analysis was also carried out to analyze proteins through purification steps. HPLC chromatograms of whey protein products and purified fractions were given in Figure 5.6. Protein peaks in WPI are quite clear and sharp due to high protein concentration with high purity of this commercial product.

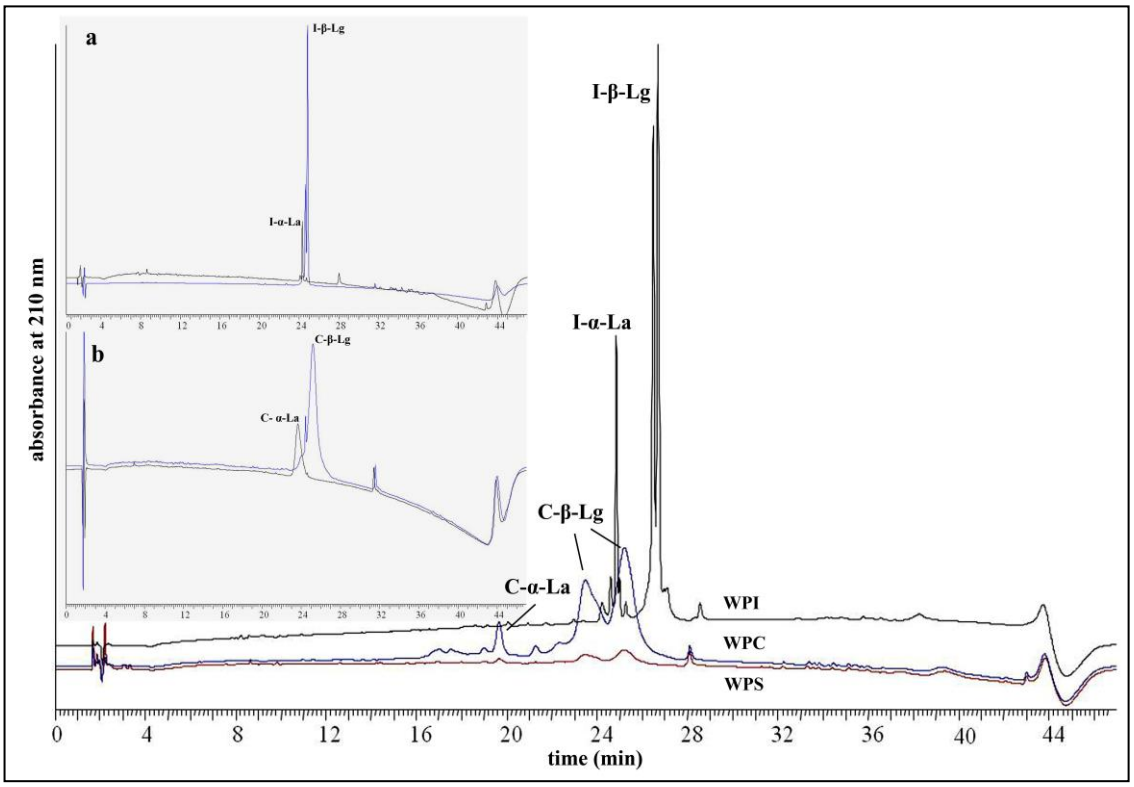

Figure 5.6. HPLC chromatograms of whey proteins. Inset chromatograms: a) α-La and β-Lg extracted from WPI (I-α-La, I-β-Lg), b) α-La and β-Lg extracted from WPC (C-α-La, C-β-Lg).

When WPS and WPC chromatograms were compared, significant difference was observed. Especially, peaks showed better intensities in WPC chromatogram. Both HPLC chromatograms and SDS-PAGE profiles agreed that proteins were well-concentrated by UF. When WPI and other two chromatograms were compared, shifts in retention times were also obsereved. The α-La in WPI left the column at 24.3 min, however α-La in WPC left the column at about 19.5 min. This shift may be due to the high mineral content of the latter. Similarly retention times for β-Lg B and β-Lg A were 26.5 and 26.7 min, but those in WPC shifted to 23.5 and 25.2. The peaks of α-La and β-Lg extracted from WPI (Figure 5.6.a) had much better resolution than the peaks of those extracted from WPC (Figure 5.6.b) due to their sources. The inset chromatograms indicated individual protein fractions of α-La and β-Lg purified from WPI and WPC. The purity of each α-La and β-Lg fraction was determined from the ratio of their peak areas to the total peak area of all peaks obtained by HPLC. According to this, the purities of WPI based α-La (I-α-La) and β-Lg (I-β-Lg) were 95 and 97% and WPC based α-La (C-α-La) and β-Lg (C-β-Lg) were 99%. HPLC chromatograms of commercial standards of whey proteins were given in Appendix A2.

Figure 5.7 shows 2-D gels of whey preparates and purified α-La and β-Lg fractions. Protein spots belonging to β-Lg were very dominant in both WPI and WPC as expected (Figure 5.7. a, b). Casein fractions, immunoglobulin, BSA, and other protein fractions were also appeared on both gels. However, purified α-La and β-Lg fractions were dominated by the spots of target proteins (Figure 5.7. c, d, e, f). The results of 2D-IEF agreed with SDS-PAGE and HPLC data indicating the purity of the target protein fractions. Some weak non-target protein spots were visible in the 2D gels of individual fractions, especially in Figure 5.7. c and e, due to the high sensitivity of the silver staining procedure. The identifications of the spots representing individual whey proteins were given in Table 2. In general, the spots observed in this study are comparable with those reported previously (Yamada et al., 2002; Lindmark-Mansson et al., 2005; Ounis et al., 2008). However, the pI value of α-La might be a little bit higher than the reported ones and closer to that of β-Lg, according to AEC elution and 2D-IEF results. In fact, these literature examples reported detailed milk and whey protein/peptide compositions. However, this study reports characteristics of newly purified major whey proteins (α-La and β-Lg). Purification procedures may lead to some alterations in some properties of the resultant product. Some researchers also reported the pI values of protein fractions isolated from whey and our results are also comparable with those (Caessens et al., 1997).

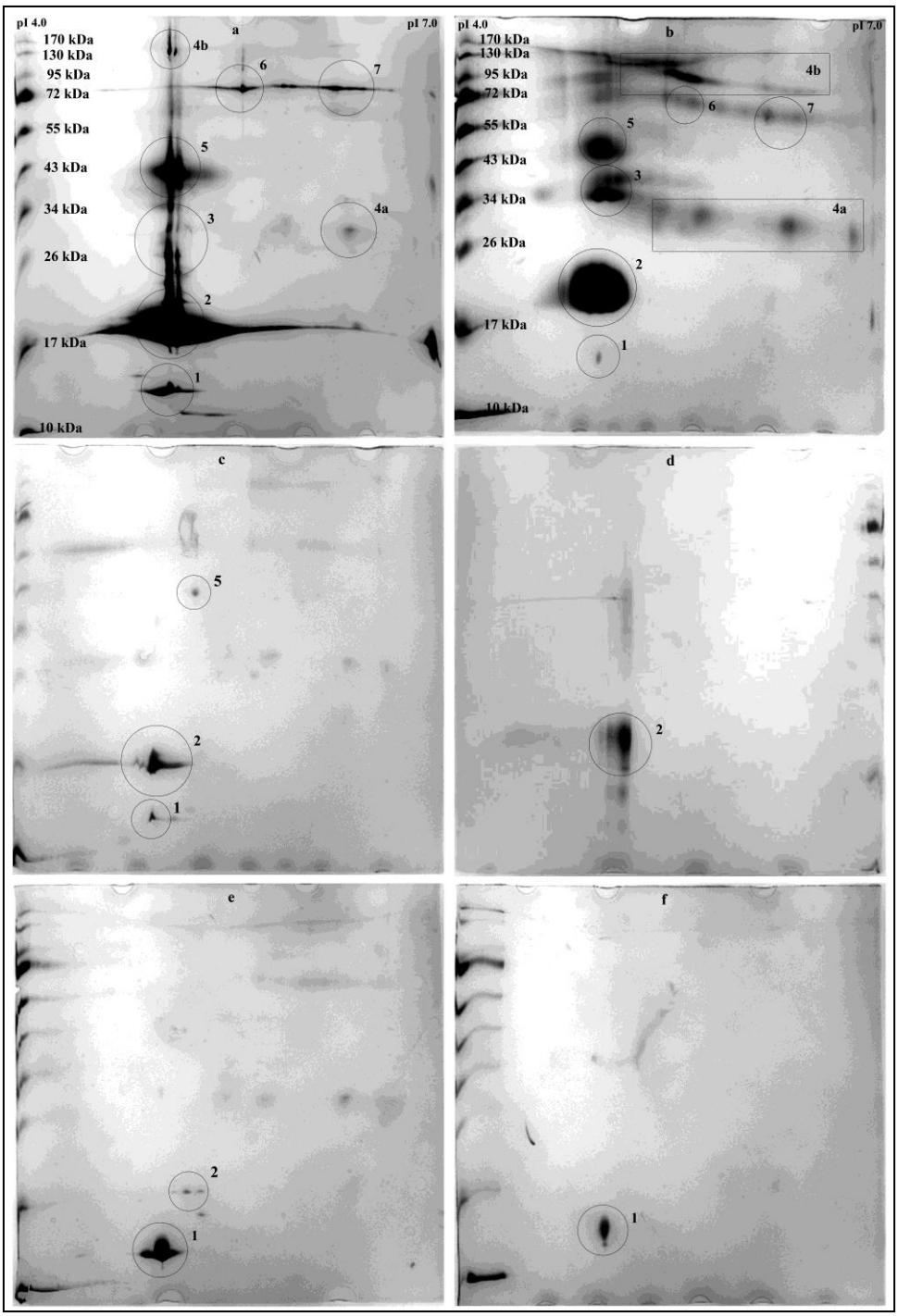

Figure 5.7. 2-D gel of whey proteins. a) WPI, b) WPC, c and d) α-La extracted from WPI and WPC (I-α-La, C-α-La), e and f) β-Lg extracted from WPI and WPC (I-β-Lg, C-β-Lg).

Table 5.6. Proteins in whey identified on two-dimensional electrophoresis gels

number[a]	protein	mwt (kDa)[b]	pI[b]
1	α-La	14.2	4.5-4.8
2	β-Lg (monomer)	18.4	5.2-5.3
3	caseins	21-25	4.9-6.3
4a	IgG light chain	22-27	5.5-8.3
4b	IgG heavy chain	55-59	5.5-8.3
5	β-Lg (dimer)	36.8	5.2-5.3
6	BSA	66.3	4.7-4.9
7	LF	78 - 86	8.0-9.0

[a] corresponding to spots on figure 6
[b] given according to Lindmark-Mansson et.al., 2005 and Ounis et.al., 2008

Figure 5.6 shows MALDI-TOF MS spectra of purified α-La fractions. Protonated (14.20, 13.63, 12.07 kDa in I-α-La; 14.18, 13.65 kDa in C-α-La) and double protonated (7.09, 6.82, 6.04 kDa in I-α-La; 7.09 kDa in C-α-La) protein peaks were observed. The molecular masses for I-α-La and C-α-La were determined as 14.2 and 14.18 kDa, respectively. Some part of the native structure of α-La may be distorted during the purification process. The peaks at 13.63/13.65 and 12.07 kDa might also be attributed to the α-La which lost a few peptides.

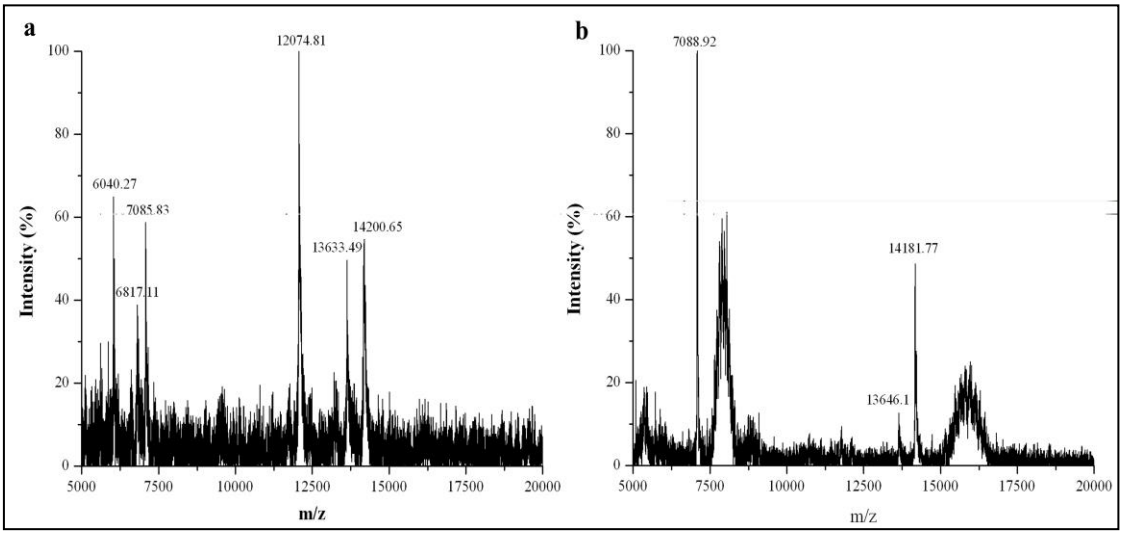

Figure 5.8. MS Spectra of α-La protein purified from a) WPI and b) WPC.

It was clearly seen that no peaks representing the non-target proteins (β-Lg and others) was appeared in the α-La fractions. This is important because, the presence of

other proteins, such as β-Lg, (even in small concentrations) disturbs the process of self-assembly of nanotubes and induces random aggregation (Graveland-Bikker and de Kruif, 2006). The results of HPLC, 2D-IEF and MALDI-TOF MS revealed that the target protein α-La was purified from the whey protein matrix successfully, which is suitable for nanotube formation.

Whey composition importantly affected this purification process and assays included in the following chapters. Elemental analysis by XRF showed differences in mineral composition of α-La from WPI and WPC (Table 5.8). Chlorine was found as the major element in the samples. Magnesium, aluminum, manganese and calcium were detected minerals as expected in whey. These cations, especially Ca^{2+} have significance in nanotube elongation and have been considered in the following chapter.

Table 5.9. Elemental composition of the standard and purified α-Lactalbumin samples

Symbol	Element	**S -α-La***		**I -α-La**		**C -α-La**	
		0.5 ml (3 % sol'n)		0.1 ml (5 % sol'n)		0.07 ml (10 % sol'n)	
		Concentration	Abs. Error	Concentration	Abs. Error	Concentration	Abs. Error
Na	Sodium	0,097%	0,014%	0,259%	0,021%	0,288%	0,022%
Mg	Magnesium	< 0,011%	(0,0)%	0,266%	0,018%	0,508%	0,022%
Al	Aluminum	0,00537%	0,00070%	0,0698%	0,0025%	0,0885%	0,0028%
Si	Silicon	0,00448%	0,00077%	< 0,00051%	(0,0)%	< 0,00051%	(0,0)%
P	Phosphorus	0,01609%	0,00038%	< 0,00030%	(0,0)%	< 0,00030%	(0,0)%
S	Sulfur	0,01047%	0,00021%	< 0,00004%	(0,0)%	< 0,00004%	(0,0)%
Cl	Chlorine	0,2554%	0,0006%	0,8042%	0,0014%	0,9708%	0,0016%
K	Potassium	< 0,0010%	(0,0)%	0,0070%	0,0012%	0,0069%	0,0013%
Ca	Calcium	0,00276%	0,00026%	0,00746%	0,00047%	0,01080%	0,00058%
Ti	Titanium	0,00040%	0,00008%	0,00117%	0,00015%	0,00098%	0,00016%
V	Vanadium	< 0,00051%	(0,0)%	0,00023%	0,00011%	< 0,00016%	(0,00016)%
Cr	Chromium	0,00165%	0,00012%	< 0,00051%	(0,0)%	< 0,00051%	(0,0)%
Mn	Manganese	0,03097%	0,00058%	0,01125%	0,00083%	0,01326%	0,00092%
Fe	Iron	0,00288%	0,00025%	< 0,00073%	(0,00073)%	< 0,00083%	(0,00083)%
Co	Cobalt	0,00071%	0,00011%	0,00223%	0,00015%	0,00315%	0,00016%
Cu	Copper	0,00366%	0,00041%	0,0420%	0,0014%	0,0583%	0,0025%
Zn	Zinc	< 0,00010%	(0,0)%	0,01568%	0,00090%	0,0317%	0,0017%
Ga	Gallium	< 0,00010%	(0,0)%	0,07010%	0,00100%	0,1260%	0,0019%
Nb	Niobium	0,00023%	0,00010%	< 0,00042%	(0,00042)%	< 0,00006%	(0,00006)%
Mo	Molybdenum	0,00071%	0,00014%	< 0,0023%	(0,0023)%	< 0,0031%	(0,0031)%
Te	Tellurium	< 0,00071%	(0,0)%	0,064%	0,016%	0,126%	0,031%
Ta	Tantalum	0,04528%	0,00072%	< 0,00020%	(0,0)%	< 0,00020%	(0,0)%

S-α-La: standard α-La protein

5.3. Conclusions

In this chapter, purification of major whey proteins (α-La, β-Lg) by UF and preparative scale AEC and SEC was presented. WP and WPI were used as protein source for extraction. Diafiltration assisted UF provided removal of lactose and concentration of proteins prior to chromatography. Strong anion exchanger, Q sepharose, in combination with the elution approach based on changing pH was shown to be an effective and promising method in separating major proteins in whey products. In beside of the target protein α-La, β-Lg was also extracted from whey preparates. Although the recovery was not highly efficient for the proteins obtained in the concentrated fractions, the main goal of this study was not to achieve a high recovery, but to obtain highly pure proteins to facilitate the nanotube growth. This goal was achieved as indicated by the results of a series of experiments including SDS-PAGE, HPLC, 2D-IEF and MALDI-TOF MS analyses. In addition, protein recovery can be increased by improving sensitivity of the liquid chromatography system used and limiting the post-processing of the fractions collected. Besides this, column matrix and elution approach are also important for succesfull purification, in fact. In the previous trails of the presented study, DEAE-Sepharose matrix was used with salt-gradient elution, but target separation was not achieved. Besides this, membrane filtration (using with 100, 30 and 10 kDa cut-off filters), and centrifugal filter units (with the same molecular cut-off values) were also tested for the purification of these proteins, but not succeded, unfortunately. Target purification was achieved by using Q-sepharose matrix with pH gradient elution. The purified WPI and WPC based α-La proteins were then used for the formation of nanotubes.

CHAPTER 6

DEVELOPMENT AND CHARACTERIZATION OF ALPHA-LACTALBUMIN NANOTUBES

6.1. Introduction

Food proteins and their building blocks, peptides have the special importance due to their ability for formation of supramolecular structures naturally by self-assembly which is identified by the spontaneous and reversible aggregation due to polymerization of molecules by non-covalent intermolecular interactions such as hydrogen bonding, electrostatic, hydrophobic and Van der Waals interactions (Rajagapol and Schneider, 2004). Enzymatic hydrolysis leads to breakdown of the proteins through smaller protein/peptide fragments depending on degree of hydrolysis. Then, naturally occurring self-assembly may give rise to fabrication of novel nanostructures from these fragments. Some researchers developed protein nanotubes in such a way from whey protein, α-Lactalbumin (α-La). It is a globular and compact protein, and resembles an ellipsoid. It has 14.2 kDa molecular weight and the ability of forming fibrillar structures. Ipsen and coworkers produced α-La gels containing novel microstructures (Ipsen et al., 2001). They reported partially hydrolyzed α-La with *Bacillus licheniformis* protease, BLP, which resulted in strong gels consisting non-branching, apperantly hollow microtubules with a uniform diameter of about 20 nm and lengths exceeding 2 μm. Graveland-Bikker and coworkers investigated the effect of calcium on nanotube growth and gel formation due to molecular self-assembly after limited hydrolysis of α-La extracted from bovine milk (Graveland-Bikker et al., 2004). They reported transparent gels with fine strands (nanotubes) having outer and inner diameters arround 20 and 7 nm, respectively. The critical calcium concentration was denoted as R = 1.5 (mole Ca^{++} / mole α-La) for the development of tubular structures leading to whitish transparent gel.

Microscopy is the key tool in nanotechnology researches. Especially, highly sophisticated TEM and AFM are used widely to visualize structures at nano scale and determine their dimensions.

Calcium plays a critical role in self-assembly process by linking peptides for

nanotube growth. The kinetics of the self-assembly process is monitored by the researchers (Ipsen et al., 2001; Graveland-Bikker et al., 2004). They studied the effect of Ca^{++} with various concentrations. They also presented the effects of some other cations such as Mg, Mn, Al, Zn by using DLS and UV-Vis spectrophotometer. In this study, both were used to monitor nanotube growth in changing Ca^{2+} and protein concentrations. Dynamic light scattering (DLS), also known as Photon Correlation Spectroscopy or Quasi-Elastic Light Scattering, is one of the most popular methods used to determine the size distribution of particles. In theory, a monochromatic light beam, such as a laser beam, sent onto a solution with spherical particles in Brownian motion undergoes a Doppler Shift. That is, the wavelength of the scattered light is different from that of the incident light due to the relative velocities of particles doing Brownian motion. This wavelength change is related to the size of the particle. It is possible to compute the sphere size distribution and give a description of the particle's motion in the medium, measuring the diffusion coefficient of the particle and using the autocorrelation function. The size distribution of the spherical particles is computed based on this relation (Clark et al., 1970). The DLS system used in this study for the particle size analysis of α-La nanostructures was operated at fixed angle (173º) and at 633nm wavelength.

During the hydrolysis of α-La, polypeptide chain is broken down and the peptides arised forms nanotubes by re-organizing readily. Actually, this is a conformational change after limited hydrolysis. Raman spectroscopy was used to investigate the conformational transitions in proteins by detecting changes in the secondary structure. It provides information related to the vibrational motions of the molecules which can be used in prediction or identification of their chemical structures (Nonaka et al., 1993). Backbone vibrations in polypeptides and proteins are usually associated with three main regions of the Raman spectrum (Tu, 1986; Diem, 1993; Miura and Thomas, 1995; Blanch et al., 2000). These are the backbone skeletal stretch region of ~870-1150 cm^{-1}, arising from C_α-C, C_α-C_β, and C_α-N stretches; the amide III region of ~1230-1340 cm^{-1}, resulting primarily in-phase combination of the N-H in-plane deformation vibrations with the C_α-N stretch; and amide I region of ~1630-1700 cm^{-1}, originating mainly from the C=O stretch.

BLP cuts α-La at aspartic and glutamic acid sites during the hydrolysis (Breddam and Meldal, 1992). Carboxylic acid groups (COO^-) at these ends exposed and become available for cation chelation. Ca^{++} ions bind peptide units at these ends and act

as salt bridges for nanotube elongation (Ipsen et al., 2001). FT-IR spectroscopy provides facility for determination of interactions of Ca^{++} and Ca^{++}-binding proteins through the coordination of COO^- groups (Nara et al., 1994; Mizuguchi et al., 1997). COO^- groups of Asp and Glu side-chains assign bands at around 1400 and 1560/1580 cm-1 and due to Ca^{++} binding some shifts were detected at these sites. Absorption in amino acid side chains provides very valuable information about molecular reaction mechanisms and structural changes in proteins. FT-IR was used to detect conformational changes in the structure of α-La during hydrolysis and nanotube growth, in this study. In theory, the absorption of infrared radiation excites vibrational transition of molecules (Barth, 2007). Molecules absorb specific frequencies which are characteristic of their structures, called resonant frequency. The frequency of the absorbed radiation matches the frequency of the bond or group that vibrates through different modes such as symmetric and antisymmetric stretching vibrational modes. In proteins, amide modes are used to analyze polypeptide backbone vibrations (Barth, 2007). Amide A band between 3310-3270 cm^{-1} and amide B band between 3100 and 3030 cm^{-1} corresponds to NH stretching vibrations. Amide I band around 1650 cm^{-1}, arises mainly from C=O stretching vibrations; amide II band around 1550 cm^{-1} arises mainly from the combination of NH bending and CN stretching vibrations; and amide III mode in the region of 1400-1200 cm^{-1} from combination of NH bending and CN stretching vibrations. The amide I vibration is mostly used to analyze secondary structure in proteins, on account of this vibration is hardly affected by the nature of side chain depending on secondary structure of backbone (Krimm and Bandekar, 1986; Barth, 2007). Amide II and III bands also provide valuable structural information in proteins.

Partial hydrolysis leads to formation of peptides that are building blocks of nanotubes. Hence, analysis of these peptides was considered as an important key in understanding of nanotube formation. Mass spectrometry (MS) is an analytical technique measuring the mass-to-charge ratio of charged particles. It is used for determining masses of particles, for identification of the elemental composition of a sample or a molecule, and for elucidating the chemical structures of molecules, such as peptides and other chemical compounds. The MS principle consists of ionizing chemical compounds to generate charged molecules or molecule fragments and measuring their mass-to-charge ratios. It is an important method to characterize proteins. Different MS configurations, with changing ion source, detector type, etc., are

available for different applications. MALDI-TOF MS (Matrix-assisted laser desorption/ionization – time of flight**)** and ESI-MS (electrospray ionization) are used for proteins / peptides, especially. In MALDI-TOF MS, the ionization is triggered by a laser beam and a matrix is used to protect the biomolecule from being destroyed by direct laser beam and to facilitate vaporization and ionization.

In this chapter, the development and characterization of α-LaNTs from both commercial and purified α-La proteins are presented. The constructed nanotubular structures were visualized by microscopic techniques. The conformational changes in the secondary structure of α-La during the hydrolysis and nanotube formation were investigated by optical spectroscopy. Studies related to nanotube growth due to the effects of Ca^{++} and protein concentration and analysis of the protein hydrolysis prior to nanotube growth were also carried out.

6.2. Experimental

6.2.1. Materials

All chemicals and standards used in this work were purchased from Sigma Chemicals Co. (St. Louis, MO). *Bacillus licheniformis* protease (BLP) with an activity of 2.4 AU-A/g was kindly provided by Novozymes A/S (Bagsvaerd, Denmark). Low protein binding filters with 0.1 micron pore size were purchased from Millipore (Merck KGaA, Darmstadt, Germany). Copper grids were supplied by Electron Microscopy Sciences (USA).

6.2.2. Methods

Microscopic analysis of α-LaNTs developed by self-assembly was carried out by TEM, STEM and AFM. Optical characterization of α-La, α-La hydrolyzates and α-LaNTs was achieved by FT-IR and Raman Spectroscopy. Studies related to nanotube growth were performed by DLS and UV-VIS Spectrophotometry. Hydrolysis process was investigated by HPLC and MALDI-TOF MS.

6.2.2.1. Enzymatic Hydrolysis of α-La (sample preparation)

The formation of α-La nanotubes were achieved considering the procedure reported previously (Graveland-Bikker et al., 2004). Three percent (w/v) of α-La (Sigma L6010) was dissolved in 75 mM Tris-HCl, pH 7.5, and $CaCl_2$ with the ratio of 2:1 (mol Calcium: mol α-La), and 4 % BLP (w/w) were added. After mixing, the solution was filtered immediately through 0.1 micron low protein binding filter to remove impurities. Then the solution was incubated at 50 ºC for 1.5 h for enzymatic hydrolysis and nanotube development through self-assembly. At the end of the incubation, samples were stored at + 4 ºC for further analysis. For Raman and FTIR spectroscopy analysis, native α-La was prepared by dissolving in tris buffer, and α-La hydrolysates were prepared by limited proteolysis of protein with BLP (4% w/w).

Nanotube development was also investigated by the purified α-La proteins. Since purified fractions had already contained calcium, only protein and enzyme were mixed and incubated under the same conditions without calcium addition. Protein concentrations of purified ones were lower than the standard, approximately 1 % for WPI based α-La and 0.5 % for WPC based α-La. The enzyme ratio was kept as the same. At the end of the incubation, samples were stored at + 4 ºC for further analysis.

6.2.2.2. TEM Analysis

Samples for TEM measurements were taken from the reaction mixture at the end of the incubation and diluted as 1000 fold. Ten µl of sample was placed onto carbon coated copper grids and dried at RT or 37 ºC. Then, the structures were examined by TEM at 80 kV (FEI Technai Spirit, The Netherlands).

6.2.2.3. STEM Analysis

Samples for STEM were taken from reaction mixture at the end of incubation (1.5 h). It was diluted as 1000 fold and 10 µl of sample was placed onto carbon coated or non-coated copper grids and dried overnight at 37 ºC. Then, the structures were examined by SEM with STEM detector at 12 kV (FEI Quanta 250FEG, The Netherlands).

6.2.2.4. AFM Analysis

Samples for AFM were taken from the reaction mixture at the end of the incubation and diluted as 1000 fold. Ten µl of a sample was placed onto mica and/or glass surfaces. After drying for overnight at 37 ºC, the structures were examined by AFM (MMSPM Nanoscope IV, Veeco, USA). A silicon AFM cantilever (Veeco, USA) was used with the following properties, f_0: 330-359 kHz and k: 12-103 N/m.

6.2.2.5. Raman Spectroscopy Assay

A confocal Raman system (S&I Germany, based on Princeton Instruments, USA) was used to obtain the Raman data of α-La samples. Five to ten µl samples were dropped onto glass slides to be placed under the objective of an Olympus microscope which directs the selected laser beam (488nm argon ion laser, 120 mW power) onto the sample and collects the Raman signal. The signal is then sent to a monochromator (700 mm focal length, Princeton Instrument) to obtain the spectrum data which is recorded by a CCD camera. The data is then sent to the computer which controls the Raman system as well. Typical resolutions based on the chosen gratings in the monochromator (150, 600, or 1800 groves/mm) change from 1-10 $cm^{-1}$and the entrance slit width of mostly 100 µm is used. A typical Raman data is obtained as the average of 50 scans with one second accumulation each. Raman shifts were recorded in the Stokes side usually from 100 to 4000 cm^{-1} away from the Rayleigh line.

6.2.2.6. FT-IR Spectroscopy Assay

FT-IR measurements were carried out at room temperature by using a Perkin-Elmer Spectrum 100 FTIR Spectrometer (Perkin Elmer Inc., Wellesley, MA) equipped with a horizontal ATR sampling accessory (ZnSe crystal) and a deuterated tri-glycine sulfate (DTGS) detector. Nearly 100µl sample were placed onto a crystal surface and the measurements were taken in the range of 4000-600 cm^{-1}. The resolution was 4 cm^{-1} and 64 scans were recorded per each spectrum with a scan speed of 1 cm/sec. A background was recorded before each measurement. Deconvolution of the data was performed with the parameters, γ: 0.75 and L: 15 cm.

6.2.2.7. Dynamic Light Scattering Assay

DLS assays were carried out using a Malvern Nano ZS Nanosizer (England). The scattering angle was 173º and the laser wavelength was 633 nm. Samples were prepared as mentioned above and placed into instrument for incubation at 50 ºC. Intensity fluctuations were detected and collected through backscattered light. Software in the system calculated the particle size as follows: The intensity autocorrelation function was obtained from fluctuations in the intensity, then the autocorrelation function was fit with a second cumulant fit to obtain diffusion coefficient. An apparent hydrodynamic radius (because particles were linear, not spherical) was obtained from the Stokes-Einstein relation.

6.2.2.8. UV-Spectrophotometry Assay

UV-spectrophotometry assays were performed using Varioscan Flash (Thermo, USA). Samples prepared through desired calcium and protein concentrations and incubated in the instrument at 50 ºC. Measurements were taken at 633nm with 5 minute-intervals for 12 hours.

6.2.2.9. HPLC Analysis for Peptides

HPLC analysis was performed by using Perkin-Elmer HPLC (USA) system with Agilent ACE C18 column with dimensions of 150x4.6 mm. All the standard solutions and sample dilutions were prepared by 0.1% TFA (v/v, in water) which was the mobile phase used in the HPLC. The mobile phases are buffer A 0.1% TFA (v/v) in water, and buffer B 0.09% TFA (v/v) in acetonitrile-water (80:20) (v/v). Elution was carried out by the linear gradient program from 0 to 100 % B in 40 minutes and then returned to starting conditions in 5 minutes. The column temperature was maintained at 40°C and the flow rate was 1 ml/min with the injection volume of 20 µl.

6.2.2.10. MALDI-TOF MS Analysis for Peptides

MS spectra of the samples were taken by a Bruker MALDI-TOF MS system

(Germany). For the analysis, hydrolysis samples withdrawn from the reaction mixture at certain time intervals of incubation were added 0.1% TFA, to lower the pH and stop the enzyme activity (Otte et.al, 2004). DHB (2-, 5- dihydro benzoic acid) ve CHCA (alpha-cyano hydroxy cinnamic acid) mixture (2:1) was used as the matrix in the analysis. One µl of protein sample (1 %) was mixed with a 5 µl of matrix solution, DHB (2-, 5-dihydro benzoic acid) and CHCA (alpha-cyano hydroxy cinnamic acid) (3:2), and 2 µl of the mixture was spotted on the MALDI plate to dry for analysis. Masses were detected with the linear mode in the ranges between 5000-20000 Da.

6.2.3. Results and Discussion

6.2.3.1. Microscopic Analysis of α-Lactalbumin Nanotubes

Partial hydrolysis of α-La by BLP in the presence of Ca^{2+} ions resulted in the formation of nanotubular structures through self-assembly. TEM images of α-LaNTs formed by using standard protein were given in Figure 6.1. The observed structures were longer than 100 nm and about 20 nm in diameter. They seemed as regular strands with uniform morphology. The dimensions and morphologies of the structures showed consistency with related works in the literature (Ipsen et al., 2001; Graveland-Bikker et al., 2004).

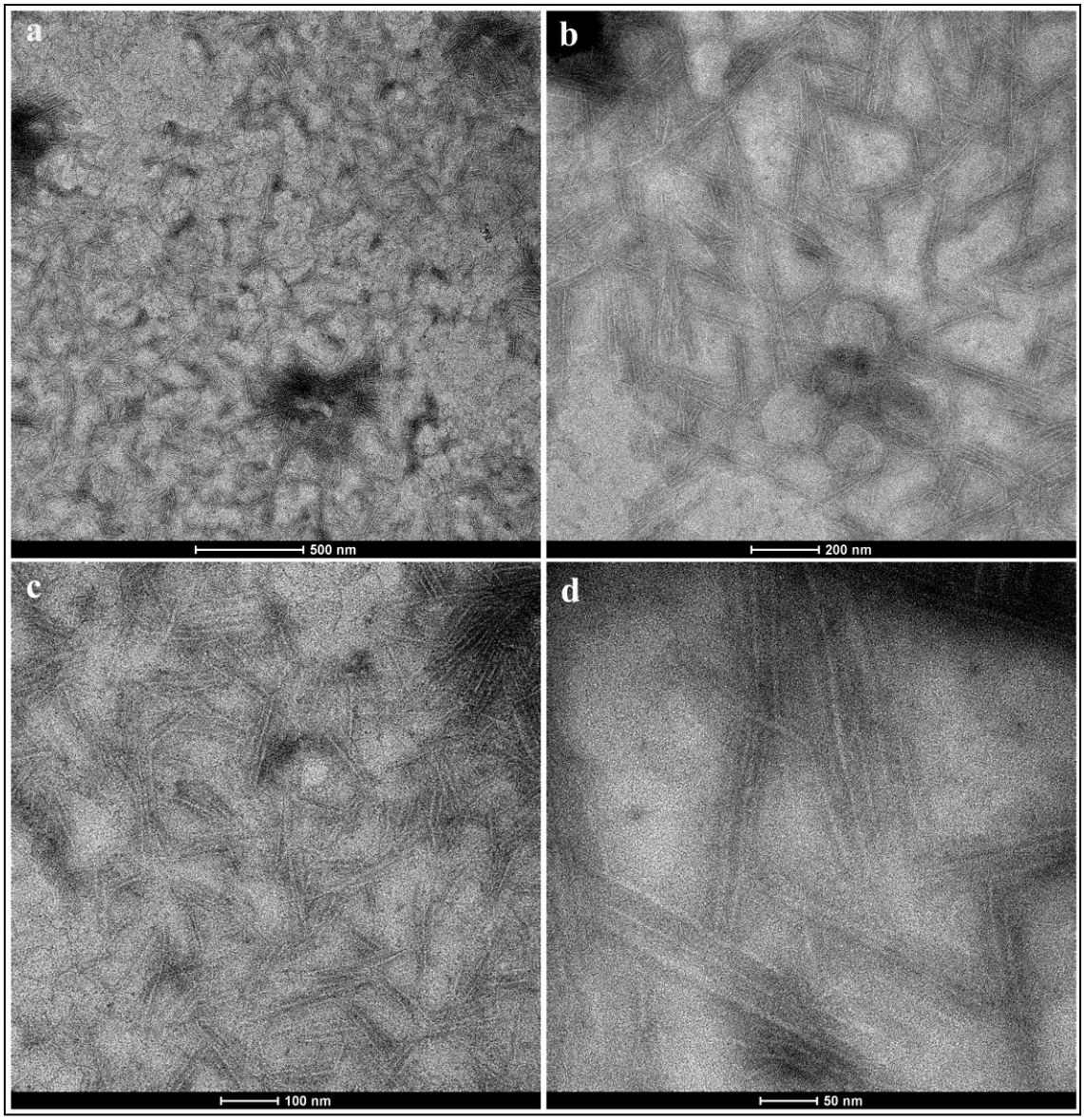

Figure 6.1. TEM images of α-LaNTs constructed from standard protein

The α-LaNTs were reported as hollow tubes in the literature (Graveland-Bikker and de Kruif, 2006). STEM observations given here agree with this. The electron beam transmitted through the hollow tubes and thus structures with brighter inner parts were captured (Figure 6.2). Also, interferences occurred at the points where the tubules crossover (Figure 6.2.b and c). Some tubules seemed as wider or thicker and this is supposed to be due to the attachment and/or overlapping of the strands (Figure 6.2.c). Typically, nanotubes were unbranched but occasionally, three-way junctions were also observed (Figure 6.2.d). These STEM images endorse TEM images of α-LaNTs.

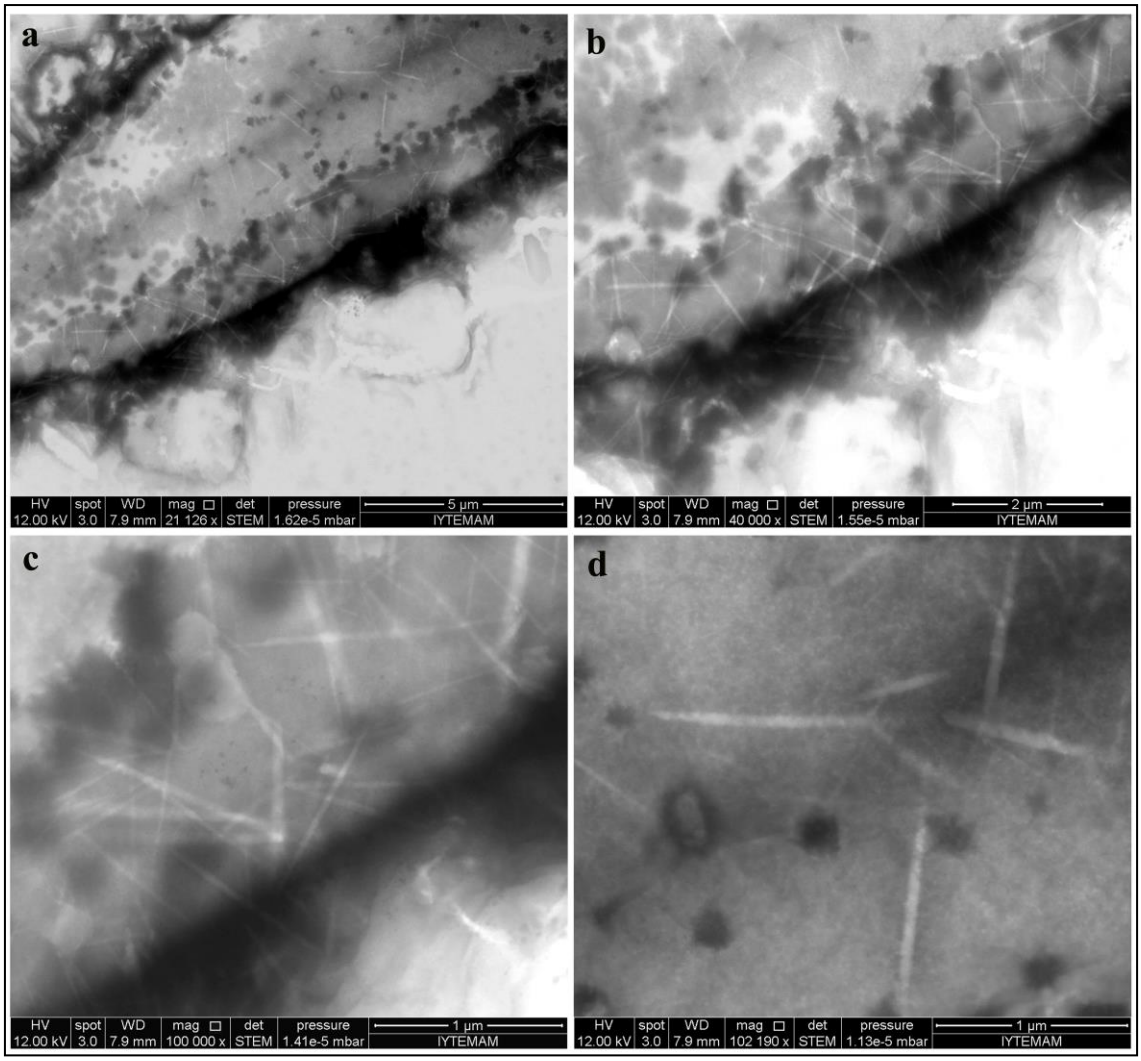

Figure 6.2. STEM images of α-LaNTs constructed from standard protein

Besides commercial standard of α-La, nanotubes were also formed by using purified proteins. Figure 6.3 and 6.4 presents STEM images of nanotubules obtained from WPI and WPC. Only few nano structures were detected in both. This is most probably due to low protein concentration of these samples. Black arrows on the images indicates nanostructures. Otte et al. (2005) reported that fibrillar structures with 5 nm width were formed when the protein concentration of α-La was 1 % due to aggregation of 8.8 kDa peptide fragments obtained by hydrolysis. Especially in the case of WPC based α-La, fibril formation might be induced mostly, instead of nanotube growth. AFM images given below were also support this.

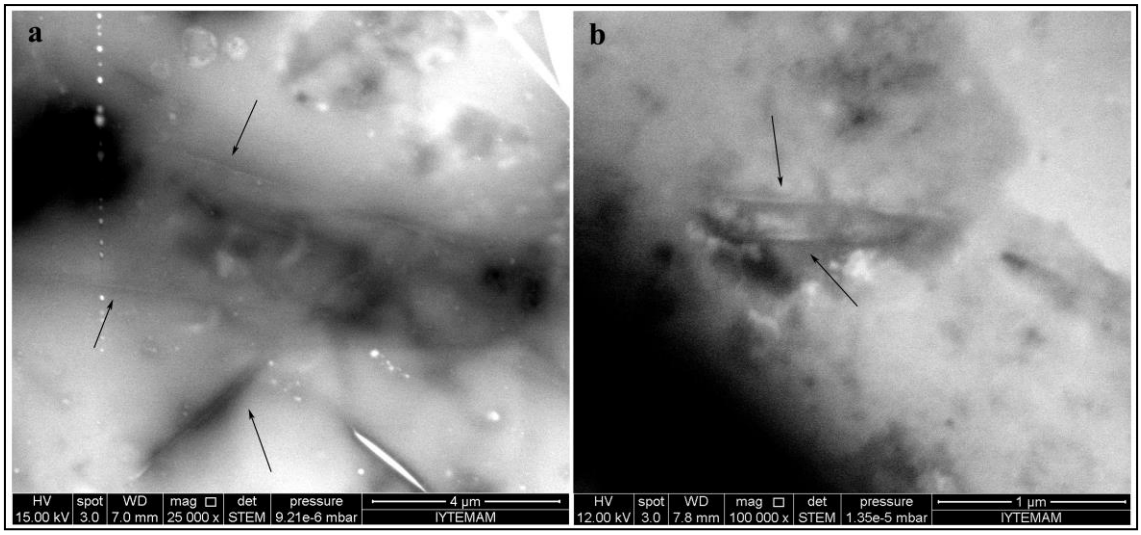

Figure 6.3. STEM images of α-LaNTs constructed from WPI based α-La (I-α-LaNTs)

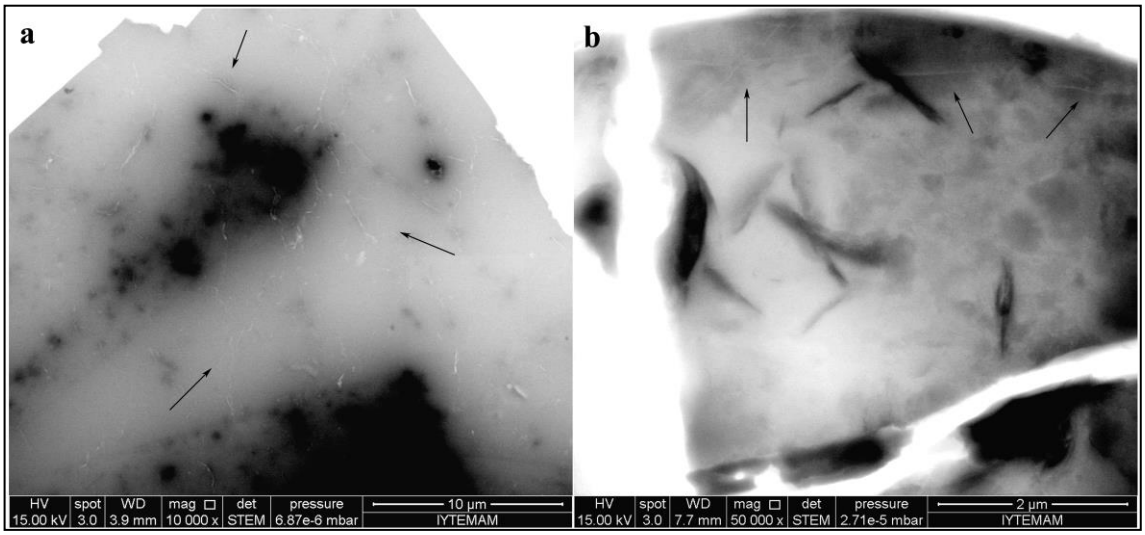

Figure 6.4. STEM images of α-LaNTs constructed from WPC based α-La (C-α-LaNTs)

Calcium ions added to medium act as brigde between peptides produced during hydrolysis and trigger nanotube formation (Ipsen and Otte, 2007). In order to test this, only α-La and BLP were mixed and incubated. Then the microscopic observations were performed to understand whether nanotubes were formed or not. It was seen clearly in figure 6.5 that, no nanotubular structures were obtained without addition of Ca^{2+} ions. This finding supports the crucial importance of Ca^{2+} ions when producing α-La nanotubes by self assembly process.

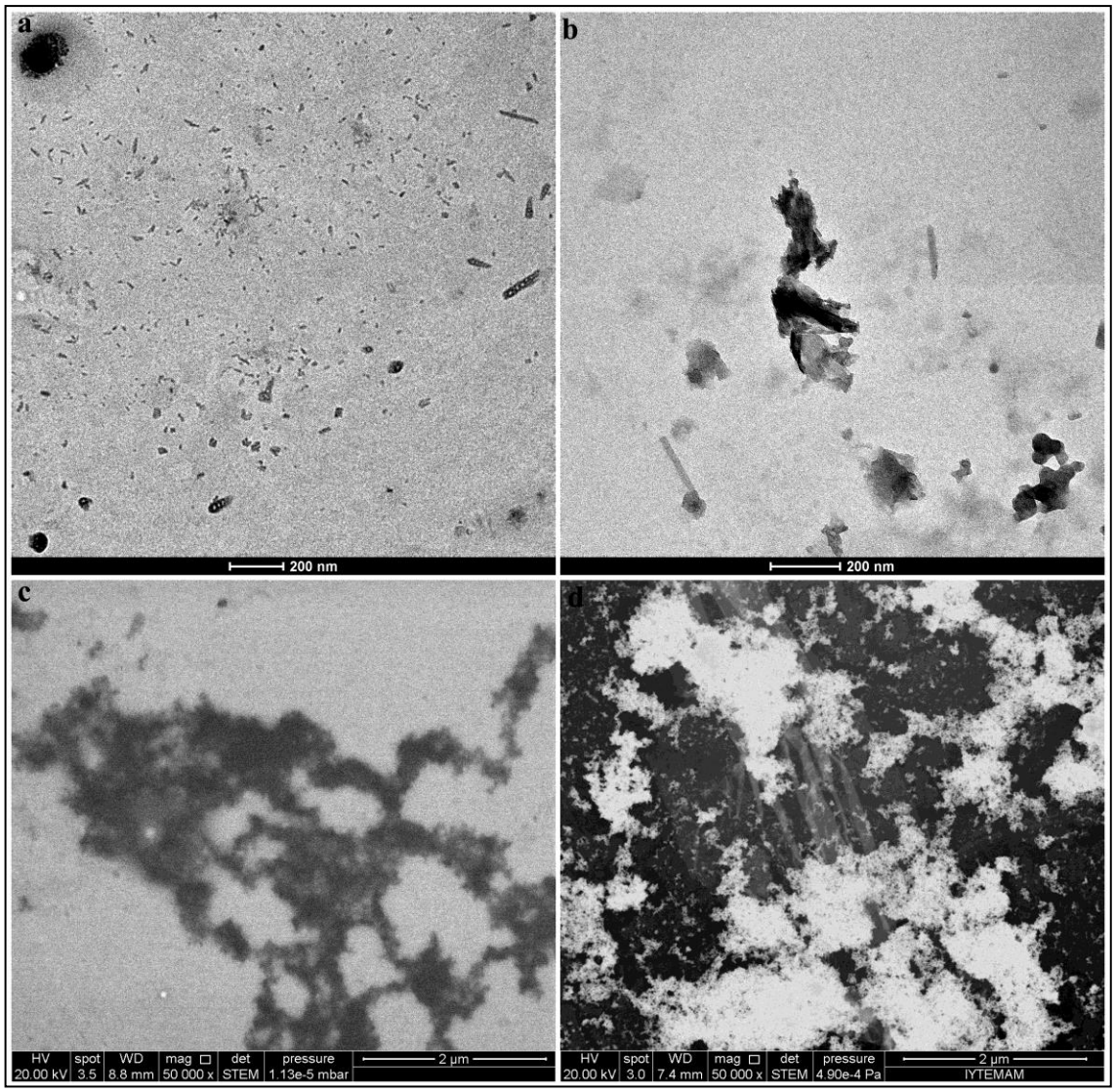

Figure 6.5. TEM (a, b) and STEM (c, d) images of α-La hydrolyzed by BLP

In addition to electron microscopy, α-LaNTs were also investigated by AFM. Figure 6.6 shows typical images of α-LaNTs prepared by molar Ca:α-La ratio of 2 (R=2) attached to a glass slide and Figure 6.7 shows α-LaNTs with Ca:α-La ratio of 5 (R=5) on a mica surface. Height, phase and surface plots were seen in Figure 6.6.a, b and c, respectively. Nanotubes were seened as attached to each other or joined end to end. The length of the linear tubules was as long as 1 micron or even longer. Apperantly, their diameters were in the range of 50-80 nm (mostly about 70 nm). Apparent width of α-LaNTs visualized by SFM (Scanning Force Microscopy) was reported as nearly 60 nm (Graveland-Bikker et al., 2006b). In fact the real nanotube dimensions, especially their widths are greater than that displayed by TEM/STEM

images. This arises from a lateral dilation caused by the force microscope tip with a nominal tip radius in between 48-52 nm.

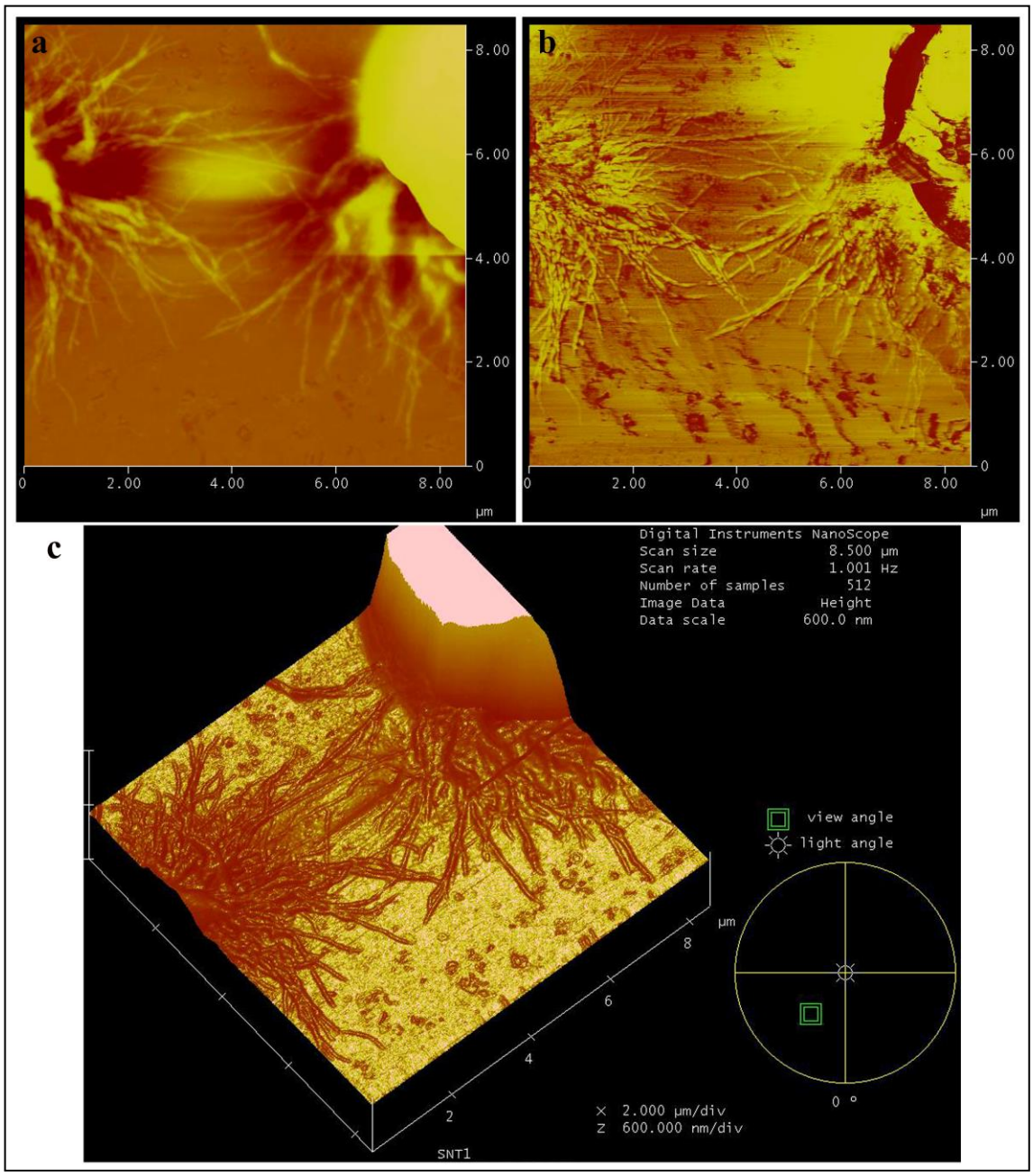

Figure 6.6. AFM images of α-LaNTs constructed from standard α-La protein with mol Ca^{++} / mol α-La (R): 3 a) height image; b) phase image; c) surface plot view

Dimensions and morphologies of the structures visualized by both techniques were in fact consistent. The nanotubes observed in the TEM/STEM images were seemed to be very regular linear rods; however those in the AFM images were seemed to be rough. TEM or other electron microscopes obtain images only in two dimensions

by sending electrons through the structures. However, AFM data are collected by tapping (or by contact mode) of a nanometer scale tip onto a surface in three dimensions, thus providing better information about the morphology. Actually, both are very sophisticated techniques for visualization of micro/nano structures.

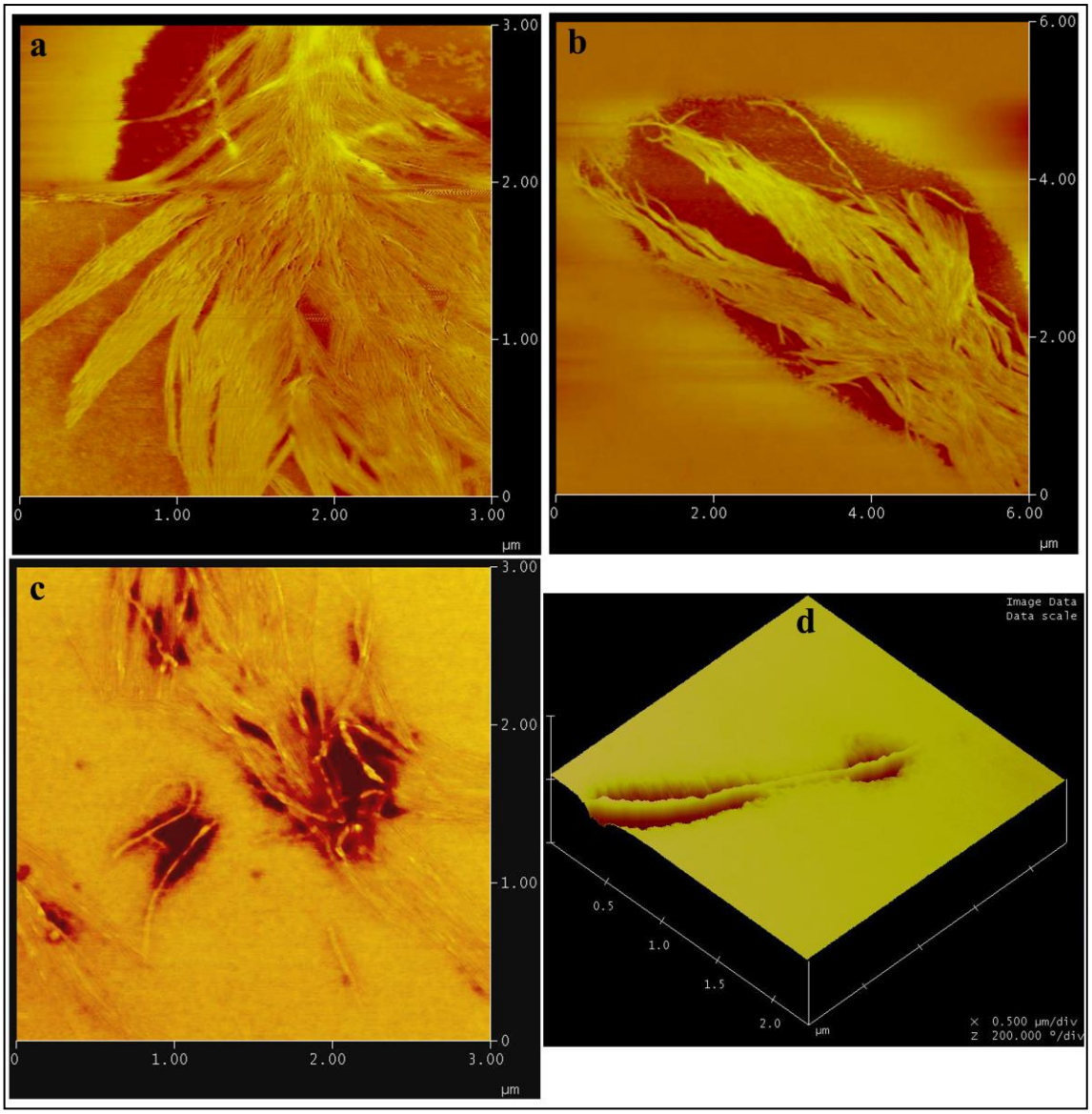

Figure 6.7. AFM images of α-LaNTs constructed from standard α-La protein with mol Ca^{++} / mol α-La (R): 5

Nanotubes in AFM images were nearly 1-2 µm or longer. In TEM images they seemed as more separately, but in AFM images they seemed as attached to each other or joined end to end mostly. Therefore, this may make difficult evaluation of their dimensions in AFM images. Dimensions could be detected better in TEM images. Nevertheless, when single structures in both images were considered, size distribution

could be given in a wider range, such as from 100 nm to one or few µm in length and 20 – 40 nm in diameter.

Besides commercial standard protein, nanotubes were also developed by purified α-lactalbumin. Figure 6.8 indicates AFM images of nanotubes formed by WPI-based α-La (Figure 6.8.a,b) and WPC-based α-La (Figure 6.8.c,d). When compared, I-α-LaNTs presented chain-like long tubular structures with a uniform width of about 20 nm, whereas C-α-LaNTs seemed as thinner fibrils leading to reticular structure.

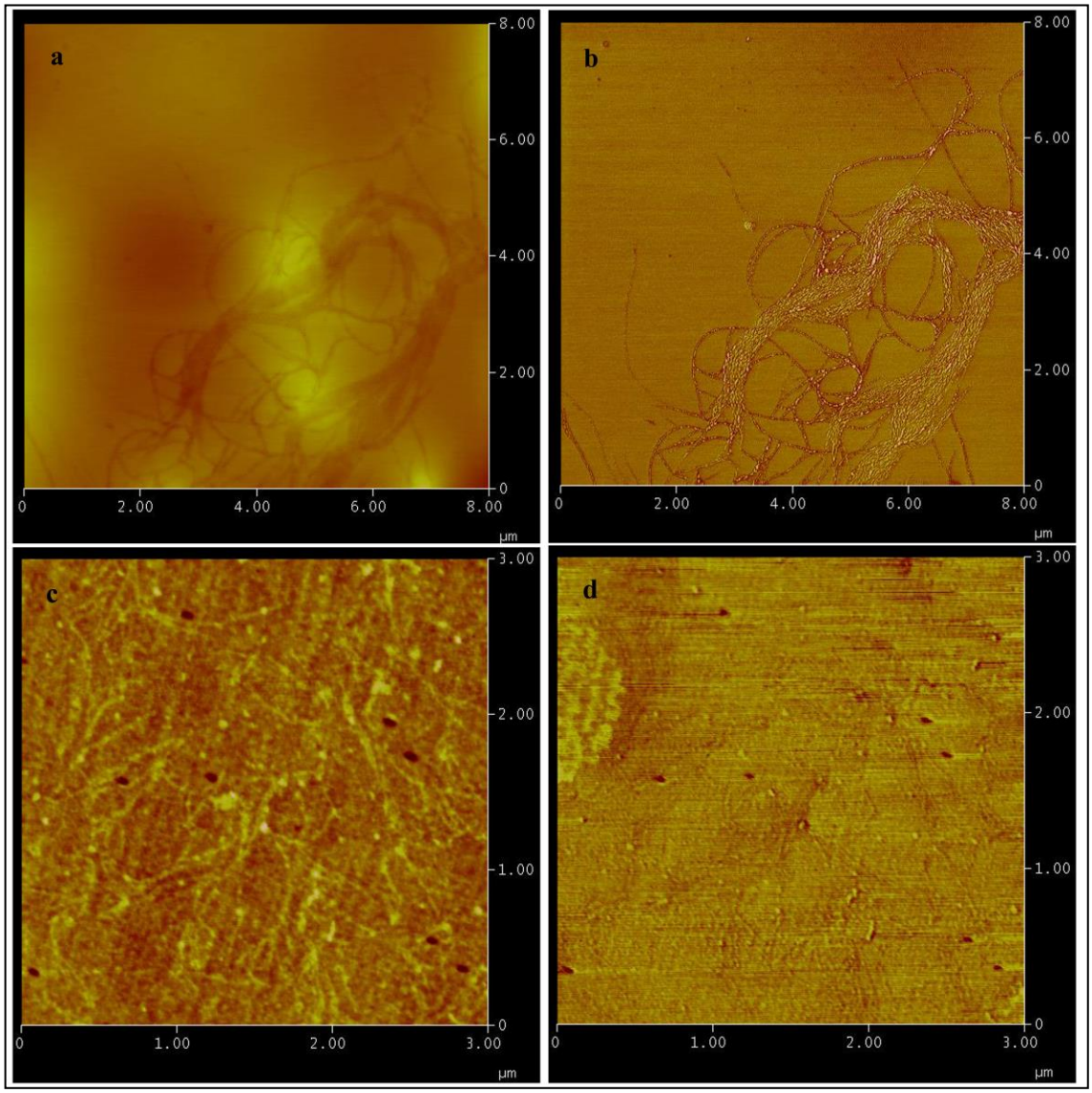

Figure 6.8. AFM images of α-LaNTs constructed from purified α-La protein a, b) I-α-LaNTs; c,d) C-α-LaNTs. a, c) Height images; b,d) Phase images

The α-LaNTs formed by standard α-La had the dimensions of 20 nm in width and one to few microns in length, approximately. Differently, the nanotubules constructed from I-α-La were longer and chain-like natively, this may lead to formation

of stronger network to be useful in application. Some studies related to applications of these nanotubes will be discussed in the next chapter.

6.2.3.2. Investigation of the Structure of α-Lactalbumin Nanotubes

Raman and FT-IR spectroscopy was used to determine the structural changes of α-La during hydrolysis and nanotube formation. Figure 6.9 represents Raman spectrum (250-1800 cm^{-1}) of α-La standard protein in 75mM Tris-HCl buffer, pH 7.5.

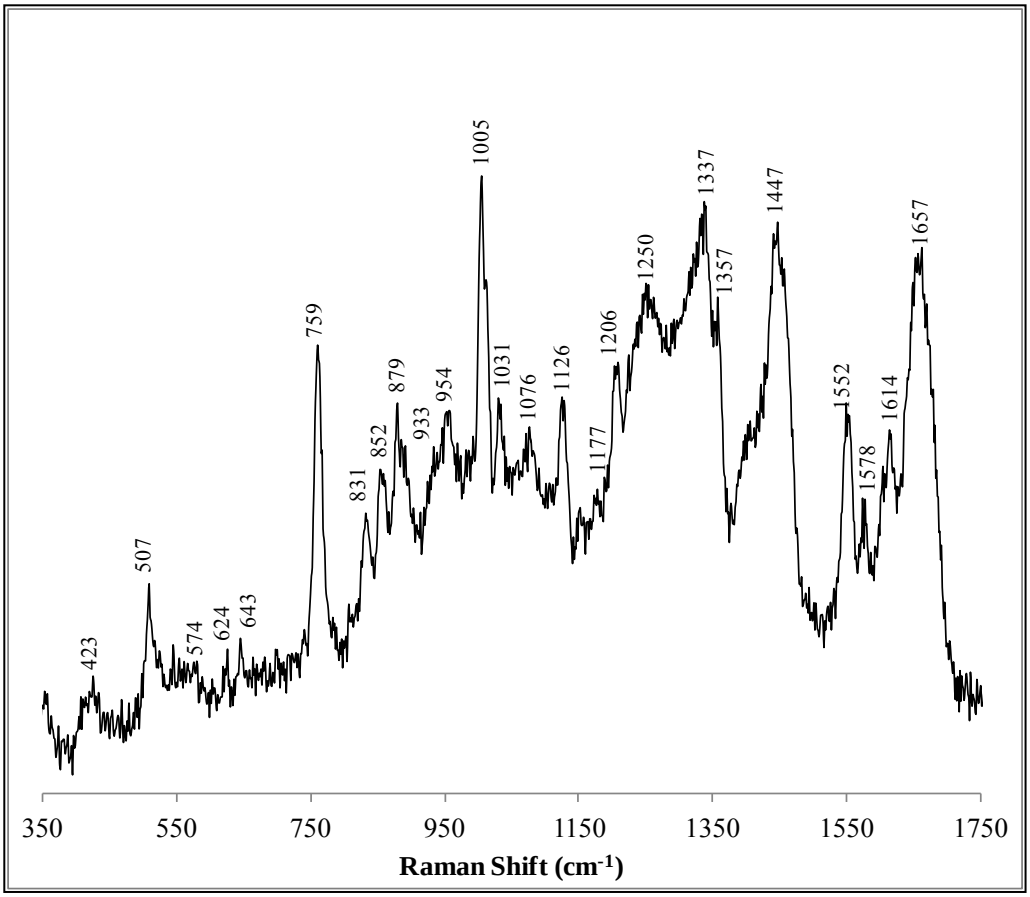

Figure 6.9. Raman spectrum of standard α-La protein in the range of 350-1750 cm^{-1}

Numerous bands were detected in spectrum as listed in table 6.1 with tentative assignments. Most of the detected peaks (Figure 6.9) correspond to molecules that of wavenumbers given in the table. Amide vibrational regions, especially amide I, amide III and backbone skeletal stretching regions are important in structural characterization of proteins. Rava and Spiro (1985) reported amide I region at 1654 cm^{-1}; amide II at

1555 cm^{-1} and amide III at 1250 cm^{-1}. In our study, they were detected as 1657, 1552 and 1250 cm^{-1}, respectively, in the range given by literature.

Table 6.1. Tentative assignments of major bands in Raman spectrum of a-La

wavenumber, cm^{-1}	**assignment**	**reference**
1662/1666	Amide I (β-sheet)	Miura and Thomas, 1995; Ashton and Blanch, 2010
1657	Amide I (α-helix)	Miura and Thomas, 1995; Ashton and Blanch, 2010
1614	Amide I (Tyr)	Rava and Spiro, 1984
1578	Trp	Ashton and Blanch, 2010
1552-1556	Amide II (Trp)	Miura et al., 1989; Ashton and Blanch, 2010
1447 / 1456	CH_2^{δ}	Nanoka et al., 1993
1357	Trp	Rava and Spiro, 1984
1337	Amide III (α-helix / Trp)	Lord and Yu, 1970; Ashton and Blanch, 2010
1328	Amide III (α-helix)	Ashton and Blanch, 2010
1250 / 1253 / 1254	Amide III (Polyproline helix II)	Miura and Thomas, 1995; Ashton and Blanch, 2010
1210	Tyr & Phe	Nanoka et al., 1993
1177	Tyr & Phe	Lord and Yu, 1970; Ashton and Blanch, 2010
1152	$C\text{-}N^{\gamma}$	Nanoka et al., 1993
1126	Trp, CH_3^{δ}	Ashton and Blanch, 2010
1075	sheet interaction$^{\gamma}$	Ashton and Blanch, 2010
1030 / 1005	Phe	Nanoka et al., 1993; Ikeda and Chen, 2004
954	disordered$^{\gamma}$	Ashton and Blanch, 2010
933	α-helix$^{\gamma}$	Ashton and Blanch, 2010
879	Trp	Nanoka et al., 1993
853 / 831	Tyr Fermi Doublet	Nanoka et al., 1993; Ashton and Blanch, 2010
759	Trp	Nanoka et al., 1993
643	C-S (g-g-g)$^{\zeta}$	Nanoka et al., 1993
624	Phe	Nanoka et al., 1993
574	Trp	Nanoka et al., 1993
507	S-S (g-g-g)$^{\zeta}$	Nanoka et al., 1993; Ikeda and Chen, 2004

$^{\nu}$ backbone skeletal stretch, $^{\delta}$ deformation mode, $^{\zeta}$ gauche-gauche-gauche conformation

Figure 6.10 shows typical Raman spectra of standard α-La protein, its hydrolysates and α-La nanotubes. Backbone skeletal region, amide III and amide I regions were presented more closely in Figure 6.11. The spectra belonging to protein and hydrolyzate gels were similar, however that of nanotubes differs. Some shifts were observed, some bands were Raman allowed, where some were lost in nanotube spectrum.

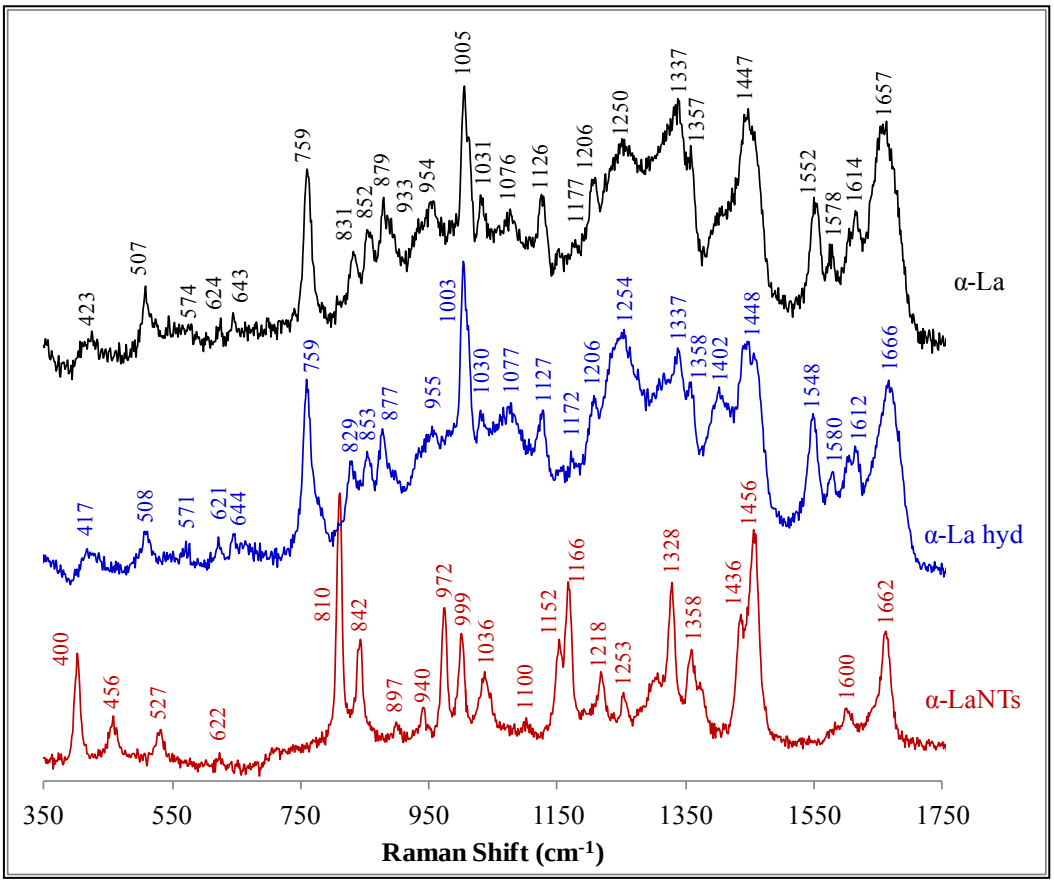

Figure 6.10. Raman spectra of α-La, α-La-hydrolyzates and α-LaNTs (standard protein)

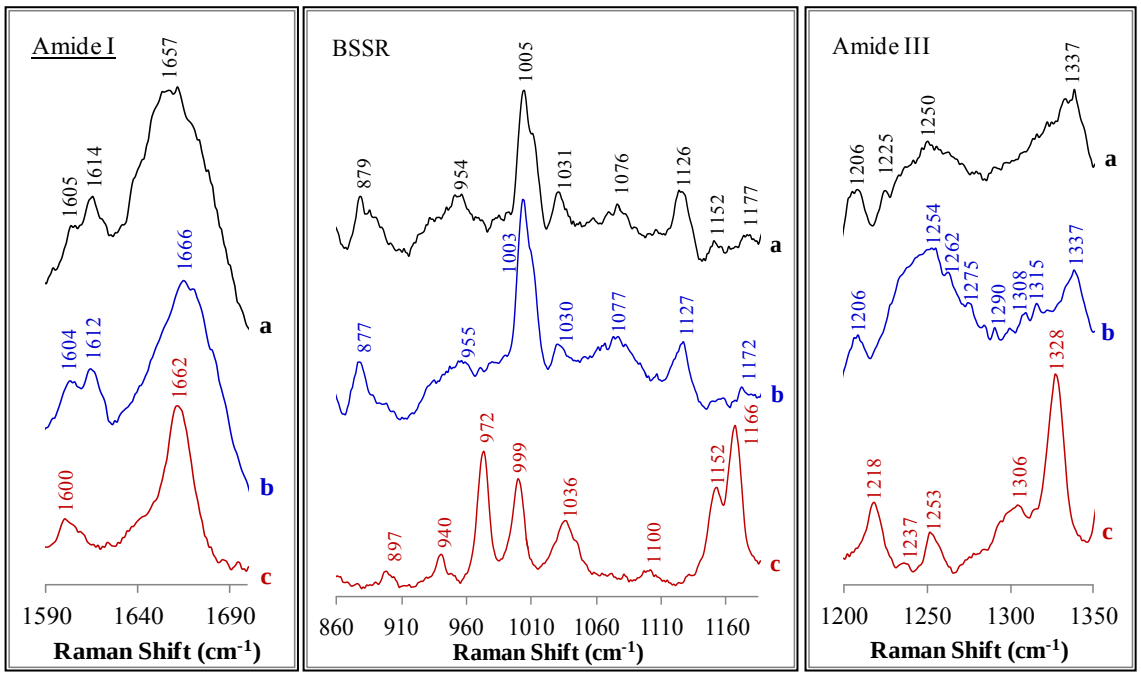

Figure 6.11. Smoothed Raman spectra of amide I, III and BSSR (backbone skeletal stretch region) regions a) α-La, b) α-La hydrolysates and c) α-LaNTs (smoothing achieved by taking average of three neighboring data)

For native α-La, amide I region indicated a large loop containing α-helix, β-sheet and disordered structures with the assignments between 1645-1680 cm^{-1} (Figure 6.9, 6.10, 6.11). This broad band is centered at 1657 cm^{-1} corresponding to a mainly helical structure mainly (Figure 6.11). In the hydrolysates, β-sheet became dominant as evident by the band at 1666 cm^{-1} (Miura and Thomas, 1995; Ashton and Blanch, 2010). The band observed at 1402 cm^{-1}, indicating a symmetric carboxylate stretch, in the hydrolysate spectrum is probably due to the exposure of free COO- groups at the digested Asp and Glu sites during the hydrolysis (Figure 6.10). No peaks at this region were seen in the nanotube spectrum. This is because the peptides are linked by Ca^{2+} ions at these COO- sites through nanotube elongation. Raman spectrum of the nanotubes exhibited stark differences from that of α-La and hydrolysates. Most probably, this is due to a novel conformational arrangement of peptides to form nanotubes. In that case, some bands become Raman active, while some others become Raman inactive. Besides, various shifts and intensity changes are also possible. Conformation-sensitive amide I region was seen near 1662 cm^{-1} with a narrower peak and reduced intensity in the nanotube spectrum. However, the bands at ~1578 cm^{-1} and 1552 cm^{-1}, representing the trptophan side chain in the amide II region was disappeared (Figure 6.10). Tryptophan band at ~1357 cm^{-1} gained intensity and sharpness in the nanotube spectrum. The other conformational-sensitive region, amide III, was detected in the region between ~1218 and 1337 cm^{-1} (Figure 6.11). Tryptophan band seen at 1337 cm^{-1} in native α-La lost intensity in hydrolysate spectrum. However, in the case of nanotubes two possibilities could be considered. This band might shift to 1328 cm^{-1} (about 11 cm^{-1}) and become sharper, or the peak at 1337 cm^{-1} become inactive and a new peak at 1328 cm^{-1} arises from the stretching of new bonds formed during nanotube formation. This band is assigned to 3_{10} helix or to residues having local order like that of 3_{10} helix at the ends of α- helices or in loops (Wilson et al., 1995; Blanch et al., 2000). The α-LaNTs occurs via β-sheet stacking, leading to 10-start right handed-helix (Graveland-Bikker et al., 2009). The presence of a band around 1310 cm^{-1} in hydrolysate (1308, 1315 cm^{-1}) and nanotube (1306 cm^{-1}) spectrum is attributed to α-helix structure (Spiro and Gaber, 1977). A broad band, assigned as polyproline II-helix, centered at 1250 cm^{-1} in α-La spectrum shifted to 1254 cm^{-1} in hydrolysate gels with an increased intensity and to 1253 cm^{-1} in nanotubes with a decreased intensity. Also intensity gains at 1262, 1275, 1290, 1308, and 1315 cm^{-1} are attributed to the increase in the number of α-helix and disordered structures in hydrolysates due to hydrolysis and gel formation (Ikeda and Li-

Chan, 2004). Additionally, the band at 1225 cm^{-1} detected in protein was disappeared in hydrolysates and nanotubes while, a new sharp band was appeared at 1218 cm^{-1} and a weak band at ~1237 cm^{-1} were detected in nanotubes. The bands at ~1230-1245 cm^{-1} are assigned as β-sheet structures (Miura and Thomas, 1995). Also, one at 1218 cm^{-1} could appear to be a distinct variant of β-strand or sheet (Barron et al., 2002). Tyrosine and phenyalanine peaks at ~1206 cm^{-1} were also dissappered in nanotubes. The weak tyrosine and phenylalanine bands at ~1177 cm^{-1} gained a little intensity in hydrolysates, but in nanotubes, they shifted to 1166 cm^{-1} with significantly increased intensity or this band disappeared and a new sharp band was born due to stretching of new bonds. Another conformation-sensitive region with backbone skeletal stretchings showed considerable changes especially in the nanotube spectrum. The weak peak at 1152 cm^{-1}, originating mainly from C-N stretchings (Nonaka et al., 1993) appeared with an intensity loss in the hydrolysate gels, but with a significant intensity gain in the nanotubes. Tryptophan band at ~1126 cm^{-1} was also detected in hydrolysates with a small intensity change, but it was disappeared in the nanotubes. The band attributed to the backbone skeletal stretch at ~1076 cm^{-1} was gained a little intensity in the hydrolysates and became inactive in the nanotubes also. Phenylalanine peaks at ~1031 and 1005 cm^{-1} were expected to shift to 1036 and 999 cm^{-1} with considerable changes in their intensities. A new peak was detected at 972 cm^{-1} in the nanotube spectrum. The bands at ~954 cm^{-1} (assigned as disordered structures), ~879 cm^{-1} (tryptophan), ~831/852 cm^{-1} (tyrosine Fermi doublet) were also detected in the hydrolysate spectrum with small shifts and intensity changes. Hovewer, they were disappeared in the nanotube spectrum which exhibited new bands at 940, 897, 842 and 810 cm^{-1}. A distinct trp band at 759 cm^{-1} became Raman inactive in the nanotube spectrum. The band around 507 cm^{-1} is assigned as disulfide bonds in gauche-gauche-gauche conformation, minor bands at around 525 and 540 cm^{-1} are assigned as those in gauche-gauche-trans and trans-gauche-trans conformations, respectively (Nakanishi et al., 1974; Kitagawa et al., 1979). S-S peak in native α-La at 507 cm^{-1} was also observed in hydrolysates with a decreased intensity and as a broader band, however the minor band at ~542 cm^{-1} was disappeared. Nanoka and coworkers studied the structure of α-La gels with Raman spectroscopy and reported that conformation of S-S bonds was altered in the native α-La after heating at 90ºC (Nanoka et al., 1993). A similarly taken data may show the loss of native forms of disulfide bonds by the alteration of conformation due to hydrolysis and gelation. The band representing disulfide bonds was detected at 527 cm^{-1}, instead at

~507 cm^{-1} in nanotube spectrum by suggesting dominant gauche-gauche-trans conformation, which is most probably arised from a rearrangement of peptides in the nanotubes. Actually, it is reported in the literature that (from the CD-spectra analysis) the secondary structure of the α-La is largely retained during nanotube formation (Graveland-Bikker et al., 2009). Our findings support this, but remarkable conformational changes were observed in nanotube structure due to rearrangement of the structural elements.

The Raman spectra of purified proteins and nanotubes developed by using them were given in Figure 6.12. It is well-known that, α-La is a cation-binding protein. The mineral content of the purified α-La samples was natively higher than that of standard. Therefore, some peaks might not be allowed to observe intensively due to cation chelation.

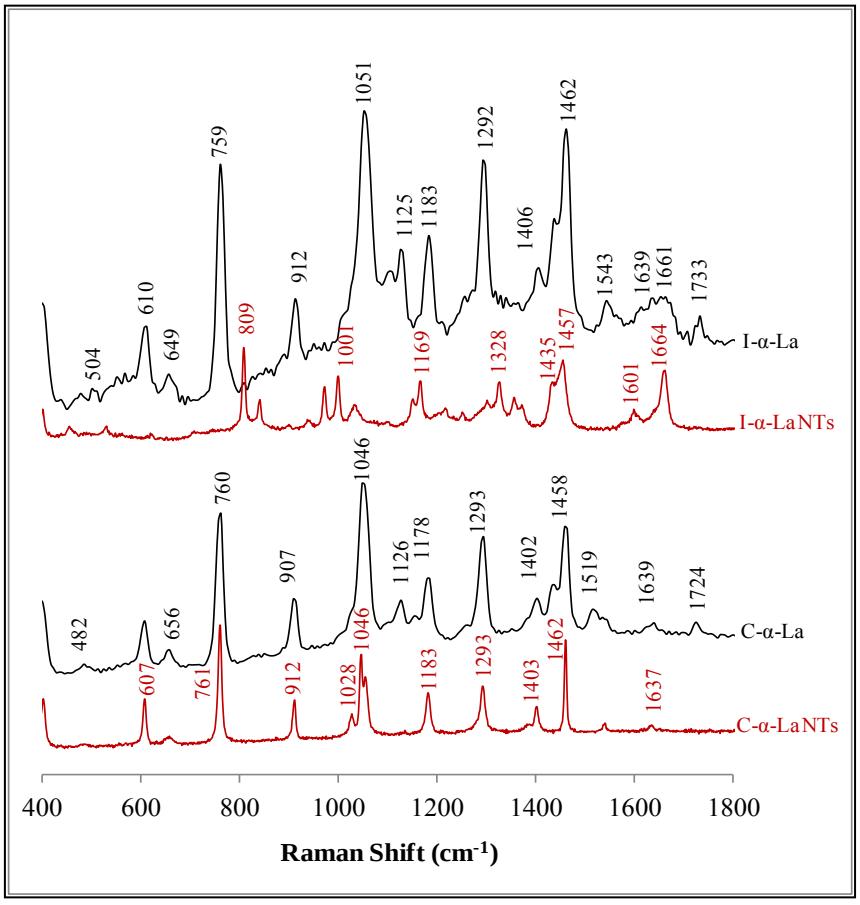

Figure 6.12. Raman spectra of the purified α-La proteins and the nanotubes constructed using them.

The spectrum of nanotubes of WPI-based α-La is almost the same with that of standard protein. However, the spectrum of WPC-based α-LaNTs was differred

significantly. In fact, the nanostructures developed from I-α-La and C-α-La were obviously different according to microscopic observations. It can be concluded that the nanotubes constructed from standard α-La and WPI-based α-La posseses identical conformation of secondary structure elements. In WPC-based nanostructures different conformations may occur.

FT-IR spectroscopy was also carried out for a better evaluation of structural changes of α-La during the hydrolysis and nanotube formation. Figure 6.13 represents Fourier-self deconvolved infrared spectra of α-La protein, α-La hydrolysates and α-La nanotubes, where the tris buffer spectra were subtracted. Enlarged amide regions are also given in Figure 6.14. In each spectrum, four broad regions are observed. They are assigned as: amide I band at ~1649 cm^{-1}, the COO^- antisymmetric stretching bands at about 1580 / 1558 cm^{-1} overlapping with amide II band at ~1550 cm^{-1}, CH_2 bending vibration band at ~1460 cm^{-1}, and the COO^- symmetric stretching band at around 1400 cm^{-1} (Figure 6.13).

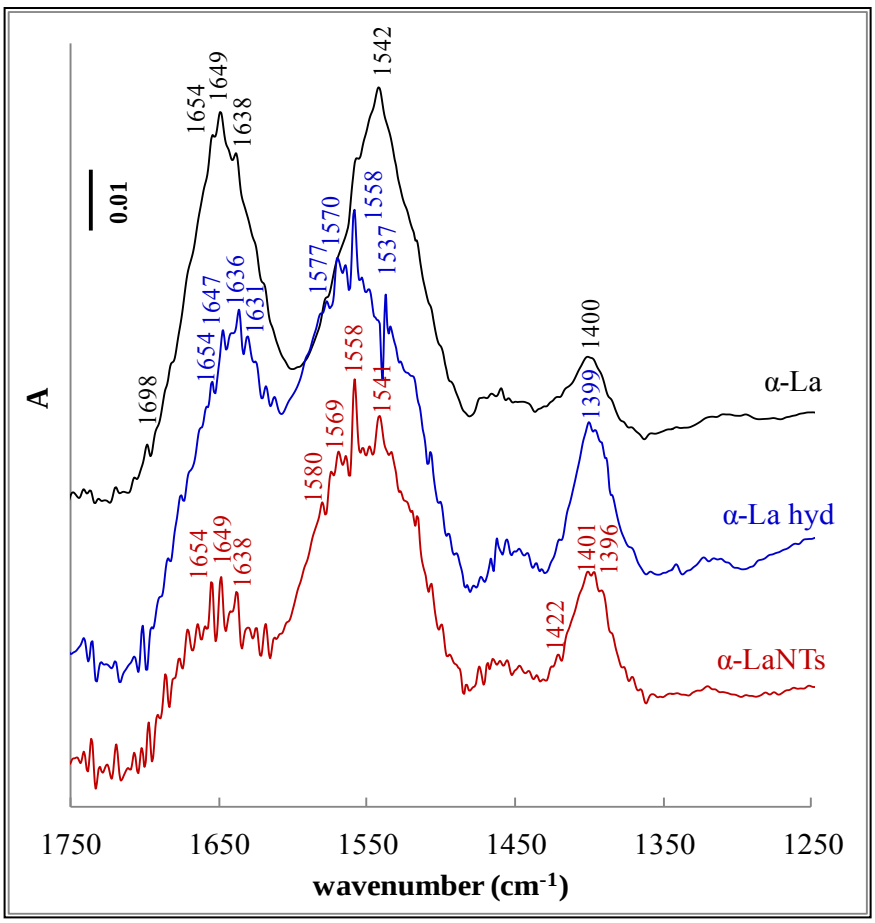

Figure 6.13. Fourier-self deconvolved spectra of standard protein of α-La, α-La hydrolysates, and α-LaNTs

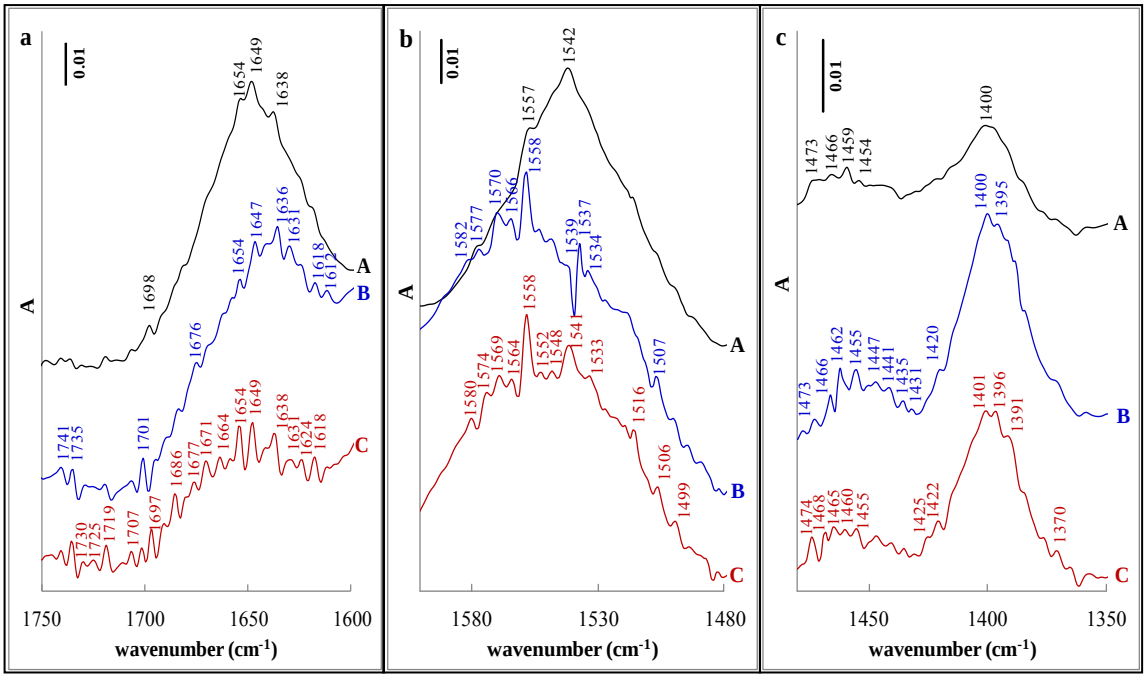

Figure 6.14. Fourier-self deconvolved spectra enlarged in the regions of a) 1715-1600 cm^{-1}; b) 1600-1480 cm^{-1}; c) 1480-1350 cm^{-1}. A) α-La, B) α-La hydrolysates and C) α-LaNTs

Numerous peaks were observed in each spectrum. Table 6.2 lists assignments of major peaks and Table 6.3 lists infrared bands of Asp and Glu side chains.

Table 6.2. Tentative assignments of major bands in FT-IR spectrum of a-La

wavenumber, cm^{-1}	amide mode	assignment	references
1688-1698	Amide I (1610-1700 cm^{-1})	β-sheet	Kong and Yu, 2007
1667-1687		β-turns	Kong and Yu, 2007
1660-1670		3_{10} helix	Jackson and Mantasch, 1995
1646-1658		α-helix/random	Jackson and Mantasch, 1995; Kong and Yu, 2007
1620-1642		β-sheet	Jackson and Mantasch, 1995; Kong and Yu, 2007
1610-1628		aggregated strands	Jackson and Mantasch, 1995
1545-1551	Amide II (1520-1560 cm^{-1})	α-helix	Ambrose and Elliot, 1951; Jackson and Mantasch, 1995
1521-1525		β-sheet	Ambrose and Elliot, 1951; Jackson and Mantasch, 1995
1260-1315	Amide III (1220-1330 cm^{-1})	α-helix	Anderle and Mendelsohn, 1987
1245-1270		random coils	Anderle and Mendelsohn, 1987; Xie and Liu, 2004
1220-1250		β-sheet	Anderle and Mendelsohn, 1987; Xie and Liu, 2005

Native α-La consists α-helix, β-sheet and random structures evident by the bands at 1698/1638 cm^{-1} and 1654/1649 cm^{-1}. When hydrolyzed, the amide I peak intensity decreased slightly, and β-sheets and turns become dominant which is evident from the new peaks detected between 1612 and 1636 cm^{-1}, and 1676/1701 cm^{-1} (Figure 6.14.a).

In case of the nanotubes, band intensities decreased significantly and numerous new peaks attributed to all secondary structure elements were appeared. They are at around 1618-1638 cm^{-1} (β-sheets/aggregated strands), 1664-1686 cm^{-1} (β-turns), 1697-1702 cm^{-1} (β-sheets). Two possibilities may be considered for this striking intensity loss in the case of the nanotubes: the decrease in the number of bonds giving the corresponding bands displayed in the native protein, and/or the decrease in the activities of these infra red-active bands of the native protein. After the tertiary structure of α-La was disturbed due to the hydrolysis, a new arrangement of peptides for nanotube formation may have caused an increase in the amount of exposed β-sheets, turns and helix structures.

Table 6.3. Asp and Glu acid side chain infrared bands*

assignments	band position, cm^{-1}	stretching
Asp	1716	ν (C=O)
	1574-1579	ν_{as} (COO^-)
	1402	ν_{s} (COO^-)
	1264-1450	δ(COH)
	1160-1253	ν (C-O)
Glu	1712	ν (C=O)
	1556-1560	ν_{as} (COO^-)
	1404	ν_{s} (COO^-)
	1264-1450	δ(COH)
	1160-1253	ν (C-O)

*taken from Barth et al. 2007. ν: stretching vibration, ν_{as}: antisymmetric stretching vibration , ν_s: symmetric stretching vibration, δ: in plane bending vibration

During hydrolysis of α-La, BLP digests the protein at aspartic (Asp) and glutamic (Glu) acid sites. Carboxy moiety released at Asp and Glu sites available for cation chelation give infrared bands at 1574-1579 cm^{-1} and 1404 cm^{-1} (for Asp), and 1556-1560 cm^{-1} and 1402 cm^{-1} (for Glu) (Barth, 2007). Mizuguchi and coworkers examined the relationship between the type of coordination and the stretching of COO^- groups in the Ca^{2+} binding site of bovine α-La (Mizuguchi et al., 1997). They reported that both Ca^{2+} free and Ca^{2+} binded α-La showed two major bands at 1588 and 1578 cm^{-1} in COO^- antisymmetric stretching region with lower intensity in the free form. Also, Ca^{2+} binding resulted in the shift at the peak arround 1400 cm^{-1} with splitting two components, 1403 and 1425 cm^{-1} by gaining intensity, through binding of Ca^{2+} to the

COO^- groups in the high affinity binding site. Similarly, in our study, the single band at 1400 cm^{-1} in the native a-La appeared as three bands at 1420, 1400 and 1395 cm^{-1} in hydrolysates by gaining significant intensities (Figure 6.14.c). In nanotube spectrum, these were detected with a very small shift (~1-2 cm^{-1}) and intensity greater than α-La and lower than hydrolysates. Also a shoulder type bands at 1425 and 1391 cm^{-1} were appeared. During hydrolysis, this high affinity calcium binding site should also be exposed, thus giving rise to the intensity increase; however, by the nanotube elongation Ca^{2+} ions link the peptides, thus fewer free sites are left and which is seen as a decrease in the intensity. Smaller intensity changes were detected in the amide II region, for the three protein samples, compared to amide I region. In the hydrolysates, the band at 1542 cm^{-1} were lost and two new peaks were appeared at 1537 and 1534 cm^{-1}, whereas in the nanotubes the band at 1541 cm^{-1} retained with lower intensity, and a new band detected at 1533 cm^{-1} (Figure 8b). The other calcium binding site (belonging to of Glu) at 1558 cm^{-1} gained much intensity in both hydrolysates and nanotubes. Two more signals appeared at 1577 and 1582 cm^{-1}, and 1574 and 1580 cm^{-1} in the hydrolysate and nanotube spectra, respectively, due to another calcium binding site of aspartic acid. The broad weak band centered at ~1460 cm^{-1} in protein gained intensity in both hydrolysates and nanotubes. In addition, numerous features were observed between 1431 and 1474 cm^{-1} arising from C-H bending vibrations (Barth, 2007).

Figure 6.15 presents FT-IR spectra of both standard and purified α-La proteins, and nanotubes formed from each of them. In amide I region, the peaks at 1620 (I-α-La) and 1617 (C-α-La) cm^{-1} became dominant in purified protein samples when compared to standard protein (Figure 6.15.a). A shift was also detected in amide II region, at 1531 cm^{-1}. However, nanotubes of these purified protein samples mostly provided identical spectra with those of standard protein (Figure 6.15.b). Although smaller shifts, they confirmed nanotube spectrum in general.

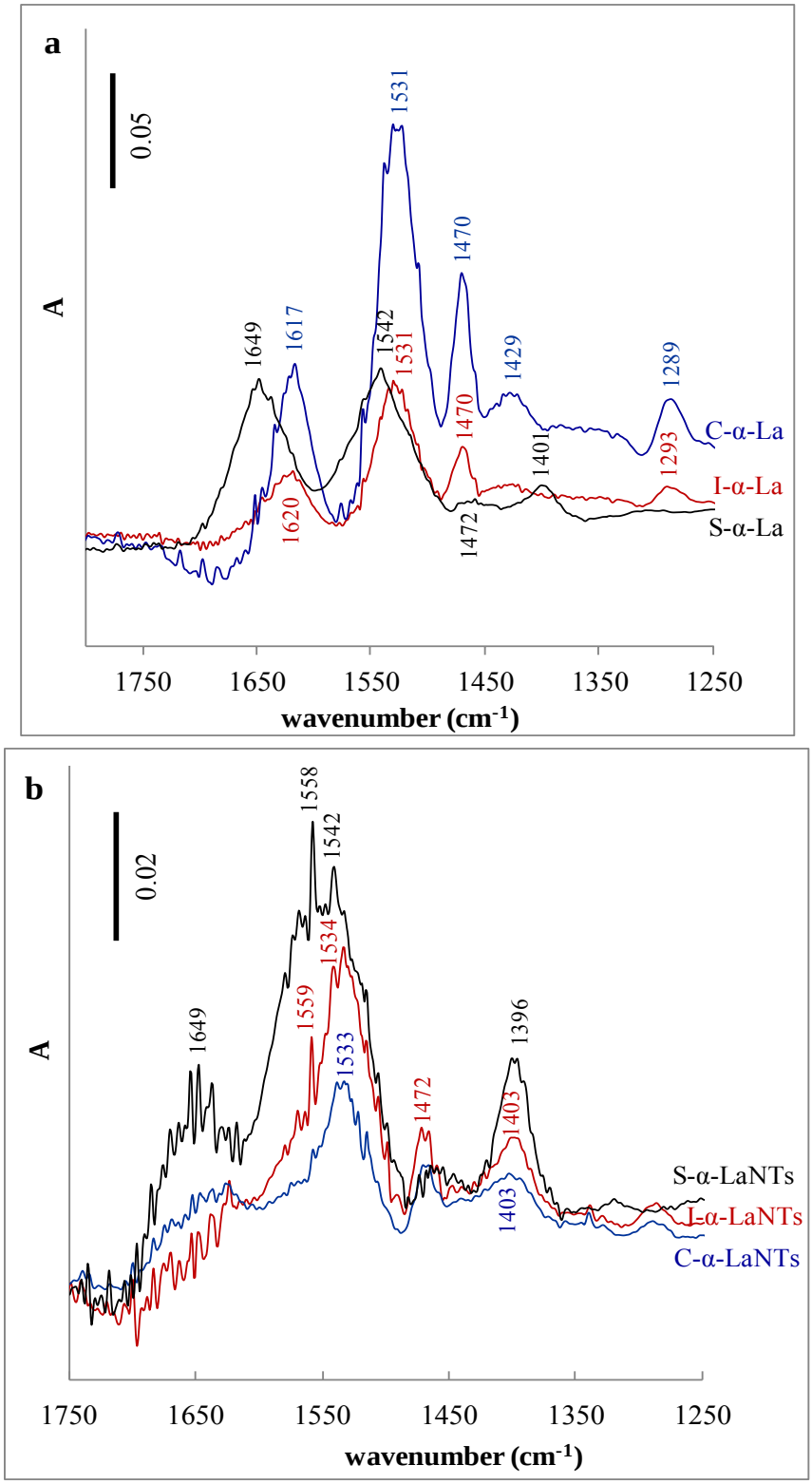

Figure 6.15. Fourier-self deconvolved spectra of a) standard (S-α-La) and purified (I-α-La, C-α-La) α-La proteins, and b) nanotubes constructed from standard (S-α-LaNTs) and purified (I-α-LaNTs and C-α-LaNTs) α-La proteins

6.2.3.3. Analysis of the Nanotube Growth

DLS and UV-spectrophotometry studies were carried out to investigate the growth of α-La nanotubes. Figure 6.16 indicates scattering intensity and particle size differences of the samples during incubation period leading to hydrolysis and nanotube growth.

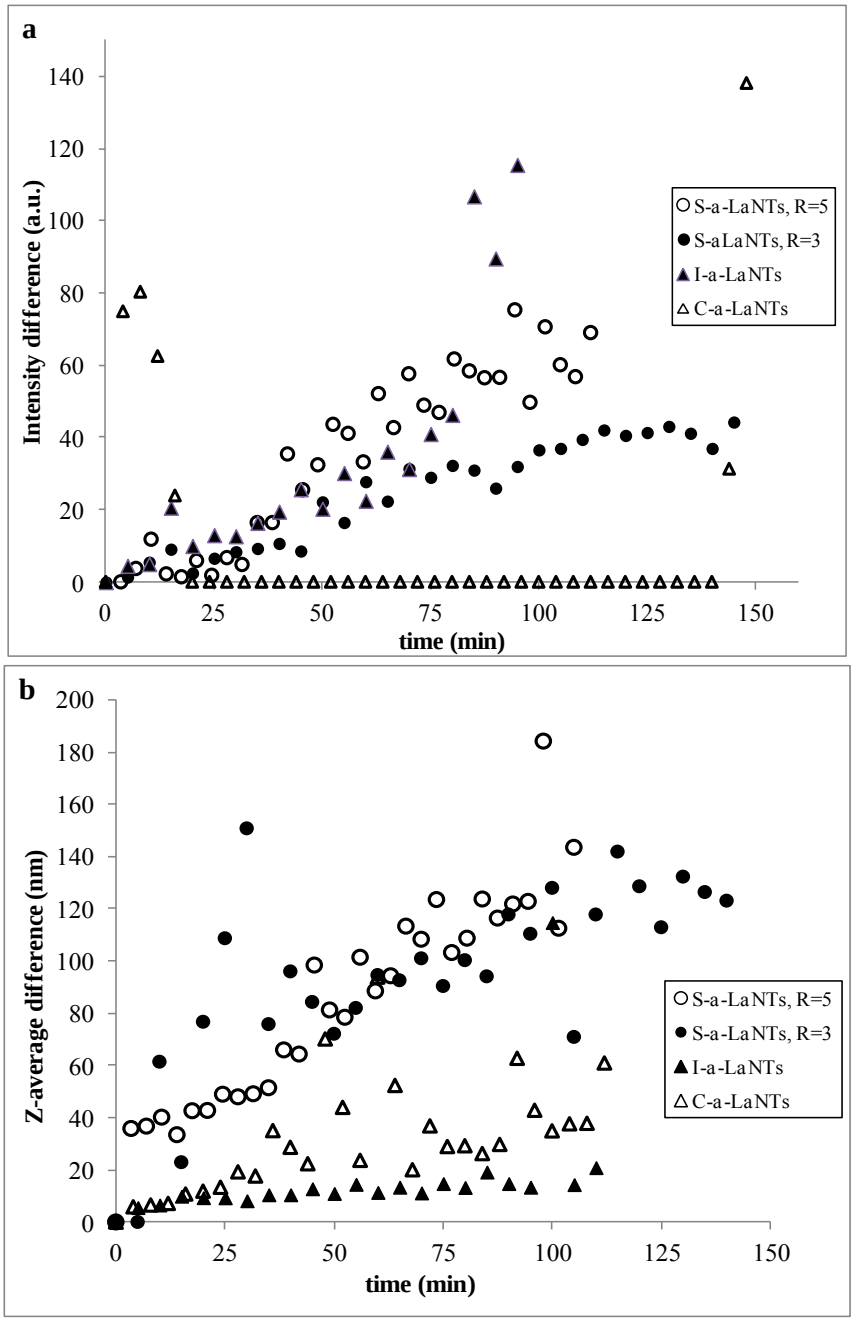

Figure 6.16. Scattering intensity distribution (a) and particle size distribution (b) with time during hydrolysis and nonotube growth of standard and purified α-La proteins

The growth kinetics of α-La nanotubes were extensively studied by Graveland-Bikker et al. (2004) under the conditions of different molar ratios of calcium to protein (R=0 to R=9), and by using different type of ions instead of calcium. In this study, two different calcium concentrations and also three different protein concentrations were tested. As shown in the figure, when the calcium concentration increased the lag period (representing hydrolysis) was decreased and intensity difference increased. This finding is consistant with the previous literature (Graveland-Bikker et al., 2004). Protein concentration is also an important parameter in this process. Protein and calcium concentrations were 0.5% and 0.0075% for I-α-La samples, and 0.3% and 0.011% for C-α-La samples (Table 5.9). However, standard a-La protein has 3% of protein and 0.0027% of calcium (Table 5.9).

The lag time for standard protein with the molar ratio of (Ca^{++} to α-La) 3 and 5 were nearly 45 min and 35 min, respectively. Sample I-α-LaNTs have lower lag time (nearly 30 min), mainly due to its higher Ca^{2+} content, however C-α-LaNTs have much longer lag time. This may be due to lower protein concentration than the instrument detection levels. During analysis, system showed warning as poor data quality in collecting data for I-α-LaNTs, and especially for C-α-LaNTs. Figure 6.16.b depicts particle size difference during nanotube growth. Both intensity and apparent hydrodynamic radius increased along incubation period. Actually, software in the system determines particle size as hydrodynamic radius by assuming spherical object. However, the structures analyzed here were linear, not spherical. Thus, the word 'apparent' was used, and difference data were given below.

Calcium ions and, also different type of ions, induced aggregation of hydrolyzed α-La and thus finally lead to gelation (Graveland-Bikker, 2005). Nanotube growth occurs due to aggregation of peptide molecules triggers gel formation. To investigate the tubular aggregation kinetics and stability of the resultant structures, photometric analysis was carried out in addition to DLS. Three different Ca^{++} and protein ratios were used and the resultant spectra were below. The gel formed in R=3 was quite transparent. As the Ca^{++} concentration increased the gel looses their transparency. Graveland-Bikker investigated the effects of Mn^{++} and Mg^{++} on tubular aggregation of α-la and reported that the former induced aggregation and gelation but the latter did not (Graveland-Bikker, 2005). In both, intensities were increased after lag period.

Figure 6.17 shows UV-spectra taken during incubation period leading to hydrolysis and nanotube growth of standard and purified a-La proteins. As mentioned

before, protein concentrations of the purified proteins were lower than that of standard protein. In order to compare growth profile of both on the basis of protein content, standard protein samples were prepared at lower concentrations (0.5% and 1%) which closer to that of purified ones. The best profile was exhibited by the nanotubular growth and gelation of standard protein (S-α-LaNTs) with 3% protein and R=3. It is followed by I-α-LaNTs having 0.5% protein and 0.0075% calcium, which corresponds approximately 3 times of that of standard protein. Then, C-α-LaNTs was the next with 0.3% protein and 0.011% calcium. The samples of S-α-LaNTs having 1% and 0.5% protein with R=3 did not lead to a significant absorbance change indicating nanostructure growth and gel formation. When all the profiles were compared, it is concluded that as the protein concentration decreased, absorbance change was also decreased. However increased calcium concentration also increases absorbance values due to aggregation and turbidity.

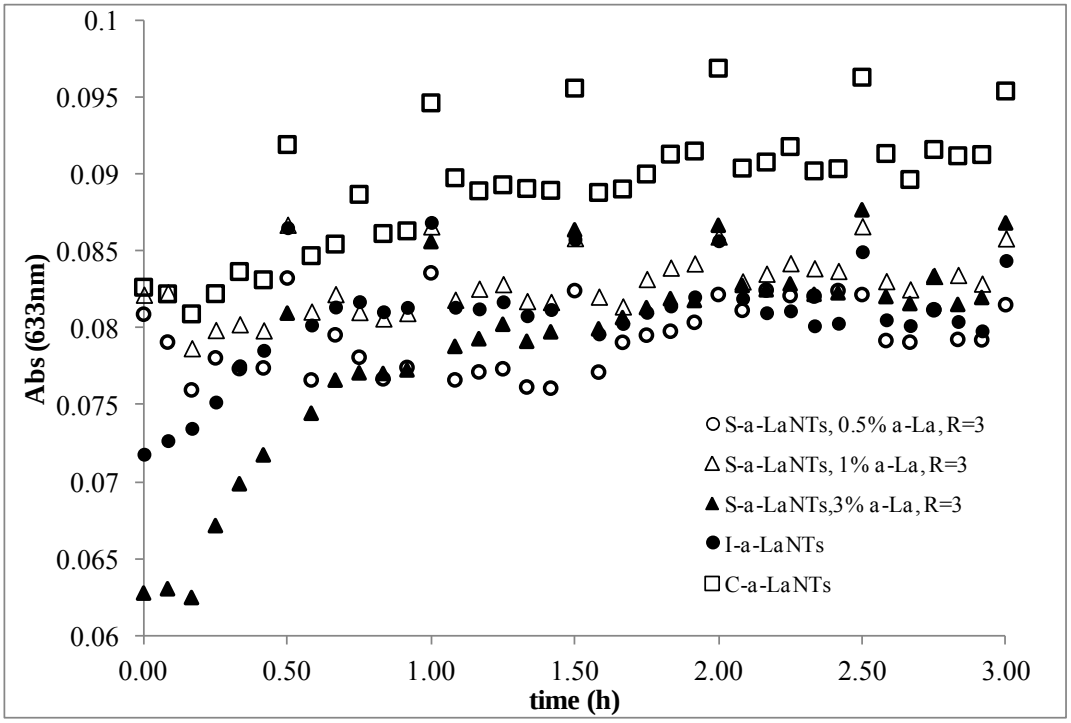

Figure 6.17. UV-spectra taken during incubation period for nanotube formation of standard and purified α-La proteins

More detailed investigation was carried out to determine the effect of both calcium and protein content on nanotube growth and gelation. Standard protein samples were prepared with changing calcium concentrations besides different protein contents. Figure 6.18, 6.19 and 6.20 presents spectra belonging to standart a-La protein with

0.5%, 1% and 3% protein concentrations, and molar ratio of Ca^{++}/a-La 3, 5, 10, respectively. After first 18 hour- incubation at 50 °C, samples were stored at 4 °C for about 48 hour, and then re-incubated in order to detect absorbance changes as an indicator of stability of the formed protein nanotubes.

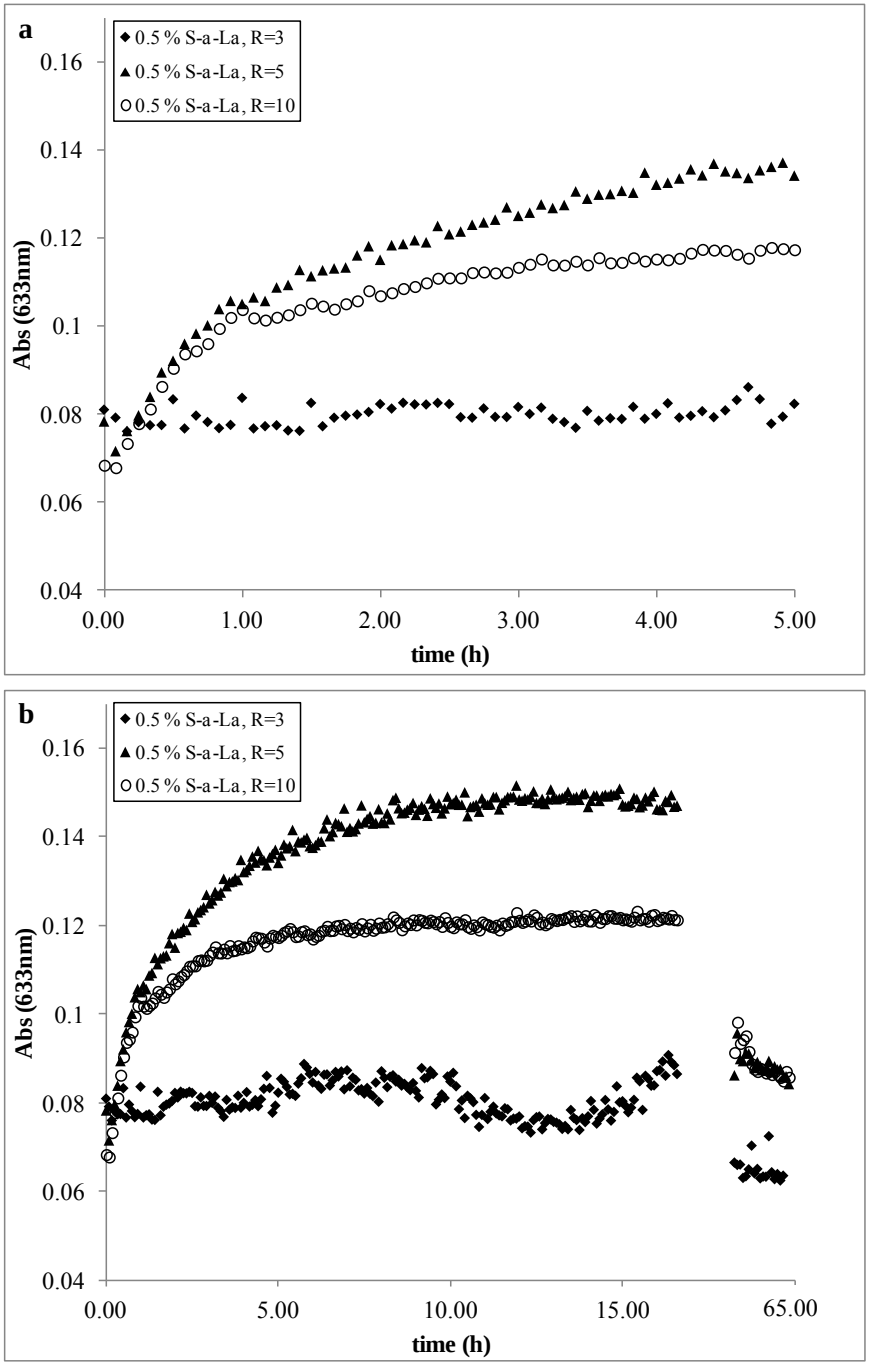

Figure 6.18. UV-spectra taken during incubation period (for nanotubular growth) of standard α-La samples with 0.5 % protein and molar ratio of Ca^{++}/α-La (R) 3, 5, and 10. a) 5-hour period, b) approximately 17-hour incubation, followed by storage at +4 ºC for 48 h and 2-hour re-incubation period

As it was clearly seen in figure 6.18, samples prepared by 0.5% protein with R=3 did not lead to significant absorbance change in UV-spectrum. But, increasing trend in absorbance was obvious in the case of increasing molar ratio of Ca^{++}/α-La (R=5, R=10). Similarly, 1% protein with R=3 did not change the absorbance, but R=5 and R=10 lead to increase in absorbance (Figure 6.19).

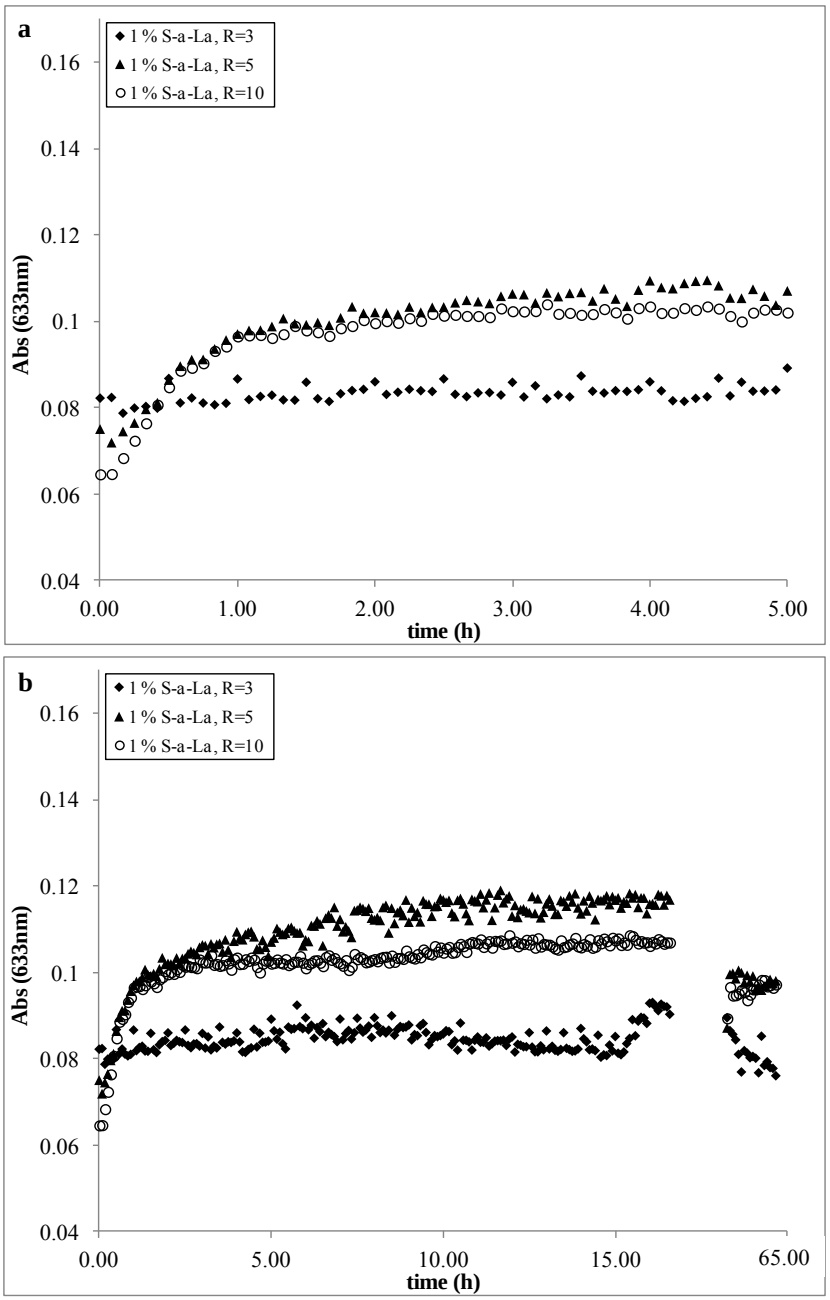

Figure 6.19. UV-spectra taken during incubation period (for nanotubular growth) of standard α-La samples with 1 % protein and molar ratio of Ca^{++}/α-La (R) 3, 5, and 10. a) 5-hour period, b) approximately 17-hour incubation, followed by storage at +4 ºC for 48 h and 2-hour re-incubation period

However, in the case of protein concentration of 3%, absorbance change was detected for all three ratios (R=3, 5, and 10) (Figure 6.20). It means that, this amout of protein is required for detecting the changes depending on the formation of new structures at R=3.

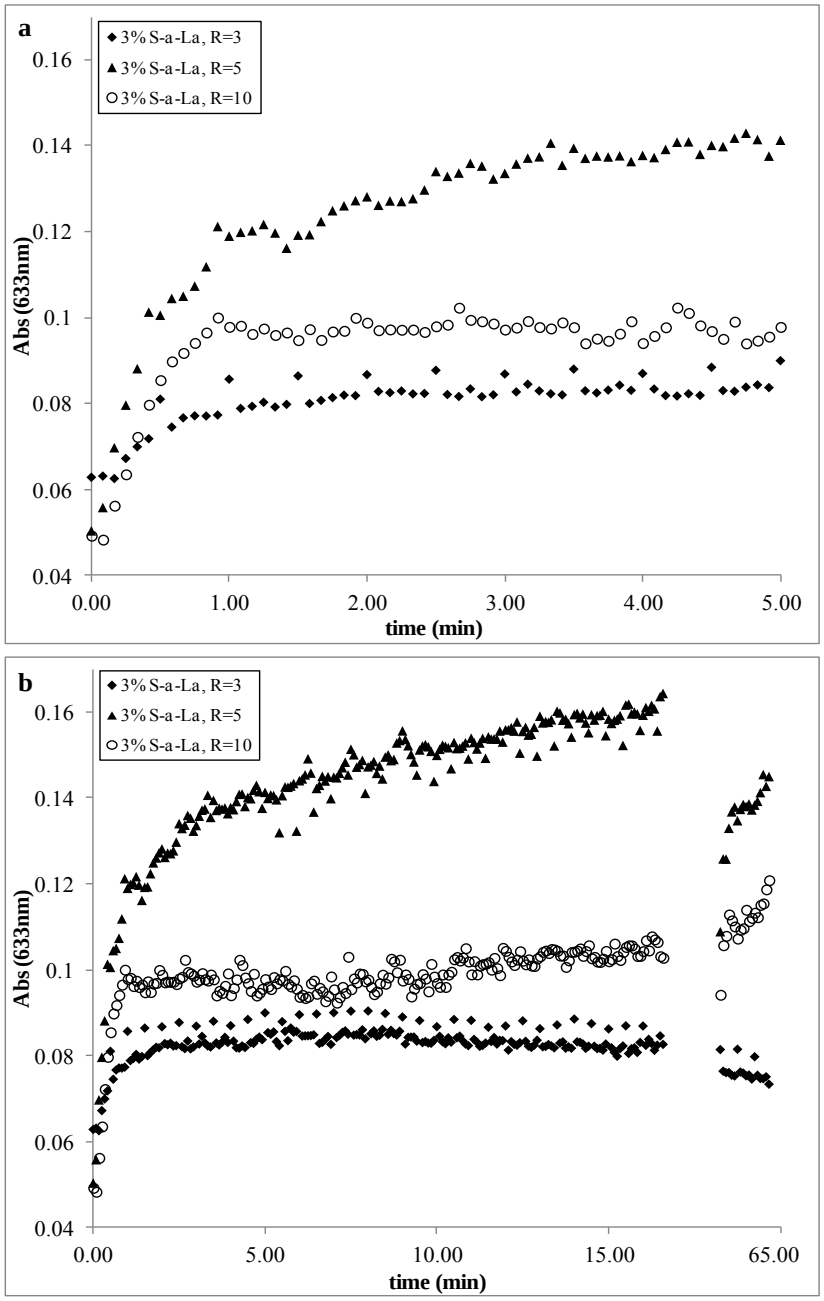

Figure 6.20. UV-spectra taken during incubation period (for nanotubular growth) of standard α-La samples with 3 % protein and molar ratio of Ca^{++}/α-La (R) 3, 5, and 10. a) 5-hour period, b) approximately 17-hour incubation, followed by storage at +4 ºC for 48 h and 2-hour re-incubation period

When compared all the cases, it is obvious that increased calcium concentrations increase absorbance, but not provide good stability if protein concentration is low.

Surprisingly, absorbances were expected to be greater than R=5 compared to R=10, however they were lower. This may be due to filtration of reaction mixture (protein, calcium and enzyme) for removal of impurities prior to incubation. Filters with 1 micron pore size may hold some amount of calcium after a critical concentration due to fouling occurred during filtration. Stability increased with increasing protein concentration, but in fact calcium and protein ratio was more critical than their individual effects.

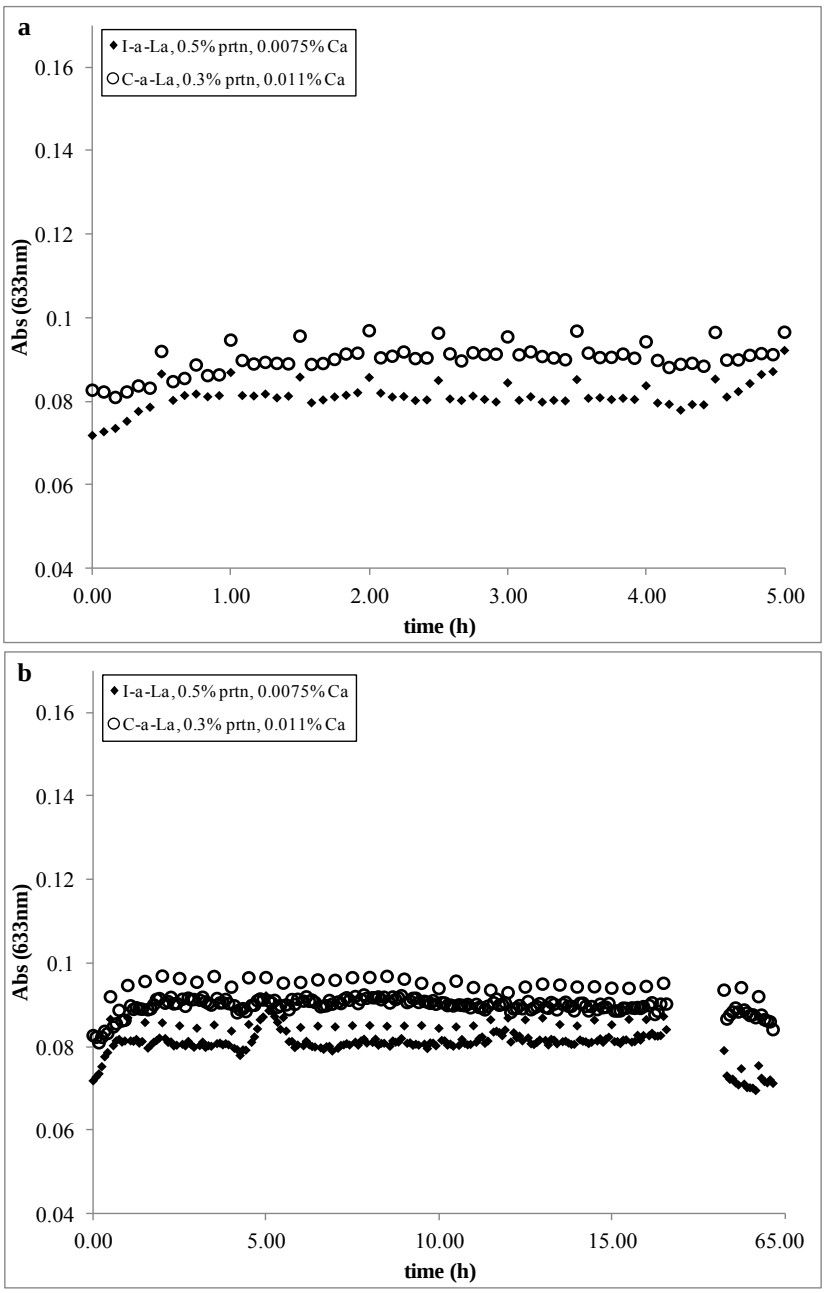

Figure 6.21. UV-spectra taken during incubation period (for nanotubular growth) of purified α-La samples a) 5-hour period, b) approximately 17-hour incubation, followed by storage at +4 ºC for 48 h and 2-hour re-incubation period

Purified proteins I-α-La and C-α-La natively had the calcium amount of 0.0075% and 0.011%, respectively. As their protein contents were low, but calcium contents were high, small changes were detected in UV-absorbance with increasing trend. The stabilities of the formed structures were comparable with those obtained by standard protein.

6.2.3.4. Analysis of the Hydrolysis of α-Lactalbumin

Peptides formed during the enzymatic hydrolysis of α-La were investigated by RP-HPLC. Chromatograms of the hydrolysates, produced by using standard α-La, at various times of incubation were given in Figure 6.22. At the beginning of the incubation (t=0 h), a large peak of non-hydrolyzed α-La protein was seen, clearly. In progressing times (t=0.5, 1, 1.5 h), as the α-La hydrolyzed the large peak of α-La loose intensity, and new peaks varying in size were formed. These peaks were belonging to peptides obtained by the hydrolysis of protein with BLP.

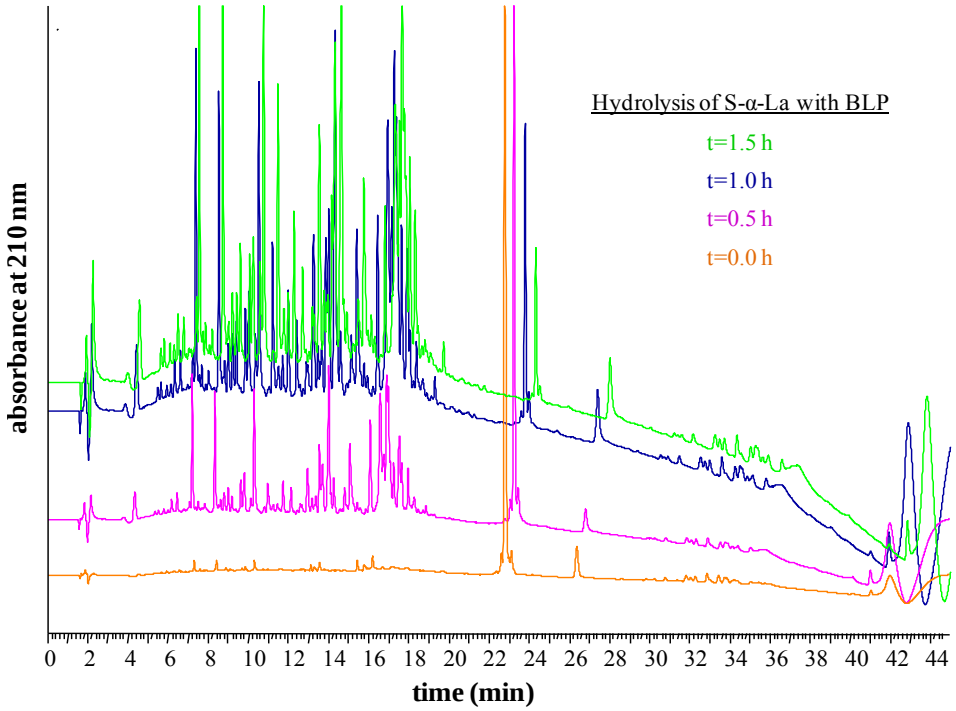

Figure 6.22. RP-HPLC chromatograms of hydrolysis products of the standard a-La protein obtained by digestion with BLP

Graveland-Bikker et al. (2004) and Otte et al. (2004) reported that all the α-La was hydrolyzed after 1 h, but in our study complete digestion was seen at about 2 h. The

researchers analyzed hydrolysis products by Liquid Chromatography Mass Spectrometry (LC-MS) and indicated the masses of the peptides formed. In the presented study, only HPLC chromatograms of peptide peaks were given. In addition, MALDI-TOF MS analysis of samplings was carried out. The results are given below.

HPLC chromatograms of hydrolysates formed by purified proteins were presented in Figure 6.23. As the protein concentrations were lower for I-α-La and C-α-La samples than standard one, nearly all protein was hydrolyzed after 1h.

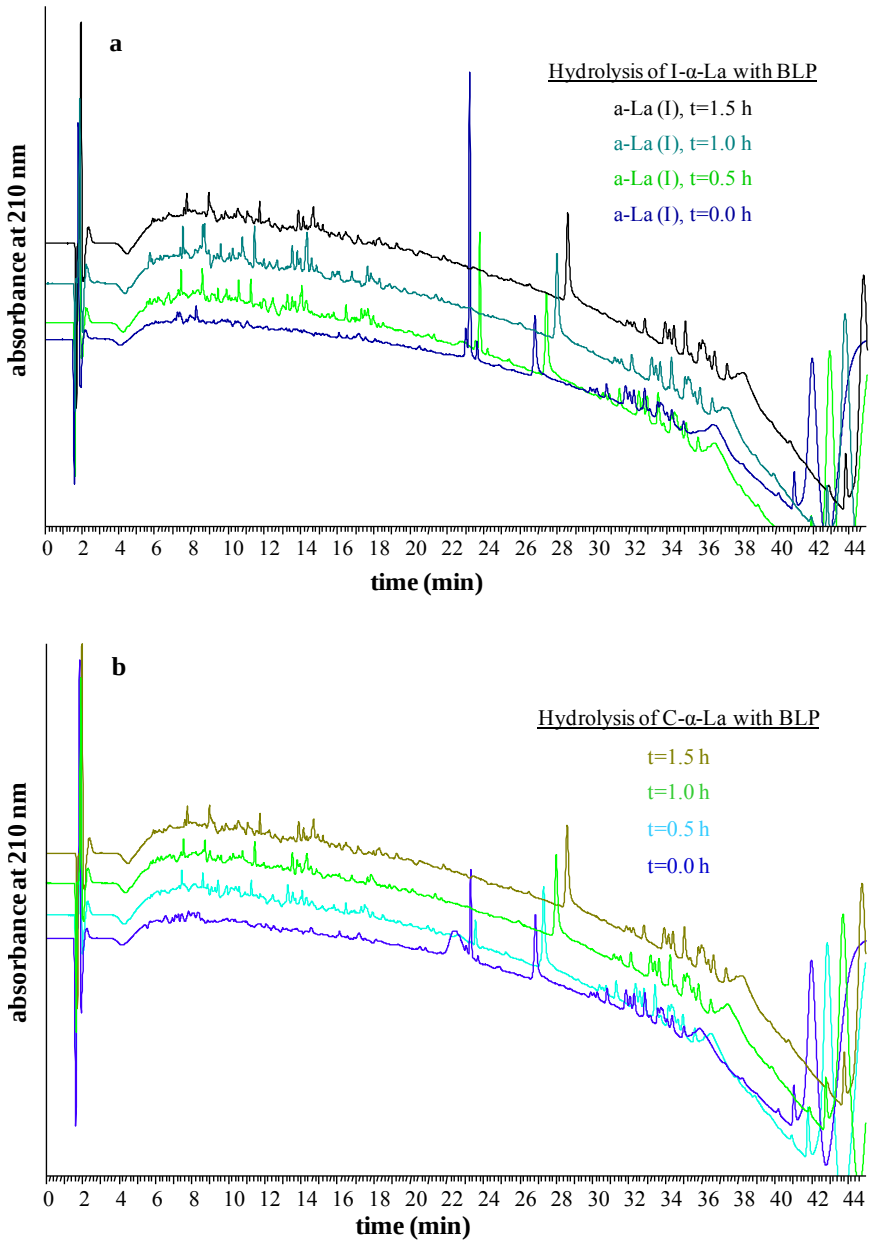

Figure 6.23. HPLC chromatograms of hydrolysis products of purified α-La proteins obtained by digestion with BLP. a) I-α-La hydrolysates, b) C-α-La hydrolysates

The hydrolysis of α-La with BLP was described by first order kinetics, previously (Graveland-Bikker et al., 2004). The hydrolysis data obtained for standard and purified α-La agreed with that finding. Digestion of α-La proteins (standard and purified) were indicated in Figure 6.24. The hydrolysis data was best fit with the log-linear model. The kinetic relations were represented as follows:

For S-α-La, $[a\text{-La}]_t = [a\text{-La}]_0 \exp(-2{,}53t)$

For I-α-La, $[a\text{-La}]_t = [a\text{-La}]_0 \exp(-3{,}62t)$

For C-α-La, $[a\text{-La}]_t = [a\text{-La}]_0 \exp(-3{,}16t)$

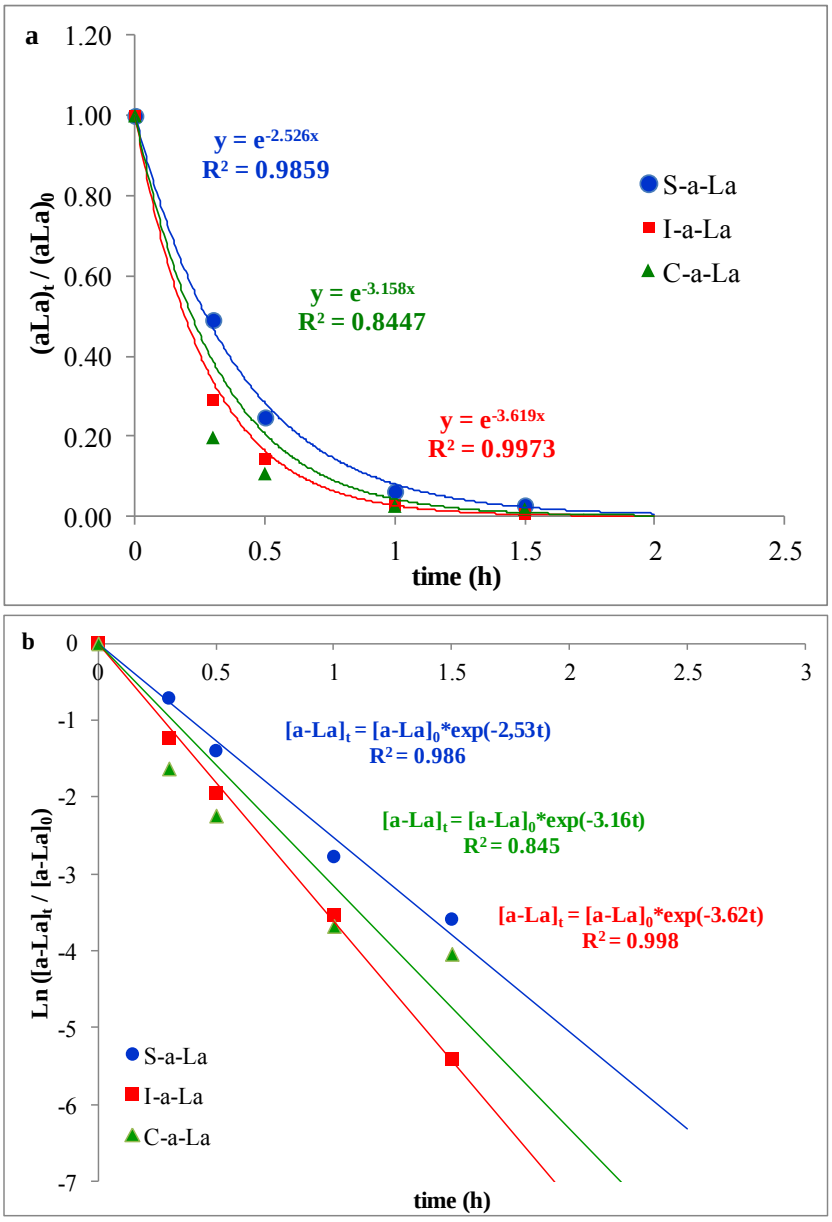

Figure 6.24. Hydrolysis kinetics of standard and purified α-La proteins. a) Degradation of α-La in logarithmic scale, b) Linearized logarithmic data of hydrolysis

The R^2 values were determined as 0.986 (S-α-La), 0.997 (I-α-La), and 0.845 (C-α-La). When compared, R^2 belonging to I-α-La was detected as the best. C-α-La was isolated from more complex and mixed media when compared to I-α-La, thus this composition might affect its hydrolysis kinetic

Peptides, building blocks of nanotubes, obtained at the end of hydrolysis were analyzed by MALDI-TOF MS in order to determine their masses. Figure 6.25 shows MS spectra of standard α-La protein hydrolysis.

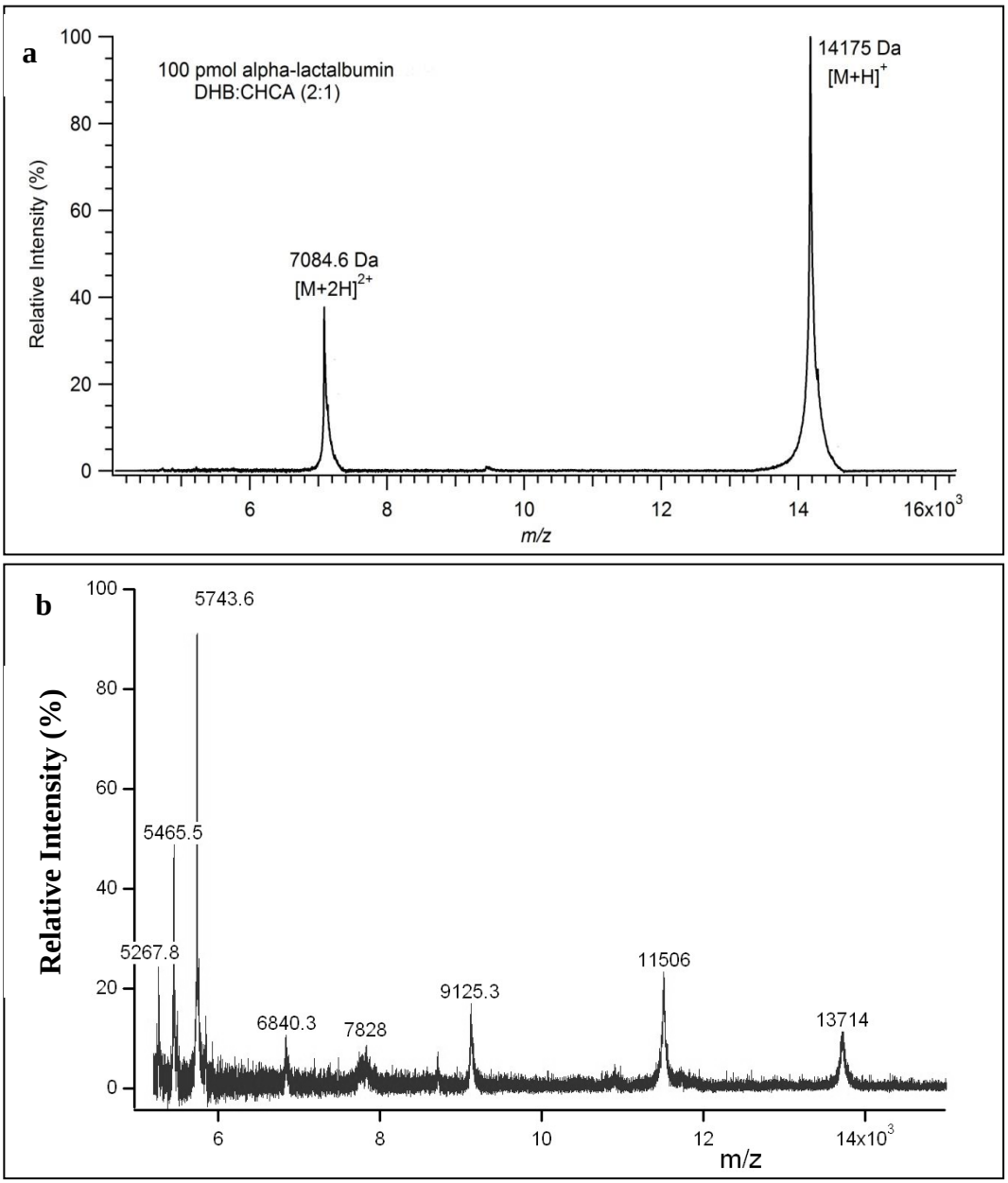

Figure 6.25. MS spectra of a) standard a-La protein and b) its peptides after hydrolysis

At the beginning protonated (14175 Da) and double protonated (7085 Da) a-La

peaks are seen (Figure 6.25.a). Nine major peptide peaks were observed with different masses (13714, 11506, 11200, 9125, 7828, 6840, 5744, 5466 and 5268 Da) at the end of hydrolysis (Figure 6.25.b).

Figure 6.26 shows MS spectra of hydrolysis of α-La purified from WPI. At the beginning two peaks of protonated (14200, 13634 Da) and double protonated (7086, 6040 Da) a-La, and one more peak (12074 Da) were seen (Figure 6.26.a). Ten major peptide peaks were observed with the masses of 8133, 7352, 7167, 6820, 6616, 5725, 5353, 5177, 4896, 4704, at the end of hydrolysis. (Figure 6.26.b).

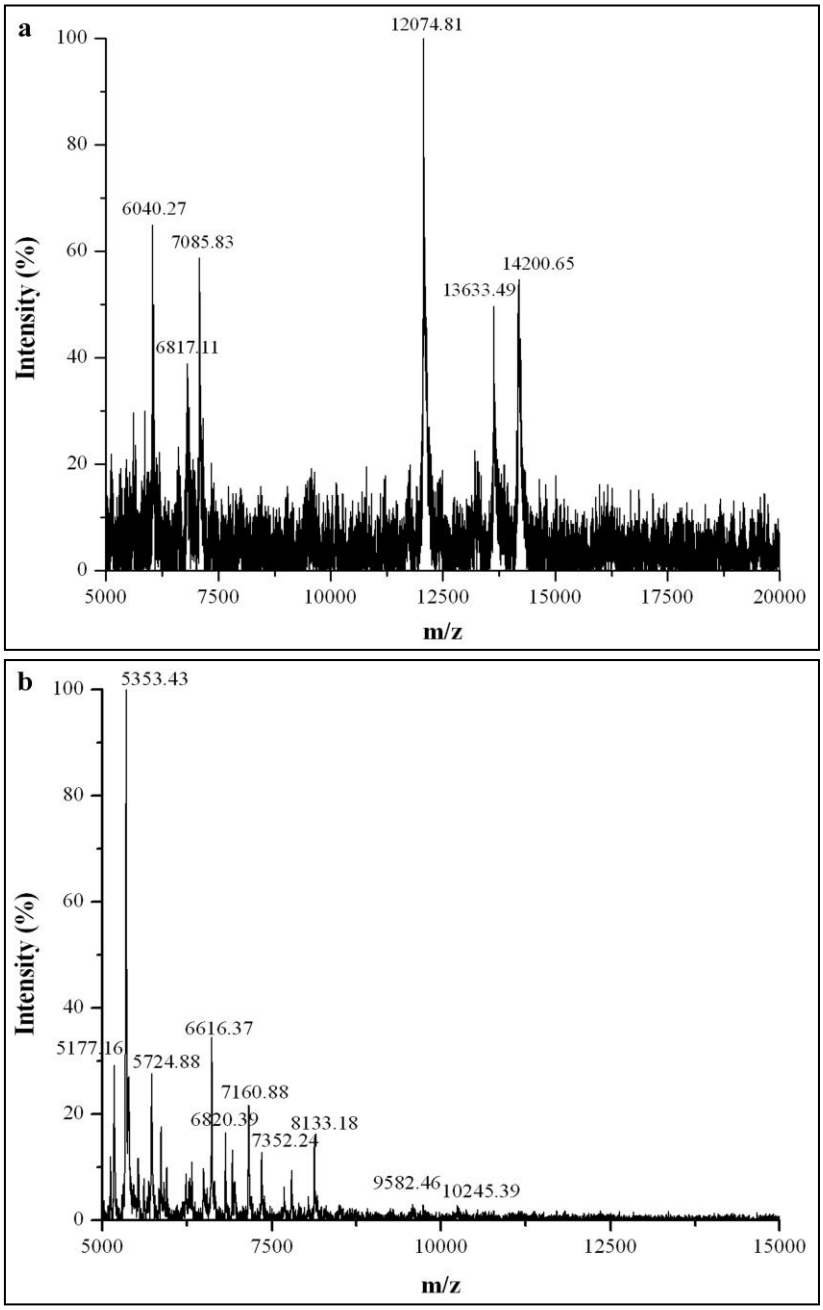

Figure 6.26. MS spectra of a) I-a-La protein and b) its peptides after hydrolysis

Figure 6.27 shows MS spectra of hydrolysis of α-La purified from WPC. At the beginning two peaks of protonated (14182, 13646 Da) and double protonated (7088, 8062 Da) a-La were detected (Figure 6.27.a). Nine major peptide peaks were observed with the masses of 9582, 8138, 7355, 7160, 6823, 6617, 5727, 5350, and 4897, at the end of hydrolysis (Figure 6.27.b).

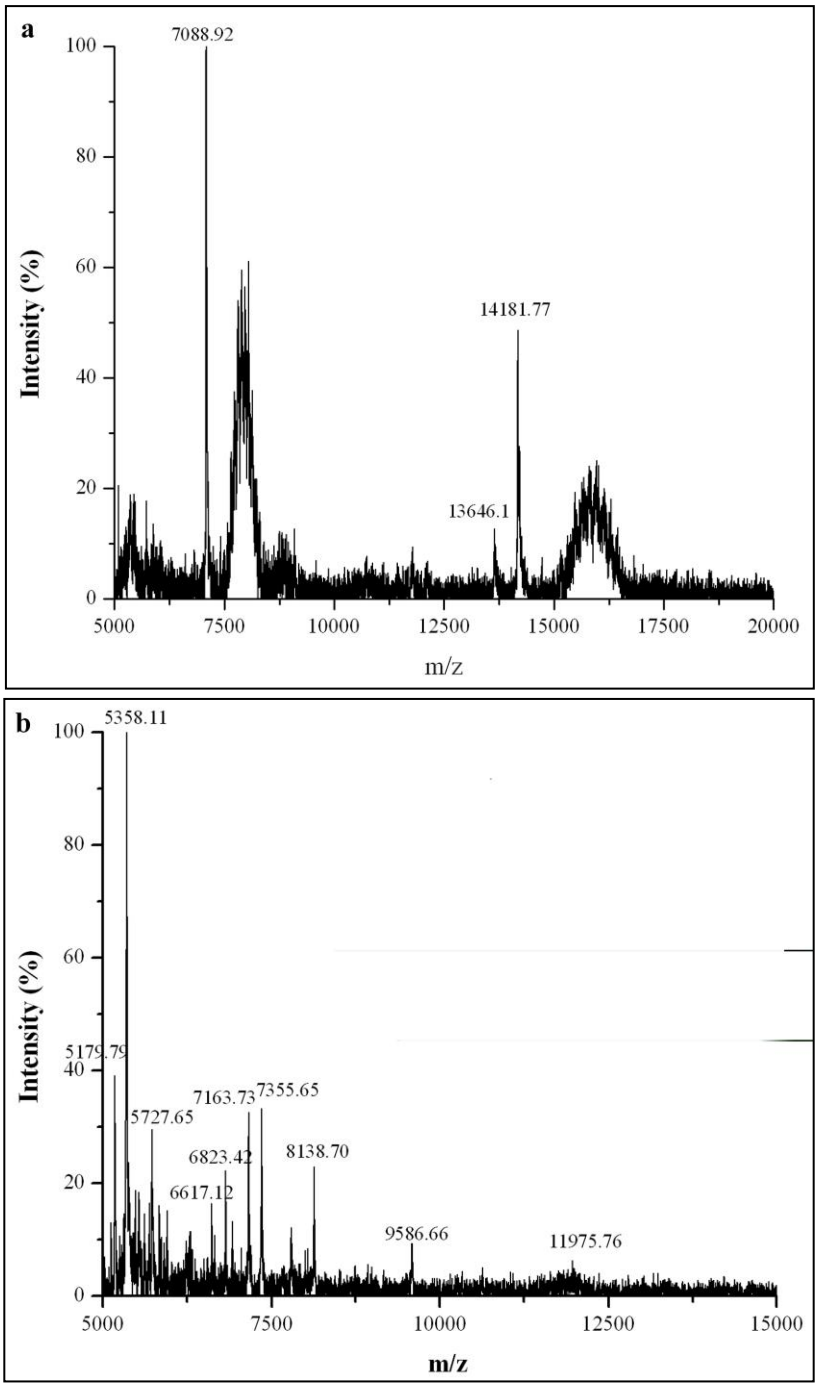

Figure 6.27. MS spectra of a) C-a-La protein and b) its peptides after hydrolysis

Mass spectrum of standard sample has difference when compared to that of purified ones. After 1.5h-incubation most of the peptides with masses lower than 10000 Da were detected in the samples of purified proteins, however three peptides with masses above 10000 Da arised from hydrolysis of standard protein (13714, 11506 and a small peak around 11200 Da). Graveland-Bikker and his collagues performed Q-TOF MS analysis for α-La peptides and reported five peptides possesing molecular masses greater than 10000 Da with masses 13928, 11570, 11253, 10268, 10111 Da identified as building blocks of nanotubes (Graveland-Bikker et al., 2009). This difference may be related to initial protein concentration. Samples with high protein concentration might enhance detection of its hydrolysis products in smaller amounts. In addition it was reported that, α-La peptides with masses around 11 kDa form nanotubes, whereas those with 8-9 kDa form linear fibrils (Ipsen and Otte, 2004). However it could not be said that there were no peptides with masses around 11 kDa in purified samples absolutely. Because microscopic observations revealed that nanotubular structures were developed from purified proteins, especially WPI-based α-La. Instead of MALDI-TOF MS, LC-MS may be more appropriate to analyze these peptides, in fact. Peptides formed at certain time intervals during hydrolysis process can be detected by RP-HPLC (Figure 6.22, 6.23) and then can be directly sent to MS for mass determinations.

6.3. Conclusions

In this chapter, development of α-LaNTs by self-assembly, microscopic analysis of the constructed nanotubes, optical characterization of the changes in the protein structure, studies in relation with the analysis of protein hydrolysis and nanotube growth were reported.

Whey protein α-La is able to form nanoscale tubular structures; namely α-La nanotubes, through self organization of peptides after partial hydrolysis by BLP. Microscopic analysis revealed that α-LaNTs were regular hollow strands with uniform morphology in consistent with the literature. Both TEM and AFM were effective in the visualization and dimensional analysis of these nanotubular structures. FT-IR and Raman Spectroscopy indicated structural conformations in α-La during the hydrolysis and nanotube growth. The native tertiary structure of α-La was destabilized, and some conformational changes were observed in the secondary structure of the protein. The β-

sheets (especially antiparallel), β-turns and random structures became dominant due to dimerization and re-arranged supramolecular structure during nanotube formation. Also, in the helix domain, 3_{10} helix structures seemed to gain importance besides α-helix. Enzymatic hydrolysis resulted in the exposure of COO^- groups at Asp and Glu side chains in the peptides. Then, calcium ions were predicted to bind peptides at these groups mainly which led to the nanotube growth. FT-IR spectroscopic analysis showed some shifts, gain and loos of intensities at the related bands due to Ca^{++} binding to COO^- groups of these specific sites. DLS and UV-spectrophotometry studies analyzing nanotubular aggregation kinetics indicated that both calcium and protein concentration affects hydrolysis and nanotube growth. Most of the protein was hydrolyzed by BLP after 1 h and new peptides with different molecular masses were formed to mediate nanotubular formation.

CHAPTER 7

INVESTIGATION OF ALPHA-LACTALBUMIN NANOTUBES IN RELATION WITH THE FOOD APPLICATIONS

7.1. Introduction

The α-Lactalbumin nanotubes possess structural and dynamic features for various applications due to their cavity, stiffness, gelation properties, inducible disassembly, enhanced stability by cross-linking, heat stability, etc. (Graveland-Bikker and de Kruif, 2006). Thus, constructed α-LaNTs are suggested for some potential food applications in such uses as gelating, viscosifying and encapsulating agents. Gelation is one of the most important functional properties of the proteins, whey based protein gels are widely used in food industry. Therefore, gelation process occurred during hydrolysis and nanotubular growth was investigated in this chapter.

Ipsen et al. (2001) reported that formation of α-La nanotubes resulted in strong gels with transparent appearance. During the hydrolysis of α-La and nanotube growth, the formation of initial network is facilitated by calcium ions, and then the gel network of the tubular strands is rearranged slowly due to hydrolytic formation of additional calcium binding sites and hydrophobic interactions between building blocks (peptides) (Ipsen et.al., 2003). As the calcium concentration increases, the gel formation occurs faster (Graveland-Bikker et al., 2004). These nanotubular gels are sensitive to pH changes and mechanical strain, but capable of partially regain structure under quiescent conditions (Ipsen and Otte, 2003). By considering current literature, gelation process occurred in the cases of hydrolysis and nanotube formation was compared in this study. Also, gelation obtained during the formation nanotubes from purified proteins was investigated. Additionally, gelation was examined in the cases of varying concentrations of protein and calcium.

Gelation is defined by the parameters, G’ (storage modulus) and G’’ (loss modulus) determined by reometer measuring responses to applied forces (strain). G is the complex dynamic modulus can be used to represent the relations between the

oscillating stress and strain. The storage (G') and loss modulus (G'') measure the stored energy, representing the elastic portion, and the energy dissipated as heat, representing the viscous portion, respectively. Viscoelasticity is the property of materials that exhibit both viscous and elastic characteristics when undergoing deformation. Elastic characteristic is a reversible deformation behavior and viscous characteristic is an irreversible deformation behavior.

As mentioned above, gelation arised from nanotube formation is an important feature in consideration with the applications. In this context, thermal stability of the constructed nanostructures and gels are also critical. Many food processes may involve various heat treatment steps. Therefore, denaturation temperature of these structures should be defined before suggesting for a target application. Differential scanning calorimetry (DSC) is a useful tool for studying thermal denaturation and conformational transition of proteins in various food systems (Arntfield et al., 1990). It measures the temperatures and heat flows associated with transitions in materials as a function of time and temperature in a controlled atmosphere. These measurements provide quantitative and qualitative information about physical and chemical changes that involve endothermic or exothermic processes, or changes in heat capacity. Thermogravimetric analysis (TGA) is also a method of thermal analysis measuring changes in physical and chemical properties of materials as a function of temperature. The sample is heated to high temperatures by continuously measuring its mass, and then weight loss or gain is determined due to decomposition, oxidation and/or loss of volatiles.

The α-La considered as the most heat stable protein. Removal of Ca^{++} in α-La native structure reduces its stability (Hiroaka et al., 1980). Nanotube growth was triggered by the addition of calcium ions. Therefore, an increase in the stability is expected, in fact. But thermal behavior of newly developed nanostructures based on α-La peptides may be different when compared to folded compact structure of the native protein. This study aims to analyze behavior of both standard and purified α-La proteins and nanotubes against thermal treatments.

One suggestion for the potential applications of α-LaNTs is the use of them for entrapment and or encapsulation of colorants and bioactive materials. The capability of binding of such active agents made these nanostructures to be considered as functional elements in transportation and target delivery. In order to test the encapsulation ability of these nanotubes, some preliminary experiments were conducted by using a bioactive

agent, epicatechin gallate (ECg). It is a valuable phenolic material extracted from green tea. Its molecular weight is 442.37 g/mol and structure is given in Figure 7.1. ECg preparate used in this study is not synthetic, it is natural extract with 98% purity.

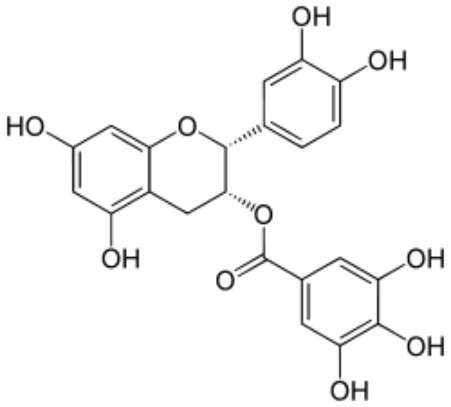

Figure 7.1. Structure of epicatechin gallate (ECg)

In this chapter, investigations related to the applications of nanotubes constructed from both commercial and purified α-La proteins in terms of analyzing gelation properties, determination of thermal stability, and examining entrapment and/or binding efficiency of a coloring agent and a bioactive material were presented.

7.2. Experimental

7.2.1. Materials

All chemicals and standards were purchased from Sigma Chemicals Co. (St. Louis, MO). *Bacillus licheniformis* protease (BLP) was kindly provided by Novozymes A/S (Bagsvaerd, Denmark). 0.1 micron low protein binding filters were purchased from Millipore.

7.2.2. Methods

Gelation analysis of nanotubes was carried out by rheometer, thermal stability of them was determined by DSC and TGA analyses, and dye-binding capability was investigated by UV-spectrophotometry. Finally, some preliminary studies by UV-

measurements were performed.to determine encapsulation/binding of catechin into nanotubes

7.2.2.1. Rheological Assays

Alpha-lactalbumin, $CaCl_2$ and BLP mix was prepared as described previously, and incubated in a rheometer (TA Instrument AR 2000ex – Rheometer, UK) at 50 °C. Experimental procedure was adapted from Graveland-Bikker et al. (2004). Samples were subjected to dynamic oscillation with a strain of 0.005 and a frequency of 0.5 Hz during the incubation. Measurements were carried out with plane and cone geometry having a cone angle of 0.1 radians and a diameter of 25 mm, and time sweep mode. In order to remove loading effects, a preshear of 1 s^{-1} was applied for 1 min prior to further measurement. Gelation was defined as the point at which G' was greater than 1 Pa. G' and G'' loss modulus were detected during analysis in the case of the nanotubes were triggered or not.

7.2.2.2. DSC Analysis

DSC analysis was carried out in TA Q10 Series (Princeton Inst. Inc., USA). Protein solutions were prepared as dissolving the 3% (w/v) protein in Tris HCl buffer, 75 mM, pH 7.5. The solutions for nanotube samples were prepared by mixing α-La (3%) with Ca^{2+} (R=3) and BLP (4%, w/w). Purified α-La (1 % (w/v) from WPI, 0.5 % (w/v) from WPC) was mixed with 4 % BLP (w/w) (BLP/α-La). The ratio (R) of calcium to protein present natively in purified fractions were 3 (mol Ca^{2+} / mol α-La from WPI) and 5 (mol Ca^{2+} / mol α-La from WPC). All the samples were incubated in DSC instruments at 50 ºC for 1.5 h firstly. Then they were scanned from 50 ºC to 200 º C and from 200 º C to -40 ºC at heating rate of 5 ºC/min. Each sample was measured at least twice, and empty DSC pans were used as reference.

DSC analysis of lyophilized samples were conducted by Shimadzu DSC 50 (Japan) by a 10 ºC/min heating rate up to 200 ºC. In both DSC analysis flowing gas was N_2.

7.2.2.3. TGA Analysis

TGA analysis was achieved by an instrument of Perkin Elmer (Diamond TG/DTA, USA). Protein samples were heated in pre-weighed pans from 30 °C to 200 °C at heating rate of 5 °C/min, under nitrogen flow.

7.2.2.4. Dye-binding and UV-Spectrophotometry Assay

UV-spectrophotometry assays were performed using Varioscan Flash (Thermo, USA). Samples prepared by mixing nanotubes of standard and purified proteins and congo red dye as a representative colorant. Control samples were also prepared by mixing α-La proteins (both standard and purified) and dye. Fifty microlitter (2.5%) congo red was added to 50µl protein /nanotube solution in well-plates and incubated in the instrument at 50 ºC. Measurements were taken at 633nm with 1 minute-intervals for nearly 1h.

7.2.2.5. Encapsulation Studies

Preliminary studies investigating the use of α-LaNTs constructed from standard protein for encapsulation of epicatechin gallate (ECg) were carried out. In order to prepare protein nanotubes loaded with bioactive agent, 0.1 mg/ml ECg was mixed with α-LaNTs and incubated at RT and +4 °C for 0 – 72 h by slow shaking. Procedure was repeated for 3 different pH's (4.0, 5.0, 7.0). During incubation, protein-flavonoid pellets were removed by ultracentrifuge (45.000*g, 30 min) in the samples taken at different time intervals (15 min, 30 min, 60 min, 3 h, 6h, 24h, 48h, 72h). ECg amounts in the medium at the beginning and after incubation period were determined by UV-spectrophotometry (275 nm). Encapsulation efficiency was calculated by using the following equation.

$$\text{encapsulation efficiency} = ((a - b) / a) * 100$$

a = bioactive material amount in the medium before incubation

b = bioactive material amount left in the medium after incubation

7.2.3. Results and Discussion

7.2.3.1. Gelation Analysis of α-Lactalbumin Nanotubes

In this part of the thesis, gelation properties of α-LaNTs constructed from standard and purified proteins were investigated in potential food applications. Protein and enzyme mixture prepared with and without calcium ions, triggering nanotube development, were incubated in a rheometer under the exposure of dynamic oscillation. Gelation times, storage and loss modules (G` and G``) data were obtained. In figure 7.2 and 7.3 the storage and loss modulus were plotted as a function of time for hydrolyzates and nanotubes of standard α-La protein. Gelation was defined at the point that G`>1 (Graveland-Bikker et al., 2004). Both figures include data collected in 2 and 6-hour period to achieve better comparison of nanotube and hydrolyzate gelation. In cases of hydrolyzates and nanotubes gelation was started at nearly 49 min and 50 min, respectively. More fluctuation in G'values belonging to α-La hydrolyzates was observed at the beginning when compared to that of α-LaNTs. After this fluctuation G` values, representing elastic behavior, of α-LaNTs' gel increased quickly and reached to nearly 12810 Pa. G' value of hydrolyzates increased slower and ended at nearly 6090 Pa. Also, G'', indicating viscous behavior, of α-LaNTs and hydrolyzates were 13790 Pa and 3759 Pa, respectively. This difference indicated that, formation of α-LaNTs increased gel stiffness. Measurements taken for about 6 h showed that nanotubular growth enhanced gelation. As it is known, proteins and their hydrolyzates are used as gelation agents in industry. Nanotubes constructed from α-La protein are certainly advisable as ingredients providing more effective gelation according to application field.

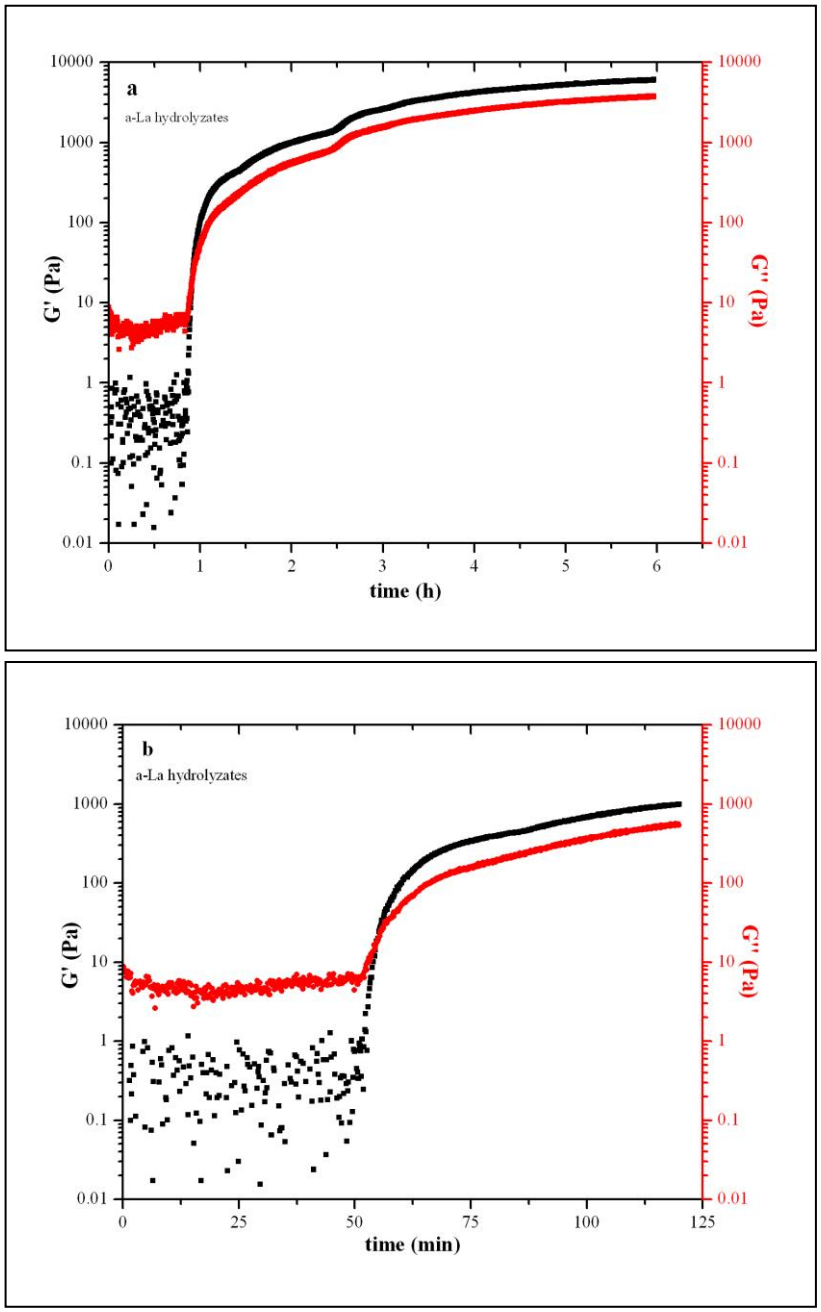

Figure 7.2. Young Modulus of the hydrolyzates of standard α-La protein a) in 6 h, b) in 2 h

Graveland-Bikker et al. (2004) reported that gelation was started after 1 h when nanotubes formed due to addition of calcium ions into incubation medium; and after 10 h when no nanotubes formed. Similarly, in the presented study, gelation was started after about 50 min in both cases. This result observed especially for protein hydrolyzates, is greatly different from that reported previously by Graveland-Bikker et al. (2010). Difference in rheometer system used for measurements might affect the results, but actual reason for this difference was not understood.

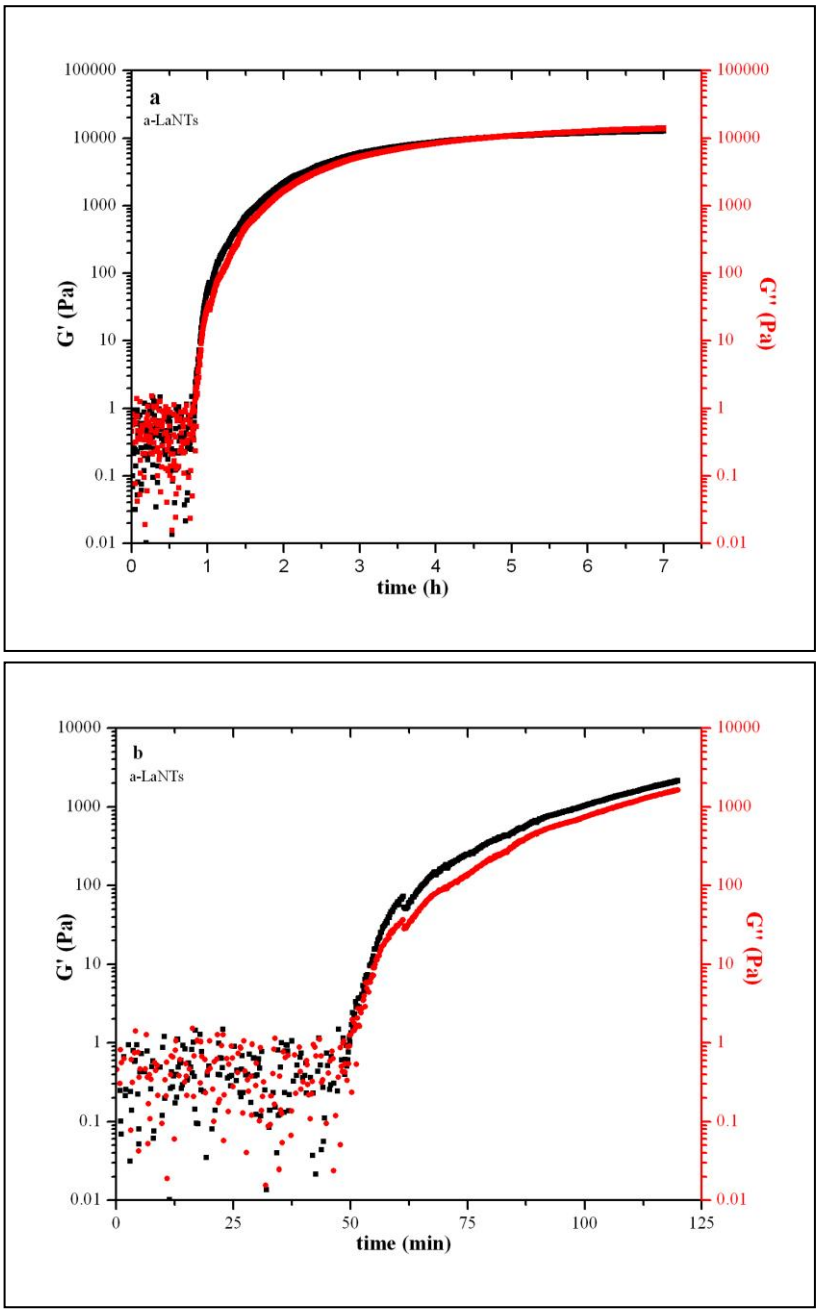

Figure 7.3. Young Modulus of the nanotubular development using standard α-La protein a) in 6 h, b) in 2 h

Figure 7.4 and 7.5 presents storage and loss modules of α-LaNTs formed by using purified proteins. G' and G''values obtained during the nanotubular growth of WPI-based α-La were determined as 1450 and 2730 Pa, respectively in 3.5 h. However, G' and G''values of nanotube growth with WPC-based α-La reached to 8942 and 3112 Pa, respectively in 45 minutes.

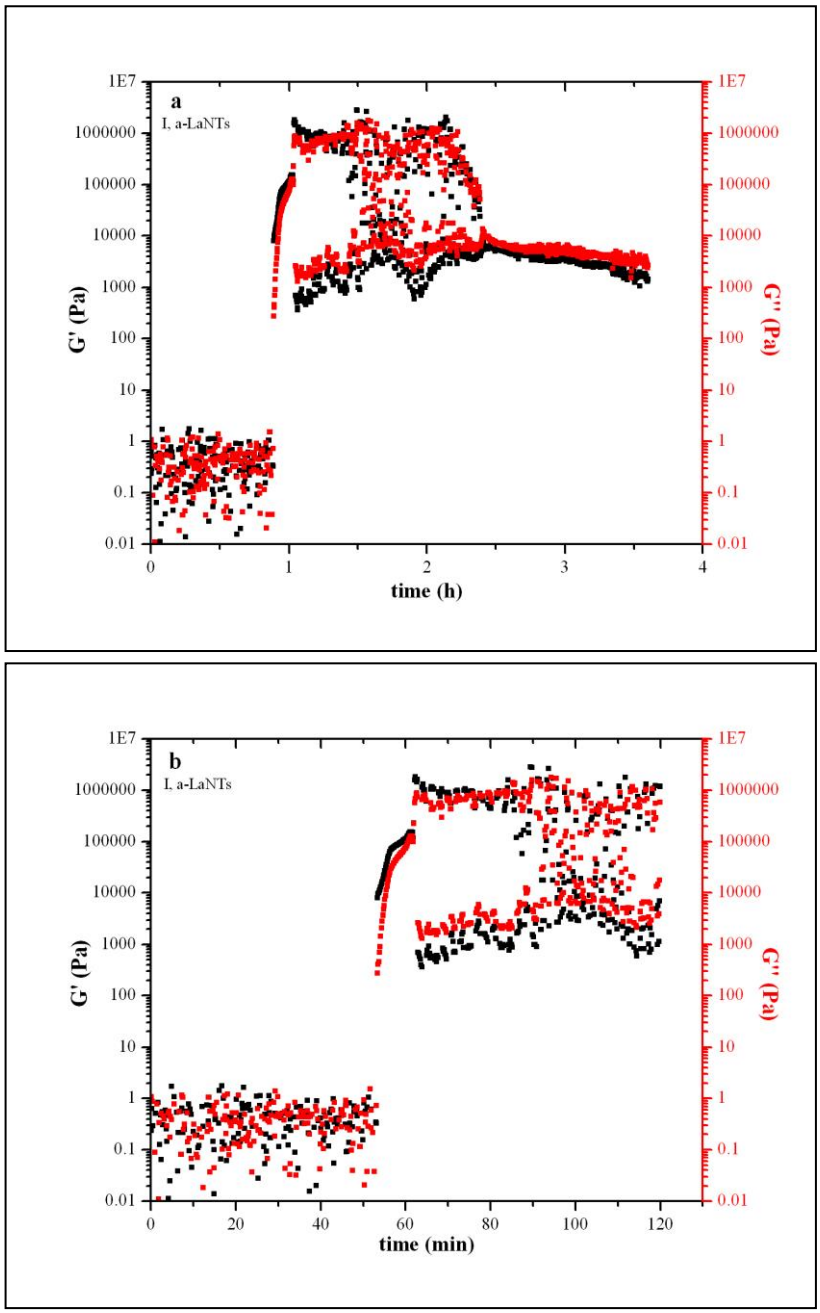

Figure 7.4. Young Modulus of the nanotubular development using purified protein, I-α-La. a) in 4 h, b) in 2 h

For the sample of C-α-LaNTs, the analysis was stopped at about 30 min, and the rest of the data were not collected because of an error occurred in the system. The data collected for I-α-LaNTs were scattered in between 1 h and 2.5 h, approximately, and then re-equilibirated. This might be arised from natural composition of the purified protein sample.

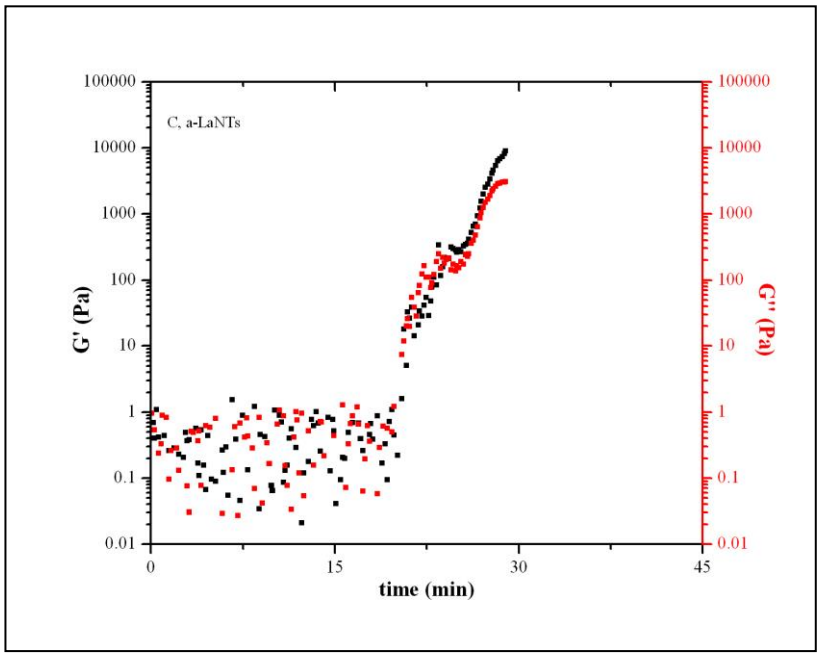

Figure 7.5. Young Modulus of the nanotubular development using purified protein, C-α-La in 45 min

Protein and calcium concentrations of the samples prepared from standard and purified proteins were different. Therefore, gelation process occurred differently in each sample. Protein amount in the purified ones were lower than that of the standard one. Besides, purified α-La samples contained higher amount of mineral than standard. Gelation started after 20 min in the C-α-La samples, but it was earlier nearly in 20 min for I-α-La samples. Clean and transparent gels were obtained by the formation of nanotubes of standard protein. White and turbid gels were observed by the growth of I-α-LaNTs. Each of them can be preferable for the target purpose in application. However, no desirable gelation was achieved by using C-α-La sample, due to very high mineral and low protein content. In order to analyze the effects of protein and mineral contents on gelation, different samples were prepared with changing protein and calcium concentrations and analyzed in rheometer. Gelation was occurred in the presence of 1% protein and triggered by increasing calcium amount (Figure 7.6.a). But, no desirable gelation was achieved when the protein concentration was dropped to 0.5%, even if calcium content was increased (Figure 7.6.b). The results revealed that protein concentration was more critical than calcium amount for gelation based on nanotubular growth.

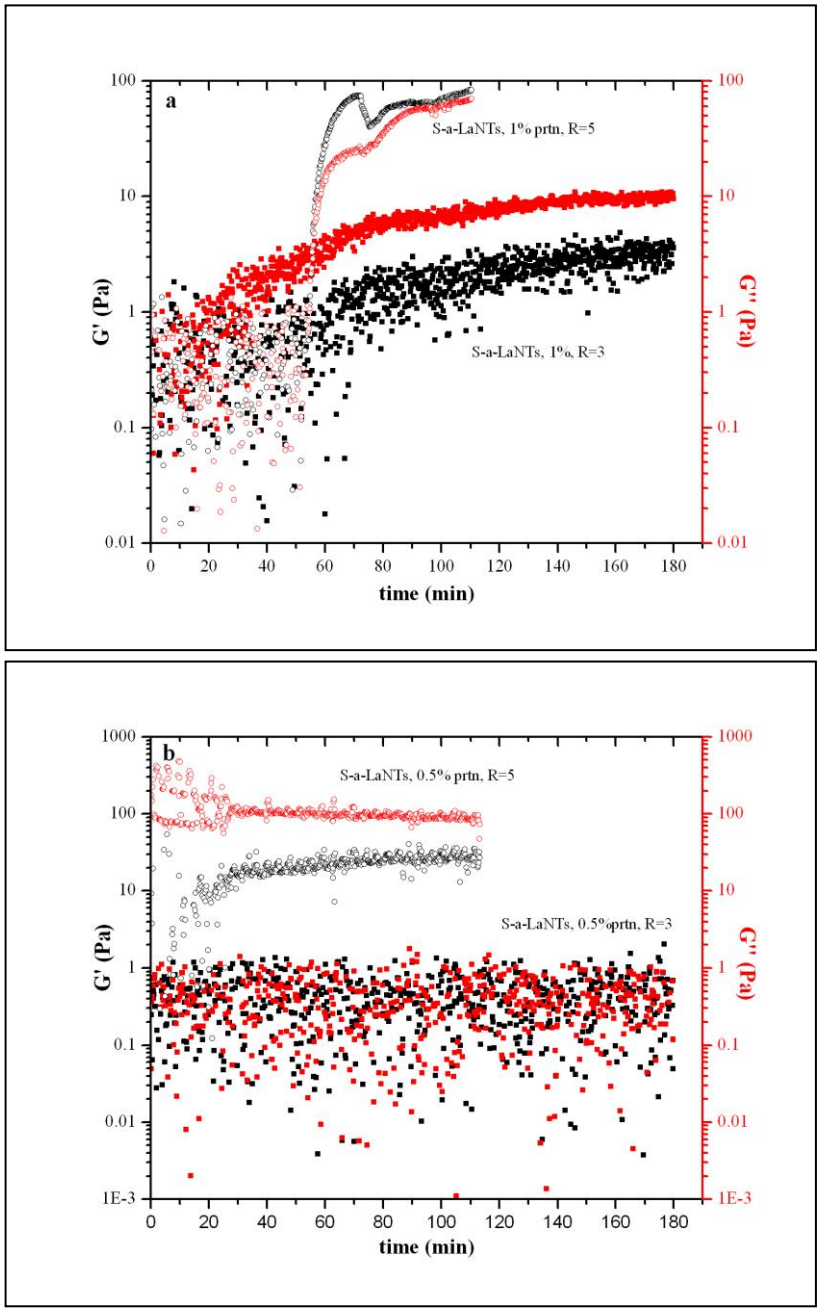

Figure 7.6. Young Modulus of nanotube growth in the case of varying Ca^{++} and α-La concentrations. a) 1 % prtn and Ca^{++}/a-La molar ratio (R) of 3 and 5, b) 0.5% prtn and Ca^{++}/α-La molar ratio of 3 and 5

Gelation process was also investigated by mixing α-LaNTs (formed using standard protein) with hemicellulose (HC). G' and G'' values were measured as 45950 and 12890 Pa, respectively. These are significantly greater than that of measured for α-LaNTs, itself. It is obvious that, addition of cellulosic fibers to the gel network established by α-La nanotubes strengthen existing network. Viscous behavior of α-La nanotubular gels and elastic behavior of α-LaNTs/HC gels are much more noticible.

Graveland-Bikker and de Kruif (2006) reported that cross-linking of a-LaNTs with dextran resulted in stiffer gels, upon increased dextran concentration. Our findings also support this.

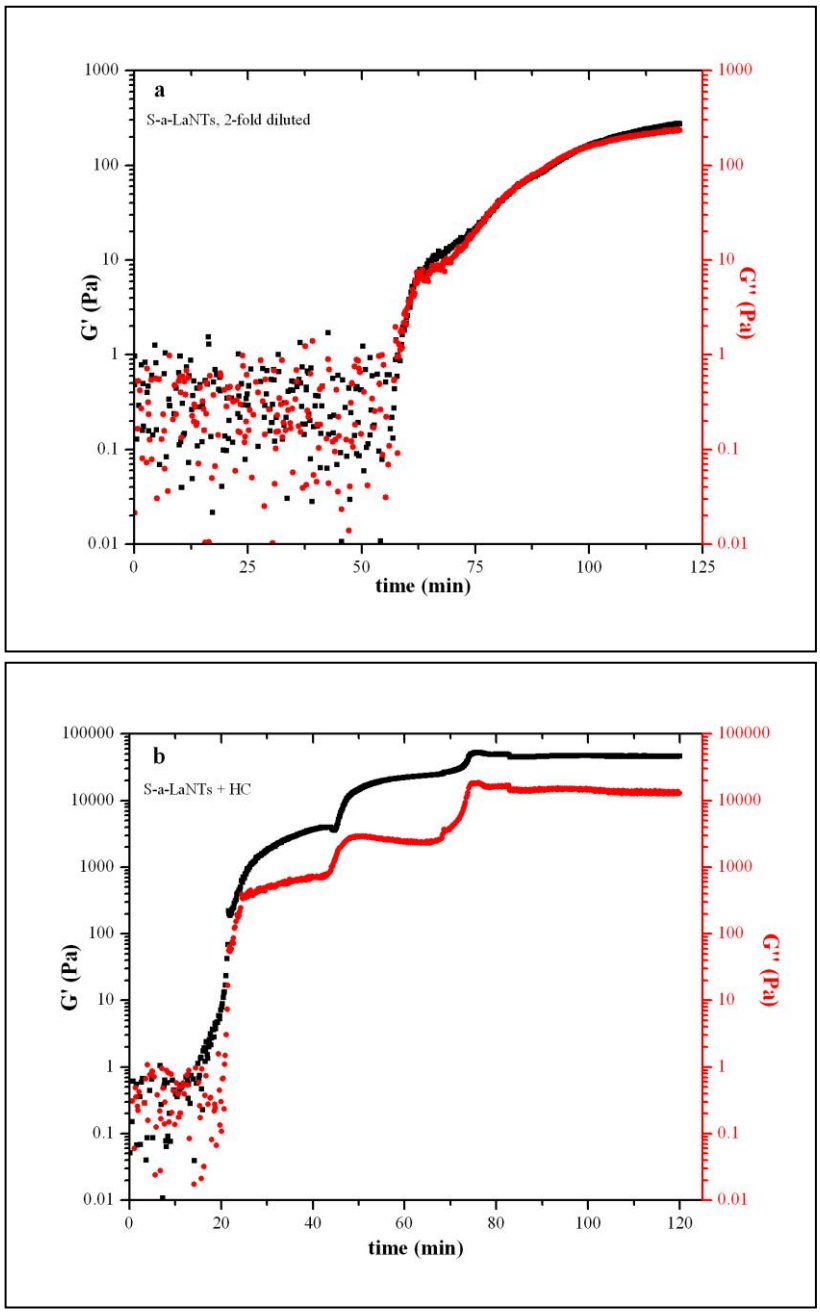

Figure 7.7. Young Modulus of S-α-LaNTs blended with hemicellulose (HC). a) S-α-LaNTs, 2-fold diluted, b) S-α-LaNTs mixed with HC

In conclusion, the growth of α-La nanotubes gives rise to formation of viscoelastic stiff gels to be used for various applications in food processing. The viscoelasticity and stiffness can be modified by blending with some polysaccharides.

7.2.3.2. Analysis of the Thermal Stability of α-Lactalbumin Nanotubes

Thermal stability of α-La protein, hydrolyzates and nanotubes was investigated by DSC and TGA. Figure 7.8.a represents DSC thermograms of protein, hydrolysate and nanotubes of standard α-La, and Figure 7.8.b represents thermograms of protein and nanotubes of purified α-La.

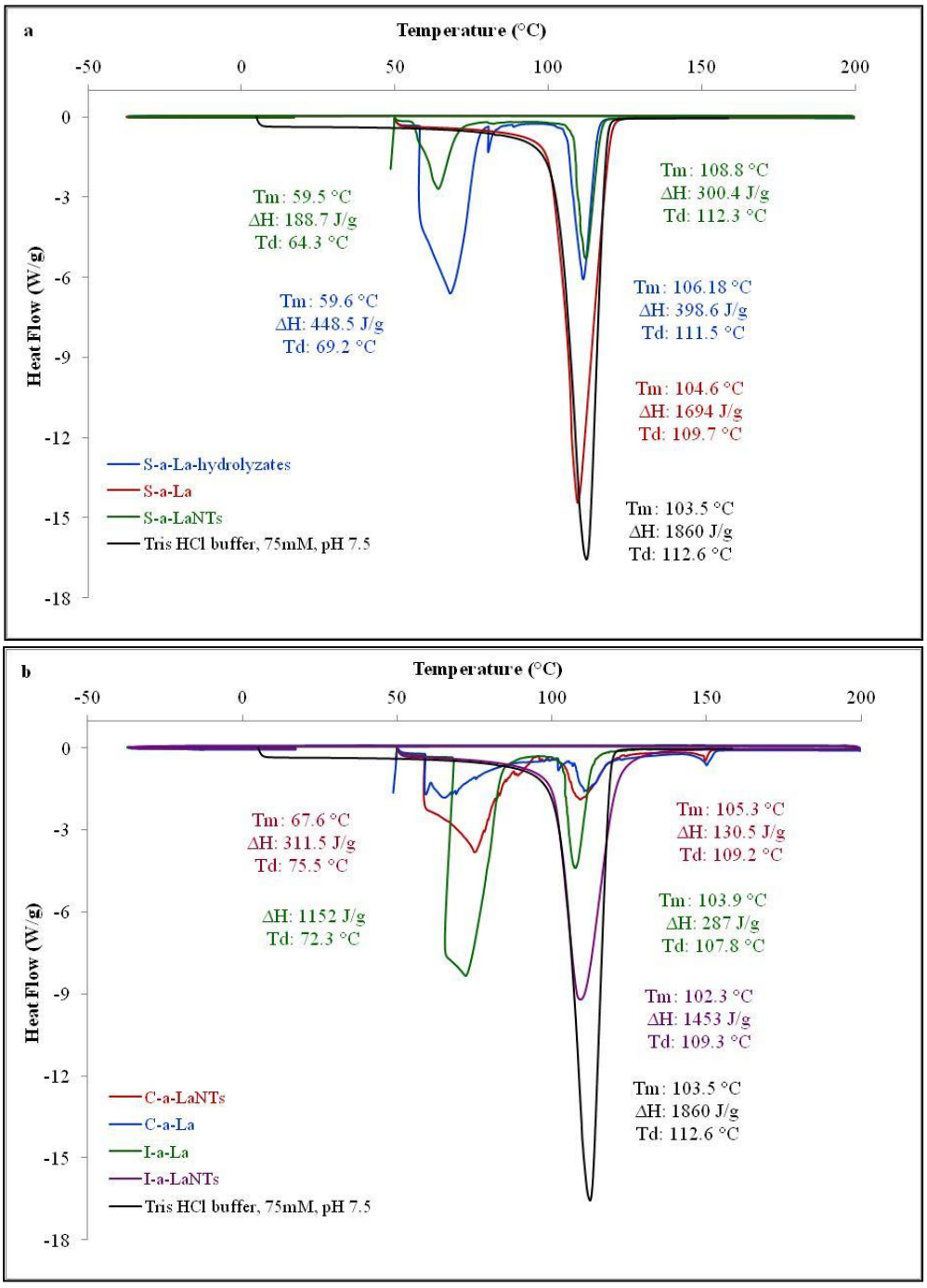

Figure 7.8. DSC thermograms of a) α-La, hydrolyzates and nanotubes of standard protein b) WPI and WPC based α-La, α-La nanotubes

Boye and Alli reported that Ca-bounded α-La showed denaturation peak at 64.3 ºC (Boye and Alli, 2000). In our study, the denaturation peak temperature detected for nanotubes and hydrolyzates produced from standard α-La were at 64.3 ºC and 69.2 ºC (Figure 7.8.a). The water evaporation peaks were detected at 100 – 110 ºC. The melting points (T_m) were shifted to lower temperatures when we ordered as nanotubes, hydrolyzates, protein and buffer; however, the enthalpy changes were decreased in reversed order.

$$T_{mNTs} > T_{mHYD} > T_{mALA} > T_{mBUF}$$
$$\Delta H_{BUF} > \Delta H_{ALA} > \Delta H_{HYD} > \Delta H_{NTs}$$

This indicated nanotubular gels entrapped much more water and phase transition (evaporation) was occurred at higher temperatures. The denaturation temperature of purified α-La (WPI-based) was about 72 ºC, and that of α-LaNTs (WPC-based) was about 75 ºC (Figure 7.8.b). This is higher than that of standard α-La, most probably due to the high mineral content in purified proteins strengthen the structure. The minerals already bounded the water in medium, thus enthalpy change decreased significantly, in both protein and nanotube samples of purified proteins.

$$\Delta H_{BUF} > \Delta H_{NTs} > \Delta H_{ALA}$$

The glass transition temperatures (T_g) were detected as about 57 – 58 ºC for hydrolyzate and nanotubular gelation. However, T_g of α-La proteins could not be detected. It is reported that determination of T_g of globular proteins is difficult due to their complex secondary and tertiary structures, which results in a gradual increase in heat capacity during glass transition (Bell and Hageman, 1996; Zhou and Labuza, 2007). However, during hydrolysis the native tertiary structure was lost and the change in heat capacity became more evident.

The results of DSC assays revealed that nanotubular structures were denatured at around 64 °C and water in the medium was strongly adsorbed by the gel network. Water in the samples might affect the heat stability of nanotubes individually. Therefore, water effect was tried to cast out by lyophilizing samples prior to DSC analysis. In this case, the denaturation peak temperatures detected for protein, hydrolysates and nanotubes produced from standard α-La were 45 °C, 38 °C and 60 °C,

respectively (Figure 7.9). Although the hydrolysate and nanotube samples were lyophilized, peaks belonging to water were observed at around 103-106 °C. These peaks were smaller than to those observed in liquid samples as given in Figure 7.8.a. This means that a little amount of water was already present possibly due to insufficient lyophilization or moisture gain during storage after lyophilization until DSC analysis. No water peak in standard α-La sample which was used in the powdered form as already had been purchased.

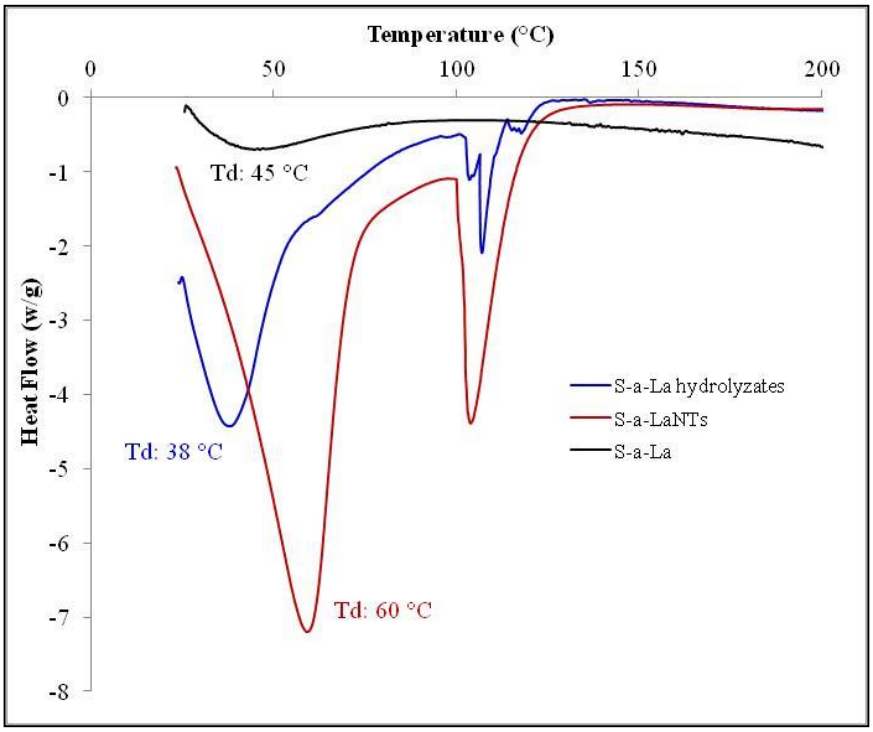

Figure 7.9. DSC thermograms of α-La, hydrolyzates and nanotubes of standard protein (lyophilized samples)

Significant difference was noticed in between denaturation temperature of hydrolyzates of liquid (69 °C) and lyophilized (38 °C) samples. Protein native structure which is folded, compact, globular and stabled by calcium binding was unfolded and destabilized during hydrolysis. New network formed by peptides might have lower thermal stability than compact native structure, especially in semi-dried form. This should need further investigation. The result of DSC analyses indicated that nanotubular structures could be stable up to ~60 °C. Food processing involving low heat treatments could be suggested for application of α-La nanotubes.

TGA curves of standard protein samples given in figure 7.10 showed that weight

loss, due to loss of water, occurred earlier and at lower temperature in α-La hydrolysates in comparison with the native α-La protein and nanotubes. This might be arised from bound of water by hydrolysate gels loosely relative to nanotubes. When compared the protein and nanotubes, weight loss was a little bit greater in nanotubes.

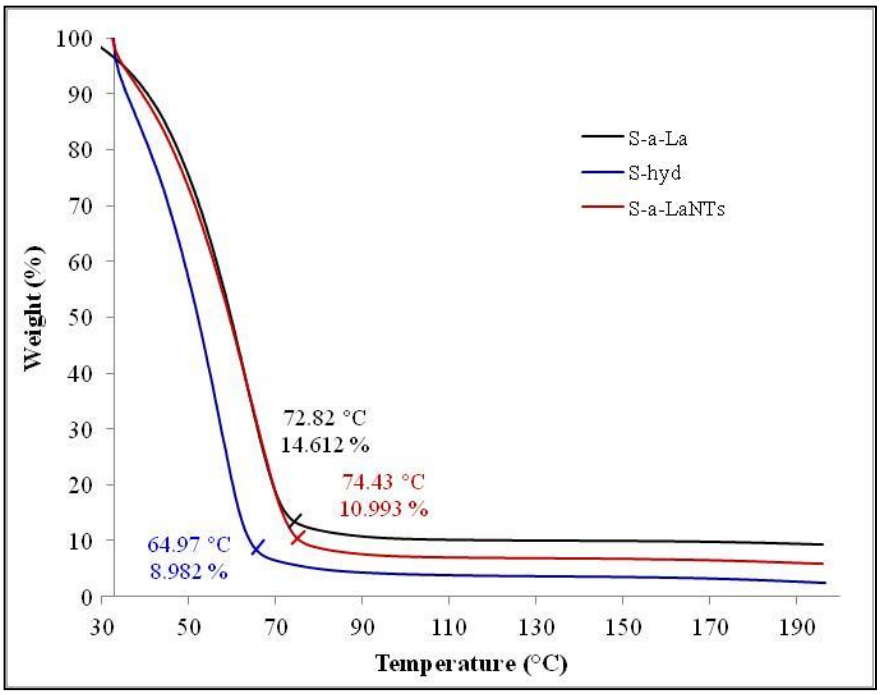

Figure 7.10. TGA curves of protein, hydrolysates and nanotubes of standard α-La protein

Table 7.1 summarizes weight losses in all samples of standard and purified proteins detected by TGA at phase transition (I), 100 °C (II) and 200 °C (III). Native protein and nanotubes were seened as more heat stable than hydrolysates.

Table 7.1. Weight losses in protein, hydrolysate and nanotube samples detected by TGA

sample	I		II		III	
	°C	%	°C	%	°C	%
S-α-La	72.82	14.612	100.00	10.254	196.00	9.245
S-α-La hyd	64.97	8.982	100.00	4.006	200.00	2.323
S-α-LaNTs	74.43	10.993	100.00	7.226	200.00	5.865
I-α-La	73.78	24.927	100.00	18.989	200.00	17.308
I-α-LaNTs	73.33	26.653	100.00	19.642	200.00	17.862
C-α-La	73.51	28.732	100.00	19.080	200.00	16.553
C-α-LaNTs	74.17	16.309	100.00	11.480	200.00	10.797

The possible reason for this was explained in the previous section (DSC results). Figure 7.11 a and b presented TGA curves of purified protein samples. No significant difference in weight loss was observed between I-α-La and I-α-LaNTs. However, remarkable weight loss was observed in C-α-LaNTs in comparison with the C-α-La. Weight loss difference was fair between S-α-La and S-α-LaNTs. When all the curves were compared, weight loss percentages were lower in the samples of purified proteins due to high mineral content.

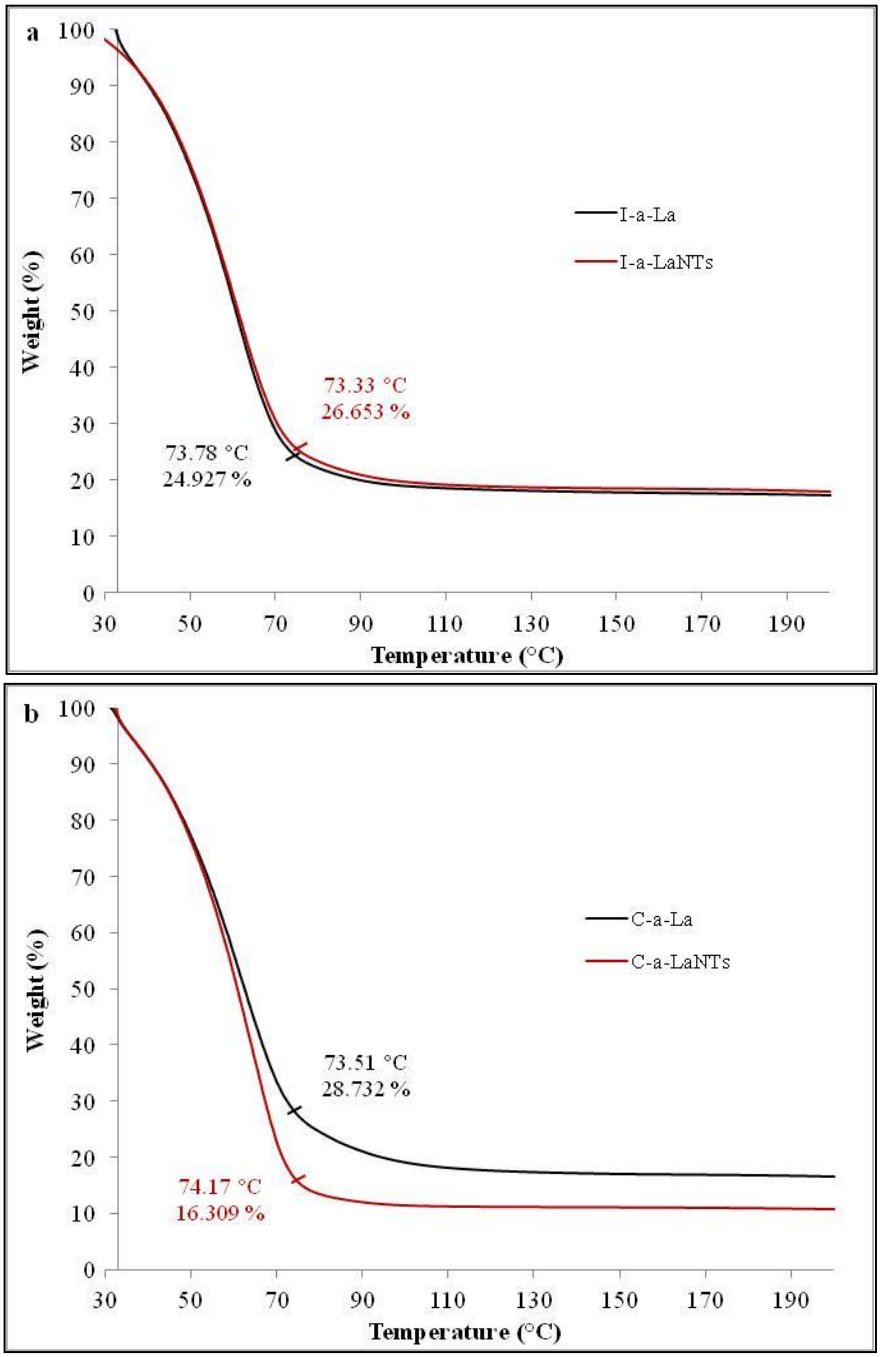

Figure 7.11. TGA curves of protein and nanotubes of a) WPI based α-La, b) WPC based α-La

7.2.3.3. Color-binding Capability of α-Lactalbumin Nanotubes

The α-LaNTs were investigated for dye binding capability. This capability is an important application area of them in food processing such as addition and stabilizing of coloring agents in food products. Congo red was chosen as representative coloring agent for this assay. It was mixed with a-La protein and a-LaNTs from both standard and purified proteins, and incubated in UV spectrophotometer. Absorbance values detected through incubation period were given in Figure 7.12. Absorbances were decreased when dye and nanotubes were mixed and incubated. This indicates the dye was absorbed by the gels of protein nanotubes and become more transparent. However, in the other cases, incubation of protein and dye mixture or incubation of them individually did not give such trends. According to this, protein nanotube gels might be effective in entrapment and carrying of such a coloring agent. The nanotubes formed by standard protein had desirable protein and calcium concentration, but purified ones were lower in protein and higher in calcium. This gave rise to obtain better trend in standard protein nanotubes and dye mixture. When the results of purified protein samples were compared with each other, I-α-La/CR mixture indicated better trend than C-α-La/CR. In fact, protein content of I-α-La was higher and calcium content was lower than those of C-α-La natively. As noticed in the results of the studies on gelation given above, both are critical parameters in gel formation, and its structure and appearance. Certain amount of protein is needed for gel formation primarily, and calcium is needed for nanotube growth to induce strong gel network. At high calcium concentrations, more random aggregates were induced, and this gave rise to formation of turbid gels (Graveland-Bikker et al., 2004). The appearances of the gels of purified proteins were not transparent as that of standard protein. The gel of I-α-La/CR mixture was clearer than the gel of C-α-La having non-uniform aggregates at the bottom of the gels. All these types of gels might be desirable according to application purpose.

The nanotubular gels can be used for various applications in food processing. One of them is the use of these gels as the carriers of natural colorants. The results of dye-binding assay revealed that the gel matrix entrapes coloring agents with transparent appearence. Therefore, the α-La nanotubular gels can be enriched with the natural coloring agents and used for coating applications, in pastry and candy industries.

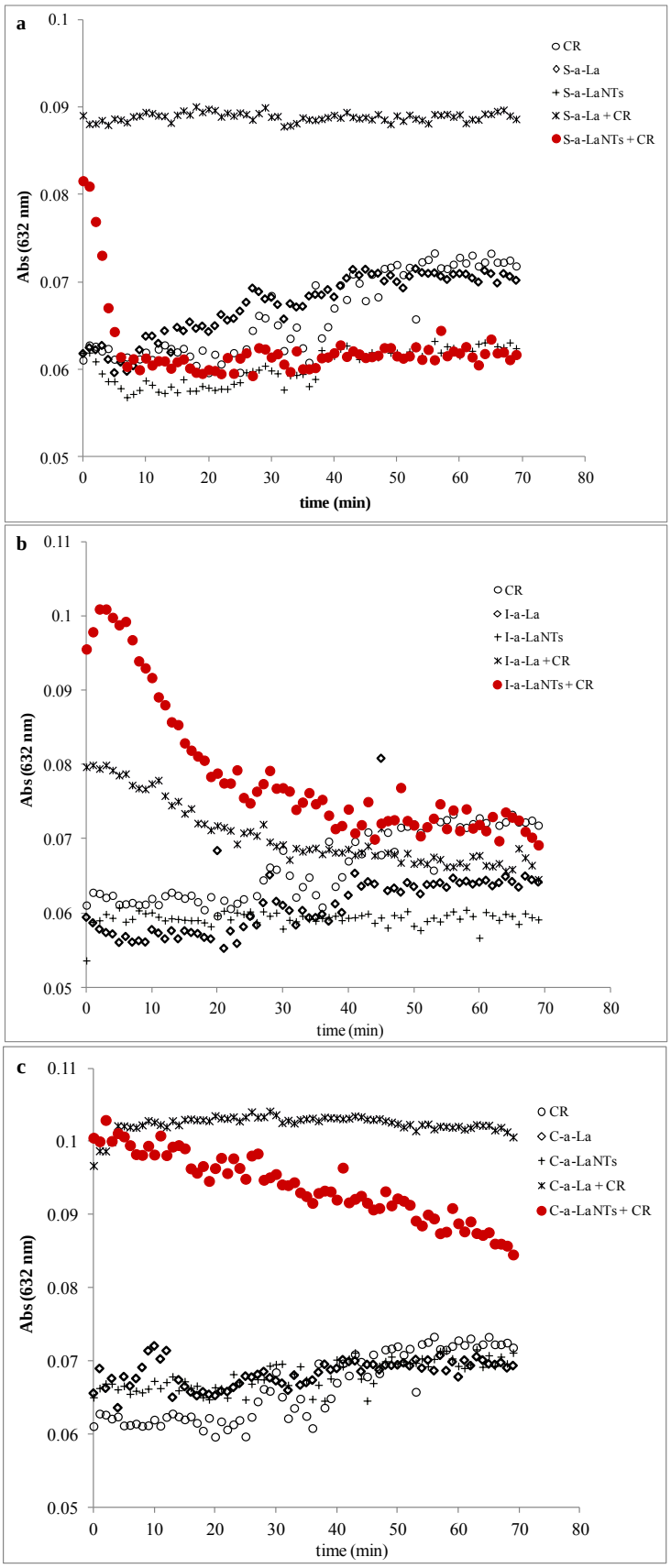

Figure 7.12. Color-binding capability of nanotubular gels formed by a) standard α-La, b) WPI-based α-La and c) WPC-based α-La proteins. CR: congo red

7.2.3.4. Encapsulation / Binding of Catechin by Nanotubes

Some experiments related to encapsulation of a bioactive material by using α-LaNTs were performed. Green tea phenolic, epicatechin gallate (ECg) was used in this studies. Nanotube- ECg mix prepared at three different pH, incubated in RT and +4 °C up to 72 h by slow shaking, and changing ECg amounts were followed by UV spectrometry. All raw data obtained are given in Appendix C1. Figure 7.13 depicts binding efficiency of ECg to α-LaNTs depending on pH. Most of catechin in the medium was cought by α-LaNTs in first 15 minute. At this time, efficiency reaches to nearly 85-88 %, at 30 minute free ECg amount increased and the efficiency dropped down to 69-75 %. Measurements taken at 1, 3 and 6 h showed an important decrease in binding of ECg by α-LaNTs, representing fluctuating efficiency between 5 - 42%. At 24 h, binding efficiency increases to 94-98 %. It was followed by a decrease in 48 h (74-75%) and an increase in 72 h (% 94-97), respectively. The results taken in these studies carried out at three different pH values were closer. This indicates that pH had no affect on binding of ECg by α-LaNTs.

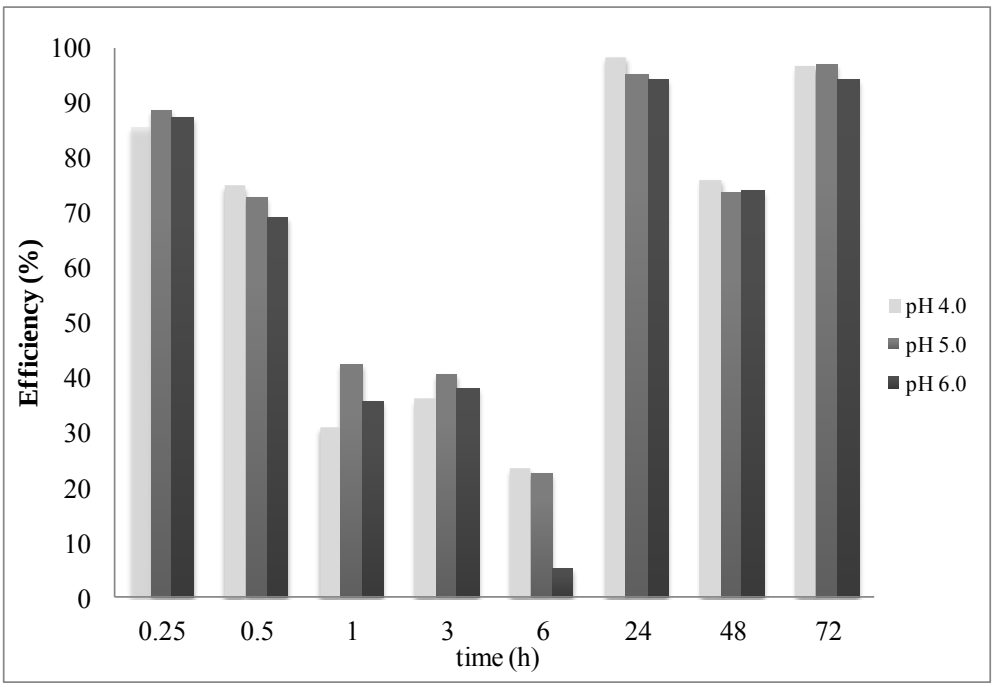

Figure 7.13. Binding efficiency of ECg to α-LaNTs depending on pH

Measurements taken in different time intervals during 72 hour-incubation indicated that binding of catechin by α-LaNTs did not occur in a stable form, but

occurred as repeated unstable binding and releasing steps. When the table C1 was analyzed, it was seen that free catechin concentration found in the medium at the beginning was 0.1 mg/ml, but this decreased and increased in the progressing sampling times. ECg was loaded by α-LaNTs highly in the first 15 – 30 th minutes, after dropping in the middle period, again it was loaded by nanotubes highly in 24 – 72 hours. The samplings at 24, 48 and 72 hours were also made from incubation at +4 °C. Both, RT and +4 °C, also gave similar results for this encapsulation study.

Nevertheless, this encapsulation trail provided a general idea about the possibility of loading a bioactive agent into the constructed α-La nanotubes. In fact, it is the first step for the development of experimental procedure and analysis of data, especially. In the following studies, more experimental trails for encapsulation and/or entrapment purposes should be carried out. In addition, more detailed identification of this binding, testing a different bioactive agent, and analysis for the most stable form of binding should be investigated.

7.3. Conclusions

In this chapter, investigations of α-La nanotubes related to gelation properties, thermal stability and capability of binding and /or entrapment of a coloring agent or bioactive material were presented. Gelation was triggered in both cases of protein hydrolysis and nanotube growth. But, more viscous and stiffer gels were obtained in the case of nanotube formation. The viscoelasticity and stiffness of these gels were modified by blending with some polysaccharides. Both protein and calcium concentrations were critically affected gel formation in terms of gelation time and gel stiffness. According to DSC analysis, thermal denaturation of the nanotube and hydrolysate gels occured at ~ 64 and 69 °C, however they were stable up to 60 and 38 °C in dried form. TGA curves indicated that α-La hydrolysates had higher weight loss at lower temperature than α-La nanotubes. This indicates that nanotubular gel network bounds water better than hydrolysate gel network. The gel matrix of nanotubes entraped coloring agents with transparent appearence. Therefore, the α-La nanotubular gels can be enriched with the natural coloring agents and used for various applications in industry. Preliminary experiments on encapsulation of ECg with nanotubes indicated that ECg interacted by α-La nanotubes but this was an unstable process. The α-La

nanotubes might be an effective matrix in loading a bioactive agent. Further studies should include more detailed analysis related to identification of binding of ECg or different bioactive agents to α-LaNTs and detection of the most stable conditions.

CHAPTER 8

CONCLUSION

Proteins and peptides extracted from various food sources are important matrices providing improved technological features in application. They have another attractive ability being researched recently, is the fabrication of nano-scale structures, promising novel potential applications in food nanotechnology concept. Alpha-lactalbumin (α-La), the second major protein in whey is able to form nanotubular structures by self-assembly after partial hydrolysis with protease. This is the main focus of the presented PhD study.

The objective of this PhD thesis was to develop and characterize whey based α-La nanotubes for food applications. In order to achieve this, both commercial and purified α-La fractions were used. The whole thesis study comprised of three major experimental section. The first experimental part included purification of α-Lactalbumin from whey powder (WP) kindly supplied from a dairy company, Pınar A.Ş. and whey protein isolate (WPI) supplied commercially. As WP was low in protein content and high in lactose as being poorly processed dairy by-product, it was subjected to ultrafiltration to eliminate lactose and concentrate target proteins prior to chromatography. The resultant retentate fraction, whey protein concentrate (WPC) and the commercial product WPI were then feed to anion exchange chromatography and size exclusion chromatography for purification of α-La individually. The purified fractions were characterized by SDS-PAGE, RP-HPLC, 2D-IEF, XRF and mass spectrometry. Finally, two target protein fractions were obtained as WPI based α-La and WPC based α-La, to be used for the development of nanotubes. In the second experimental part, protein nanotubes were constructed using commercial standard and purified fractions of α-La. Nanotube development was occured by self assembly of peptide molecules after partial hydrolysis of protein with BLP enzyme, as reported in previous studies cited many times within the thesis. The constructed nanotubes were characterized by series of experiments with various techniques. These includes microscopic analysis of nanotubes with TEM and AFM, optical investigation of the constructed structures by Raman and FT-IR Spectroscopy and analysis of nanotube growth by DLS and UV-Spectrophotometry, and analysis of hydrolysis process and

peptides by HPLC and MALDI-TOF MS. The last experimental section consisted investigation of α-La nanotubes in relation with the food applications. Gelation ability, thermal stability, and capability of binding and/or entrapment of a colorant and a bioactive agent were studied. The results were discussed in detailed in the subsequent chapters. The main conclusions were presented in the following according to experimental order.

Lactose removal and concentration of target proteins were achieved by diafiltration assisted ultrafiltration mostly after three UF runs. Target protein α-La, and besides β-lg were purified individually from WPI and WPC. SDS-PAGE, HPLC, 2D-IEF and MS studies all indicated the high purity (nearly 95 % for WPI based α-La (I-α-La), and 99 % for WPC based α-La (C-α-La)) of α-La fractions. Protein recovery was also comparable with the current literature.

According to microscopy, α-La nanotubes were uniform hollow structures longer than 100 nm up to few microns with approximately 20 nm width, in consistency with the literature. Standard protein based nanotubes were regular strands mostly in bundled form, but the nanotubes of I-α-La were longer and exhibited chain-like fashion. Those of C-α-La were shorter, thinner and fibril-like regular structures. Secondary structure of α-La protein was dominated by α-helix structure, but in the cases of hydrolysates and nanotubes β-sheets became dominant. During hydrolysis native tertiary structure disturbs due to unfolding and β-structures are exposed. Nanotube growth occurs via β-sheet stacking, which most probably detected by optical spectroscopy. Asp and Glu sites which BLP cuts during hydrolysis are involved in calcium binding, thus this sites detected by infrared spectroscopy should be critical in nanotube elongation. Calcium to protein concentration ratio affects critically nanotube formation and stability. A certain level of protein and calcium was needed for this. Approximately, 95% of protein was hydrolyzed after 1h and new peptides (building blocks of nanotubes) were formed with different masses. Hydrolysis process was explained by the first order kinetic in consistant with the current literature. Both hydrolysis process and nanotube growth resulted in gel formation. But, in the case of nanotubes gelation started a little bit earlier and gel stiffness was increased remarkably. Nanotubes of standard protein produced transparent gels, but theose of purified proteins lead to formation of turbid gels due to low protein and high mineral content. The gels of all nanotube samples entrapped the coloring agent by enhancing transparency. Turbidity and aggregation increased in the gels of nanotubes of purified proteins, especially in C-

α-La. According to preliminary studies on encapsulation, binding of catechin to nanotubes occured as reversible with low stability.

Our findings indicated that α-La nanotubular structures can be suggested for thickening and gelation purposed industrial applications involving low and moderate heat treatments. Desirable transparency can be obtained by changing amount of calcium required for nanotube formation. Gel strength and elasticity can be improved by blending nanotubes with some polysaccharides such as cellulosic fibers. The color-binding capability of these nanotubes or nanotubular gels could make them available for use as the carriers of natural colorants.

This PhD thesis presented development and characterization of whey based α-La protein nanotubes, and some studies related to application of them. The remarkable differences of this work from proviously reported ones can be given as follows. One of them is the use of α-La protein fractions already purified from whey in beside of standard α-La for nanotube formation. This enabled comparison of a purified material with standard one in producing a functional ingredient by investigating characteristics and applicability. In fact, the main purpose behind this was to produce a value-added functional product by using a by-product as raw material. The other difference was investigation of structural changes in protein by optical spectroscopy during hydrolysis and nanotube growth. The other one was that investigation of calcium binding sites most probably involved in nanotube elongation by infra-red spectroscopy. These both issues related to α-La nanotubes have been reported as the first time according to our knowledge. In addition, analysis of thermal stability of the nanotubes by the given methods and studies on entrapment of a coloring agent by the nanotubular gels resulted in new findings. Further studies should include more detailed work related to food applications of these nanotubes. Gelation characteristic of nanotubes needs considerable care in combination with the practical applications. The use of nanoparticles in foods may lead to various concerns. Although these nanostructures are dairy based, their safety should be emphasized strongly by careful investigations. In this thesis work, α-La nanotubes were developed by self-assembly process. Future studies will include development of such protein nanotubes by layer by layer assembly in more controlled dimensions using porous inert templates with PFT technique described in chapter 3.

Food nanotechnology is newly developing research and application area. There are limited number of research study have been published. This PhD thesis work will hopefully make contributions to proceeding nanotechnology researches in food concept.

REFERENCES

Acharya, K.R.; Stuart, D.I.; Walker, N.P.C.; Lewis, M.; Phillips, D.C. Refined Structure of Baboon α-Lactalbumin at 1.7 Â Resolution Comparison with C-Type Lysozyme. *Journal of Molecular Biology* **1989**, 208, 99-127.

Acharya, K.R.; Ren, J.S.; Stuart, D.I.; Phillips, D.C.; Fenna, R.E. Crystal Structure Of Human α-Lactalbumin at 1.7 Å Resolution. *Journal of Molecular Biology* **1991**, 221, 571–581.

Ai, S.; Lu, G.; He, Q.; Li, J. Highly Flexible Polyelectrolyte Nanotubes, *Journal of American Chemical Society* **2003**, 125, 11140-11141.

Allianz and OECD Opportunities and Risks of Nanotechnology, Munich: Allianz **2005**

Alonso-Fauste, I.; Andrés, M.; Iturralde, M.; Lampreave, F.; Gallart, J.; Álava, M.A. Proteomic Characterization by 2-DE in Bovine Serum and Whey From Healthy and Mastitis Affected Farm Animals. *Journal of Proteomics*, **2012**, 75, 3015-3030.

Anderle, G.; Mendelsohn, R. Thermal Denaturation Of Globular Proteins Fourier Transform-Infrared Studies of the Amide III Spectral Region. *Biophysical Journal,* **1987**, 52, 69-74.

Anderson, P.J.; Brooks, C.L.; Berliner, L.J. Functional Identification of Calcium Binding Residues in Bovine α-Lactalbumin *Biochemistry*, **1997**, 36(39), 11648–11654.

Ambrose, E.J.; Elliot, A. Infrared Spectroscopic Studies of Globular Protein Structure. *Proceedings of the Royal Society of London. Series A* **1951**, 208 75-90.

Arntfeld, S.D.; Ismond, M.A.H.; Murray, E.D. Thermal Analysis of Food Proteins in Relation to Processing Effects. In *Thermal Analysis of Foods*; Harwalkar, V.R., Ma, C.Y. Eds.; Elsevier Applied Science, New York **1990**, p 51-91.

Aschaffenburg, R.; Drewry, J. Improved Method for The Preparation Of Crystalline Beta-Lactoglobulin and Alpha-Lactalbumin From Cow's Milk. *Biochemistry,* **1957**, 65, 273–277.

Ashton, L.; Blanch, E.W. pH-induced Conformational Transitions in α-lactalbumin Investigated with Two-dimensional Raman Correlation Variance Plots and Moving Windows, *Journal of Molecular Strucure* **2010**, 947, 132-138.

Badger, T.M.; Ronis, M.J.J.; Hakkak, R. Developmental Effects and Health Aspects of Soy Protein Isolate, Casein and Whey In Male and Female Rats. *International Journal of Toxicology* **2001**, 20, 165–174.

Barron, L.D.; Blanch, E.W.; Hecht, L. Unfolded Proteins Studied by Raman Optical Activity. *Advences in Protein Chemistry* **2002**, 62, 51-90.

Barth, C.A.; Behnke, U. Nutritional Significance of Whey and Whey Compenents. *Nahrug* **1997**, 41(1), 2–12.

Barth, A. Infrared Spectroscopy of Proteins. *Biochimica et Biophysica Acta* **2007**, 1767 1073–1101

BCC Research, NANO31D, January **2011**

Bell, L.N.; Hageman, M.J. Glass Transition Explanation for the Effect of Poly-Hydroxy Compounds on Protein Denaturation in Dehydrated Solids. *Journal of Food Science* **1996**, 61, 372–378

Birktoft, J.J.; Breddam, K. Glutamyl Endopeptidases. *Methods in Enzymology* **1994**, 244, 114-126.

Blanch, E.W.; Morozova-Roche, L.A.; Hecht, L.; Noppe, W.; Barron, L.D. Raman Optical Activity Characterization of Native and Molten Globule States of Equine Lysozyme: Comparison with Hen Lysozyme and Bovine α-Lactalbumin. *Biopolymers (Biospectroscopy)* **2000**, 57, 235–248.

Bosselaers, I.M.; Caessens, P.R.; Van Boekel, M.S.; Alink, G.M. Differential Effects of Milk Proteins, BSA and Soy Protein on 4NQO- or MNNG-induced SCEs in V79 Cells. *Food Chemistry and Toxicology* **1994**, 32, 905–911.

Bouwmeester, H.; Dekkers, S.; Noordam, M.Y.; Hagens, W.I.; Bulder, A.S.; de Heer, C.; ten Voorde, S.E.C.G.; Wijnhoven, S.W.P.; Marvin, H.J.P.; Sips, A.J.A.M. Review of Health Safety Aspects of Nanotechnologies in Food Production, *Regulatory Toxicology and Pharmacology* **2009**, 53(1), 52-62.

Boye, J.I.; Alli, I. Thermal Denaturation of Mixtures of α-Lactalbumin and β-Lactoglobulin: a Differential Scanning Calorimetric Study. *Food Research International* **2000**, 33, 673-682.

Bramaud, C.; Aimar, P.; Daufin, G. Whey protein fractionation: Isoelectric Precipitation of α-Lactalbumin Under Gentle Heat Treatment. *Biotechnology and Bioengineering,* **1997**, 56, 391–397.

Breddam, K.; Meldal, M. Substrate Preferences of Glutamic-Acid-Specific Endopeptidases Assessed by Synthetic Peptide Substrates Based on Intramolecular Fluorescence Quenching. *European Journal of Biochemistry* **1992**, 206**,** 103-107.

Brew, K.; Castellino, F.J.; Vanaman, T.C.; Hill, R.L. The Complete Amino Acid Sequence Of Bovine α-Lactalbumin. *Journal of Biological Chemistry* **1970**, 10, 4570–4582.

Brew, K.; Grobler, J.A. α-Lactalbumin. In *Advanced dairy chemistry: Proteins* (Vol.1); Fox, P. F. Ed.; Elsevier Science Publishers LTD, Essex, **1992**.

Bryant, C.M.; McClements, D.J. Molecular Basis of Protein Functionality with Special Consideration of Cold-Set Gels Derived From Heat-Denatured Whey. *Trends in Food Science & Technology* **1998**, 9, 143–151.

Caessens, P.W.J.R.; Visser, S.; Gruppen, H. Method for the Isolation of Bovine β-Lactoglobulin from a Cheese Whey Protein Fraction and physicochemical Characterization of Purified Product. *International Dairy Journal* **1997**, 7, 229–235.

Cayot, P.; Lorient, D. Structure-Function Relationships of Whey Proteins. In *Food Proteins and Their Applications*; Damodaran, S.; Paraf, A. Eds; Marcel Dekker, NewYork, **1997**; p 225-256

Chandra, N.; Brew, K.; Acharya, K.R. Structural Evidence for the Presence of a Secondary Calcium Binding Site in Human α-Lactalbumin. *Biochemistry* **1998**, 37, 4767-4772.

Chau, C.F.; Wu, S.H.; Yen, G.C. The Development of Regulations for Food Nanotechnology, *Trends in Food Science & Technology* **2007**, 18, 269-280.

Cheang, B.; Zydney, A.L. Separation of α-Lactalbumin and β-Lactoglobulin Using Membrane Ultrafiltration. *Biotechnology and Bioengineering* **2003**, 83, 201–209.

Cheryan, M. Ultrafiltration and Microfiltration Handbook, Technomic Publishing Co. Inc., USA, **1998**.

Chen, H.; Weiss, J.; Shadidi, F. Nanotechnology in Nutraceuticals and Functional Foods, *Food Technology* **2006**, 30-36.

Cheremisinoff, N.P. Membrane Seperation Technologies In *Handbook of Water and Waste Water Treatment Technologies*; Elsevier Inc., **2002**, p 335-371.

Chrysina, E.D.; Brew, K.; Acharya, K.R. Crystal Structure of Apo- and Holo-Bovine α-Lactalbumin at 2.2-A Resolution Reveal an Effect of Calcium on Inter-Lobe Interactions. *The Journal of Biological Chemistry* **2000**, 275, 37021-37029.

Clare, D.A.; Catignani, G.L.; Swaisgood, H.E. Biodefense Properties of Milk, the Role of Antimicrobial Proteins and Peptides. *Current Pharmaceutical Design* **2003**, 9, 1239–1255.

Clark, N.A.; Lunacek, J.H.; Benedek, G.B. A Study of Brownian Motion Using Light Scattering, *American Journal of Physics* **1970**, 38(5), 575-585.

Creusot, N.; Gruppen, H. Enzyme-Induced Aggregation and Gelation of Proteins, *Biotechnology Advances* **2007**, 25, 597–601.

Decher, G. Fuzzy Nanoassemblies: Toward Layered Polymeric Multicomposites, *Science* **1997**, 277, 1232-1237.

Decker, K.J. Wonder Waters: Fortified and Flavoured Waters. *Food Product Design* **2003**, 13(5), 57-74.

Demirci, M.; Şimşek, O.; Kurultay, Ş. Sütçülük Yan Ürünleri ve Gıda Sanayinde Kullanımları. Süt Mikrobiyolojisi Ve Katkı Maddeleri. VI. Süt ve Süt Ürünleri Sempozyumu Tebliğler Kitabı. (Editör Prof. Dr. Mehmet Demirci), **2000**, 219-226.

de Wit, J.N. Functional Properties of Whey Proteins. In *Developments of dairy chemistry* (Vol. 4); Fox, P.F. Ed.; Applied Science, London, **1989**.

de Wit, J.N. Nutritional and Functional Characteristics of Whey Proteins in Food Products. *Journal of Dairy Science* **1998**, 81, 597–602.

Dickinson, E. Milk Protein İnterfacial Layers and the Relationship to Emulsion Stability and Rheology. *Colloids and Surfaces B-Biointerfaces* **2001**, 20, 197–210.

Diem, M. Introduction to Modern Vibrational Spectroscopy. Wiley-Interscience, New York, **1993**.

Douberly, Jr.G.E.; Pan, S.; Walters, D.; Matsui, H. Fabrication of Protein Tubules: Immobilization of Proteins on Peptide Tubules, *Journal of Physical Chemistry B*, **2001**, 105, 7612-7618.

Doultani, S.; Turhan, K.N.; Etzel, M.R. Fractionation of Proteins From Whey Using Cation Exchange Chromatography. *Process Biochemistry* **2004**, 39, 1737-1743.

Eigel, W.N.; Butler, J.E.; Ernstrom, C.A.; Farrell, H.M.; Harwalkar, V.R.; Jenness, R. Nomenclature of Proteins of Cow's Milk: Fifth revision. *Journal of Dairy Science* **1984**, 67, 1599-1631.

ElAmin, A. Nanotechnology Targets New Food Packaging Products. **2005**. Available from: http://www.foodproductiondailyusa.com/news/ng.asp?id¼63147

ElAmin, A. Nanocantilevers Studied for Quick Pathogen Detection. **2006**. Available from: http://www.foodproductiondaily-usa.com/news/ng.asp?id¼70159

ETC Group. Action Group on Erosion, Technology and Concentration. The Potential Impacts of Nano-Scale Technologies on Commodity Markets: The Implications for Commodity Dependent Developing Countries. **2005**. Available from: http://www.etcgroup.org/upload/publication/45/01/southcentre.commodities.pdf

Evans, E.W. Uses of Milk Proteins in Formulated Foods. In *Developments in Food Proteins*; Hudson, B. J. F. Ed.; Applied Science, London, **1982**.

Ferrari, D.M.; Bianco, R.; Froche, C.; Loperena, L.M. Baker's Yeast Production From Molasses/Cheese Whey Mixtures. *Biotechnology Letters* **2001**, 23, 1-4.

Fernández, A.; Menéndez, V.; Riera, F. A.; Álvarez, R. Caseinomacropeptide Behaviour in a Whey Protein Fractionation Process Based on α-Lactalbumin Precipitation. *Journal of Dairy Research* **2011**, 78, 196–202.

Fletcher, A. Nanotech antioxidant system: food ingredients of the future. **2006**. Available from: http://www.foodnavigator.com/news/ng.asp?id¼64914

Foegeding, E.A.; Davis, J.P.; Doucet, D.; McGuffey, M.K. Advances in Modifying and Understanding Whey Protein Functionality. *Trends in Food Science & Technology* **2002**, 13, 151–159.

Fong, B.Y. ; Norris, C.S. ; Palmano, K.P. Fractionation of Bovine Whey Proteins and Characterisation by Proteomic Techniques, *International Dairy Journal* **2008**, 18, 23–46.

Fox, P.F. The Milk Protein System. In *Developments in Dairy Chemistry* (Vol. 4); In Fox, P.F. Ed.; Applied Science, London, **1989**.

Gardner, E.. Brainy Food: Academia, Industry Sink Their Teeth into Edible Nano. **2003**. Small Time Correspondent. www.smalltimes.com.

Garfin, D.E. Two-dimensional Gel Electrophoresis: A Review. *Trends in Analytical Chemistry* **2003**, 22(5) 263-272.

Galvani, M.; Hamdan, M.; Righetti, P.G. Two-Dimensional Gel Electrophoresis/Matrix-Assisted Laser Desorption/Ionisation Mass Spectrometry Of Commercial Bovine Milk. *Rapid Communications* in *Mass Spectrometry* **2001**, 15, 258-264.

Geankoplis, C.G. Transport Process and Unit Operations, Third Edition, Prentice-Hall International Inc., **1993**.

Gerberding, S.J.; Byers, C.H. Preparative Ion-Exchange Chromatography of Proteins From Dairy Whey. *Journal of Chromatography A* **1998**, 808, 141–151.

Gill, H.S.; Cross, M. L. Anticancer Properties of Bovine Milk. *British Journal of Bovine Milk* **2000**, 84, 161–165.

Goers, J.; Permyakov, S.; Permyakov, E.; Uversky, V.; Fink, A. Conformational Prerequisites for Alpha-Lactalbumin Fibrillation. *Biochemistry* **2002**, 41, 12546-12551.

Graveland-Bikker, J.F.; Ipsen, R.; Otte, J.; de Kruif, C.G. Influence of Calcium on the Self-Assembly of Partially Hydrolyzed α-Lactalbumin. *Langmuir* **2004**, 20, 6841-6846.

Graveland-Bikker, J.F. Self-Assembly of Hydrolysed α-Lactalbumin into Nanotubes, PhD Dissertation, Utrecht University, The Netherlands, **2005**.

Graveland-Bikker, J.F.; Fritz, G.; Glatter, O.; de Kruif, C.G. Growth and Structure of α-Lactalbumin Nanotubes, *Journal of Applied Crystallography* **2006a**, 39, 180–184.

Graveland-Bikker, J.F.; Schaap, I.A.T.; Schmidt, C.F.; de Kruif, C.G. Structural and Mechanical Study of a Self-Assembling Protein Nanotube. *Nano Letters* **2006b**, 6, 616–621.

Graveland-Bikker, J.F.; de Kruif, C.G. Unique Milk Protein Based Nanotubes: Food and Nanotechnology Meet, *Trends in Food Science & Technology* **2006**, 17, 196-203.

Graveland-Bikker, J.F.; Koning, R.I.; Koerten, H.K.; Geels, R.B.J.; Heeren, R.M.A.; de Kruif, C.G. Structural Characterization of α-Lactalbumin Nanotubes. *Soft Matter* **2009**, 5, 2020–2026.

Hamouda, T.; Baker, Jr.J.R. Antimicrobial Mechanism of Action of Surfactant Lipid Preparations in Enteric Gram-Negative Bacilli. *Journal of Applied Microbiology* **2000**, 89, 397-403.

Hartgerink, J.D.; Granja, J.R.; Milligan, R.A.; Ghadiri, M.R. Self-Assembling Peptide Nanotubes, *Journal of American Chemical Society* **1996**, 118, 43-50.

Hazen, C. Formulating Function into Beverages. *Food Product Design* **2003**,12(10), 36-70.

Heller, L. Flavor Firm Uses Nanotechnology for New İngredient Solutions. **2006**. Available from: http://www.confectionerynews.com/news/ng.asp?id¼69008

Hiraoka, Y.; Segawa, T.; Kuwajima, K.; Sugai, S.; Moroi, N. α-Lactalbumin: a Calcium Metallo-Protein. *Biochemical and Biophysical Research Communications* **1980**, 95, 1098-1104.

Hou, S.; Wang, J.; Martin, C.R. Template-Synthesized Protein Nanotubes, *Nano Letters*, **2005**, 5(2), 231-234.

IFST (Institute of Food Science and Technology), Nanotechnology. 2006. Available from http://www.ifst.org/uploadedfiles/cms/store/ATTACHMENTS/Nanotechnology.pdf

Ikeda, S.; Li-Chan, E.C.Y. Raman Spectroscopy of Heat-Induced Fine-Stranded and Particulate β-Lactoglobulin Gels. *Food Hydrocolloids* **200**4, 18, 489–498.

Ipsen, R.; Otte, J.; Qvist, K.B. Molecular Self-Assembly of Partially Hydrolysed α-Lactalbumin Resulting in Strong Gels with a Novel Microstructure. *Journal of Dairy Research* **2001**, 68, 277-286.

Ipsen, R.; Otte, J. Nano-Structuring by Means of Proteolysis Rheology of Novel Gels From α-Lactalbumin. *Annual Transactions of the Nordic Rheology Society* **2003**, 11, 89-93.

Ipsen, R.; Otte, J. Self-Assembly of Partially Hydrolysed α-Lactalbumin *Biotechnology Advances* **2007**, 25, 602-605.

Jackson, M.; Mantsch, H.H. The use and misuse of FTIR spectroscopy in the determination of protein structure. *Critical Reviews in Biochemistry and Molecular Biology* **1995**, 30(2), 95-120.

Jung, Y.A.; Choi, D.Y.; Hong, S.B.; Row, K.H. Mobile Phase Composition for Resolving Whey Proteins in Reversed-Phase High Performance Liquid Chromatography. *Korean Journal of Chemical Engineering* **2003**, 20(4), 705-708.

Kaittanis, C.; Naser, S.A.; Perez, J.M. One-Step, Nanoparticle-Mediated Bacterial Detection with Magnetic Relaxation. *Nano Letters* **2007**, 7(2), 380-383.

Kakudo, S.; Kikuchi, N.; Kitadokoro, K.; Fujiwara, T.; Nakamura, E.; Okamoto, H.; Shin, M.; Tamaki, M.; Teraoka, H.; Tsuzuki, H.; Yoshida, N. Purification, Characterisation, Cloning and Expression of a Glutamic Acid-Specific Protease From *Bacillus licheniformis* ATCC 14580. *The Journal of Biological Chemistry* **1992**, 267, 23782-23788.

Kamau, S.M., Cheison, S.C.; Chen, W.; Liu, X.M.; Lu, R.R. Alpha-Lactalbumin: Its Production Technologies and Bioactive Peptides. *Comprehensive Reviews in Food Science and Food Safety* **2010**, 9, 197-212.

Kavacık, B.; Topaloğlu, B. Peynir Altı Suyu ve Gübre Karışımından Biyogaz Üretimi. 7. Ulusal Çevre Mühendisliği Kongresi, *Yaşam Çevre Teknoloji,* İzmir, Ekim 2007.

Kentsis, A.; Borden, K.L.B. Physical Mechanisms and Biological Significance of Supramolecular Protein Self-Assembly. *Current Protein and Peptide Science* **2004**, 5, 125-134.

Kitagawa, T.; Azuma, T.; Hamaguchi, K. The Raman Spectra of Bence-Jones Proteins. Disulfide Stretching Frequencies and Dependence of Raman Intensity of Tryptophan Residue on Their Environments. *Biopolymers* **1979**, 18, 451-465.

Kong, J.; Yu, S. Fourier Transform Infrared Spectroscopic Analysis of Protein Secondary Structures. *Acta Biochimica et Biophysica Sinica* **2007**, 39(8), 549–559.

Konrad, G.; Kleinschmidth, T. A New Method for Isolation of Native α-Lactalbumin From Sweet Whey. *International Dairy Journal* **2008**, 18, 47-54.

Krimm, S.; Bandekar, J. Vibrational Spectroscopy and Conformation of Peptides, Polypeptides, and Proteins. *Advances in Protein Chemistry* **1986**, 38, 181–367.

Kristiansen, K.R.; Otte, J.; Ipsen, R.; Qvist, K.B. Large Scale Preparation of β-Lactoglobulin A and B by Ultrafiltration and Ion-Exchange Chromatography. *International Dairy Journal* **1998**, 8, 113-118.

Laemmli, U.K. Cleavage of Structural Proteins During the Assembly of the Head of Bacteriophage T4. *Nature* **1970**, 227, 680–685.

Li, Y.; Tseng, Y.D.; Kwon, S.Y.; Despaux, L.; Bunch, J.S.; Mceuen, P.L. Controlled Assembly of Dendrimer-Like DNA. *Nature Materials* **2004**, 3, 38-42.

Liang, M.; Chen, V.Y.T.; Chen, H.L.; Chen, W. A Simple and Direct Isolation of Whey Components From Raw Milk by Gel Filtration Chromatography and Structural Characterization by Fourier Transform Raman Spectroscopy. *Talanta* **2006**, 69, 1269–1277.

Lindmark-Mansson, H.; Timgren, A.; Alde´n, G.; Paulsson, M. Two-Dimensional Gel Electrophoresis of Proteins and Peptides in Bovine Milk. *International Dairy Journal* **2005**, 15, 111–121.

Lord, R.C.; Yu, N.T. Laser-Excited Raman Spectroscopy of Biomolecules. I. Native Lysozyme and Its Constituent Amino Acids. *Journal of Molecular Biology* **1970**, 50(2), 509–524.

Lu, G.; Ai, S.; Li, J. Layer-by-Layer Assembly of Human Serum Albumin and Phospholipid Nanotubes Based on a Template. *Langmuir* **2005**, 21, 1679-1682.

Lu, G.; Komatsu, T.; Tsuchida, E. Artificial Hemoprotein Nanotubes, *Chemistry Communications* **2007**, 2980–2982.

Lucena, E.M.; Álvarez, S.; Menéndez, C.; Riera, F.A.; Álvarez, R. α-Lactalbumin Precipitation From Commercial Whey Protein Concentrates. *Separation and Purification Technology* **2007**, 52, 446–453.

Madureira, A.R.; Pereira, C.I.; Gomes, A.M.P.; Pintado, M.E.; Malcata, F.X. Bovine Whey Proteins – Overview on Their Main Biological Properties, *Food Research International* **2007**, 40, 1197–1211.

Mailliart, P.; Ribadeau-Dumas, B. Preparation of β-Lactoglobulin and β-Lactoglobulin-Free Proteins From Whey Retentate by NaCI Salting Out at Low pH. *Journal of Food Science* **1988**, 53, 743–745.

Markus, C.R.; Olivier, B.; de Haan, E.H. Whey Protein Rich in a-Lactalbumin Increases the Ratio of Plasma Tryptophan to the Sum of the Other Large Neutral Amino Acids and Improves Cognitive Performance in Stress-Vulnerable Subjects. *American Journal of Clinical Nutrition* **2002**, 75, 1051–1056.

MacIntosh, G.H.; Regester, G.O.; Leu, R.K.; Royle, P.J.; Smithers, G.W. Dairy Proteins Protect Against Dimethylhydrazine Induced Intestinal Cancers in Rats. *Journal of Nutrition* **1995**, 125, 809–816.

McIntosh, H.G.; Royle, P.J.; Leu, R.K.L.; Regester,G.O.; Johnson, M.A.; Grinsted, R.L.; Kenward, R.S.; Smithers, G.W. Whey Proteins as Functional Food Ingredients. *International Dairy Journal* **1998**, 8, 425-434.

Miura, T.; Takeuchi, H.; Harada, I. Tryptophan Raman Bands Sensitive to Hydrogen Bonding and Side-Chain Conformation. *Journal of Raman Spectroscopy* **1989**, 20 667–671.

Miura, T.; Thomas, G.J.Jr. Raman Spectroscopy of Proteins and Their Assemblies. In *Subcellular Biochemistry (Proteins: Structure, Function and Engineering);* Biswas, B.B. and Roy, S. Eds.; Plenum, New York, **1995**, p 55–99.

Mizuguchi, M.; Nara, M.; Kawano, K.; Nitta, K. FT-IR Study of the Ca^{2+}-Binding to Bovine α-Lactalbumin. *FEBS Letters* **1997**, 417, 153-156.

Nakanishi, M.; Takesada, H.; Tsuboi, M. Conformation of the Cystine Linkages in Bovine α-Lactalbumin as Revealed by Its Raman Effect. *Journal of Molecular Biology* **1974**, 89, 241-243.

Technical Information of Nano-Silver Powder. *Nanosilver* **2004**. Available from: http://www.nano-silver.net/eng/index.php

Nara, M; Tasumi, M.; Tanokurab, M.; Hiraoki, T.; Yazawa, M.; Tsutsumi, A. Infrared Studies of Interaction Between Metal Ions and Ca^{++}-Binding Proteins. *FEBS Letters* **1994**, 349, 84-88.

Nel, A.; Xia, T.; Madler, L.; Li, N. Toxic Potential of Materials at the Nanolevel. *Science,* **2006**, 311, 622-627.

Newman, H. New Use for Vegetable Oil: It's Like Bleach, But Edible. **2002**. Available from: www.freep.com/tech.

Neyestani, T.R.; Djalali, M.; Pezeshki, M. Isolation of α-Lactalbumin, β-Lactoglobulin, and Bovine Serum Albumin From Cow's Milk Using Gel Filtration and Anion-Exchange Chromatography Including Evaluation of Their Antigenicity *Protein Expression and Purification* **2003**, 29, 202–208.

Nickols-Richardson, S.M. Nanotechnology: Implications for Food and Nutrition Professionals. *Journal of American Diet Association* **2007**, 107(9), 1494-7.

Nonaka, M.; Li-Chan, E.; Naki, S. Raman Spectroscopic Study of Thermally Induced Gelation of Whey Proteins. *Journal of Agriculture and Food Chemistry* **1993**, 41, 1176-1181.

Oberdorster, G.; Maynard, A.; Donaldson, K.; Castranova, V.; Fitzpatrick, J.; Ausman, K. Principles for Characterizing the Potential Human Health Effects From Exposure to Nanomaterials: Elements of a Screening Strategy. *Particle and Fibre Toxicology* **2005**, 2(8).

OilFresh_ 1000, Frying Oil Reforming Catalytic Device. **2005**. Available from http://www.oilfresh.com/of1000.html

Ong, S.E.; Pandey, A. An Evaluation of the Use of Two-Dimensional Gel Electrophoresis in Proteomics. *Biomolecular Engineering* **2001**, 18, 195–205.

Ormrod, D.J., Miller, T.E. The Anti-İnflammatory Activity of a Low Molecular Weight Component Derived From the Milk of Hyperimmunized Cows. *Agents and Actions* **1991**, 32, 160–166.

Ostrovsky, A.V.; Kalinichenko, L.P.; Emelyanenko, V.I.; Klimanov, A.V.; Permyakov, E.A. Environment of Tryptophan Residues in Various Conformational States of α-Lactalbumin Studied by Time-Resolved and Steady-State Fluorescence Spectroscopy *Biophysical Chemistry* **1988**, 30(2), 105–112.

Otte, J.; Lomholt, S.B.; Ipsen, R.; Stapelfeldt, H.; Bukrinsky, J.T.; Qvist, K.B. Aggregate Formation During Hydrolysis of β-Lactoglobulin with a Glu and Asp Specific Protease From *Bacillus licheniformis. Journal of Agricultural and Food Chemistry* **1997**, 45, 4889–4896.

Otte, J.; Ipsen, R.; Ladefoged, A.M.; Sorensen, J. Protease-Induced Aggregation of Bovine α-Lactalbumin: Identification of the Primary Associating Fragment. *Journal of Dairy Research* **2004**, 71, 88-96.

Otte, J.; Ipsen, R.; Bauer, R.; Bjerrum, M.J.; Waninge, R. Formation of Amyloid-Like Fibrils Upon Limited Proteolysis of Bovine α-Lactalbumin, *International Dairy Journal* **2005**, 15, 219-229.

Ounis, W.B.; Gauthier, S.F.; Turgeon, S.L.; Roufik, S.; Pouli, Y. Separation of Minor Protein Components From Whey Protein Isolates by Heparin Affinity Chromatography. *International Dairy Journal* **2008**, 18, 1043–1050.

Permyakov, E.A.; Kalinichenko, L.P.; Morozova, L.A.; Yarmolenko, V.V.; Burstein, E.A. α-Lactalbumin Binds Magnesium Ions: Study by Means of Intrinsic Fluorescence Technique. *Biochemical and Biophysical Research Communications* **1981**, 102, l-7.

Permyakov, E.A.; Morozova, L.A.; Burstein, E.A. Cation Binding Effects on the pH, Thermal and Urea Denaturations in α-Lactalbumin. *Biophysical Chemistry* **1985**, 21, 21-31.

Permyakov, S.E.; Veprintsev, D.B.; Brooks, C.L.; Permyakov, E.A.; Berliner, L.J. Zinc Binding in Bovine α-Lactalbumin: Sequence Homology May Not Be a Predictor of Subtle Functional Features. *Proteins: Structure, Function and Genetics* **2000**, 40, 106-111.

Permyakov, E.A.; Shnyrov, V.L.; Kalinichenko, L.P.; Kuchar, A.; Reyzer, I.L.; Berliner, L.J. Binding of Zn(II) Ions to Alpha-Lactalbumin. *Journal of Protein Chemistry* **1991**, 10, 577-584.

Pike, A.C.W.; Brew, K.; Acharya, K.R. Crystal Structures of Guinea-Pig, Goat and Bovine α-Lactalbumins Highlight the Enhanced Conformational Flexibility of

Regions That are Significant for Its Action in the Lactose Synthase. *Structure* **1996**, 4, 691-703.

Pintado, M.E.; Macedo, A.C., Malcata, F.X. Review: Technology, Chemistry and Microbiology of Whey Cheese. *Food Science and Technology International* **2001**, 7, 105–116.

Polat, Z. Integrated Approach to Whey Utilization Through Natural Zeolite Adsorption/Desorption and Fermentation. PhD Dissertation, İzmir Institute of Technology, İzmir, Turkey, **2009**.

Puyol, P.; Pe´rez, M.D.; Ena, J.M.; Calvo, M. Interaction of β-Lactoglobulin and Other Bovine and Human Whey Proteins With Retinol and Fatty Acids. *Agricultural and Biological Chemistry* **1991**, 10, 2515–2520.

Rajagapol, K.; Schneider, J.P. Self-Assembling Peptides and Proteins for Nanotechnological Applications, *Current Opinion in Structural Biology* **2004**, 14, 480-486.

Rava, R.P.; Spiro, T.G. Ultraviolet Resonance Raman Spectra of Insulin and α-Lactalbumin With 218-and 200-nm Laser Excitation. *Biochemistry* **1984**, 24, 1861-1865.

Roach, S. Nanotechnology Passes First Toxicity Hurdle. **2006**. Available from: http://www.foodproductiondaily-usa.com/news/ng.asp?id¼69557

Sanguansri, P.; Augustin, M.A. Nanoscale Materials Development - A Food Industry Perspective. *Trends in Food Science & Technology* **2006**, 17, 547-556.

Santos, M.J.; Teixeira, J.A.; Rodrigues, L.R. Fractionation of the Major Whey Proteins and Isolation of β-Lactoglobulin Variants by Anion Exchange Chromatography. *Separation and Purification Technology* **2012**, 90, 133–139.

Santoso, S.S.; Vauthey, S.; Zhang, S. Structures, Function and Applications of Amphiphilic Peptides. *Current Opinion in Colloid & Interface Science* **2002**, 7, 262-266.

Scanlon, S.; Aggeli, A. Self-Assembling Peptide Nanotubes. *Nanotoday* **2008**, 3, 22-30.

Semo, E.; Kesselman, E.; Danino, D.; Livney, Y.D. Casein Micelle as A Natural Nano-Capsular Vehicle for Nutraceuticals. *Food Hydrocolloids* **2007**, 21, 936-942.

Shefer, A.; Shefer, S.D. Multicomponent Controlled Release System for Oral Care, Food Products, Nutraceutical and Beverages. US2005/0112235 A1. United States Patent Application, **2005**.

Sözer, S.; Yaldız, O. Sığır Gübresi Ve Peynir Altı Suyu Karışımlarından Biyogaz Üretimi Üzerine Bir Araştırma, *Akdeniz Üniversitesi Ziraat Fakültesi Dergisi* **2006**, 19(2), 179-183.

Spiro, T.G.; Gaber, B.P. Laser Raman Scattering As A Probe of Protein Structure *Annual Review of Biochemistry* **1977**, 46, 553-572.

Sugai, S.; Ikeguchi, M. Conformational Comparison Between Alpha-Lactalbumin and Lysozyme. *Advances in Biophysics* **1994**, 30, 37-84.

Svendsen, I.; Breddam, K. Isolation and Amino Acid Sequence of A Glutamic Acid Specific Endopeptidase From *Bacillus licheniformis*. *European Journal of Biochemistry* **1992**, 204, 165-171.

Stuart, D.I.; Acharya, K.R.; Walker, N.P.C.; Smith, S.G.; Lewis, M.; Philips, D.C. Alpha-Lactalbumin Possesses A Novel Calcium Binding Loop. *Nature* **1986**, 324, 84-87.

Tian, Y.; He, Q.; Cui, Y.; Li, J. Fabrication of Protein Nanotubes Based on Layer-by-Layer Assembly *Biomacromolecules* **2006**, 7, 2539-2542.

Tu, A.T. Peptide Backbone Conformation and Microenvironment of Protein Side Chains in Spectroscopy of Biological Systems In: *Spectroscopy of Biological Systems.* Clark, R.J.H.; Haster, R.E. Eds.; John Wiley & Sons, New York, **1986**, p 47–112.

Wang, Q.; Allen, J.C.; Swaisgood, H.E. Binding of Vitamin D and Cholesterol to β-Lactoglobulin. *Journal of Dairy Science* **1997**, 80, 1054–1059.

Weiss, J.; Takhistov, P.; Mcclements, D.J. Functional Materials in Food Nanotechnology. *Journal of Food Science* **2006**, 71(9), 107-116.

Wilson, G.; Ford, S.J.; Cooper, A.; Hecht, L.; Wen, Z.Q.; Barron, L.D. Vibrational Raman Optical Activity of Alpha-Lactalbumin: Comparison With Lysozyme, and Evidence for Native Tertiary Folds in Molten Globule States. *Journal of Molecular Biology* **1995**, 254(4), 747–760.

Wong, D.W.S.; Camirand, W.M.; Pavlath, A.E. Structures and Functionalities of Milk Proteins. *Critical Reviews in Food Science and Nutrition* **1996**, 36, 807-844.

Wu, S.Y.; Pe´rez, M.D.; Puyol, P.; Sawyer, L. β-Lactoglobulin Binds Palmitate Within Its Central Cavity. *Journal of Biological Chemistry* **1999**, 274, 170–174.

Xie, M.X.; Liu, Y. Studies on Amide III Infrared Bands for the Secondary Structure Determination of Proteins. *Chemical Journal of Chinese Universities* **2003**, 24(2), 226-231.

Yamada, M.; Murakami, K.; Wallingford, J.C.; Yuki, Y. Identification of Low Abundance Proteins of Bovine Colostral and Mature Milk Using Two-Dimensional Electrophoresis Followed by Microsequencing and Mass Spectrometry. *Electrophoresis* **2002**, 23, 1153–1160.

Ye, X.; Yoshida, S.; Ng, T.B. Isolation of Lactoperoxidase, Lactoferrin, α-Lactalbumin, β-Lactoglobulin B and β-Lactoglobulin A From Bovine Rennet Whey Using Ion

Exchange Chromatography, *The International Journal of Biochemistry & Cell Biology* **2000**, 32, 1143–1150.

Yoshida, S. Isolation of β-Lactoglobulin and α-Lactalbumin by Gel Filtration Using Sephacryl S-200 and Purification by DEAE Ion Exchange Chromatography, *Journal of Dairy Science* **1990**, 73, 2292-2298.

Yu, L.; Banerjee, I.A.; Gao, X.; Nuraje, N.; Matsui, H. Fabrication and Application of Enzyme-Incorporated Peptide Nanotubes *Bioconjugate Chemistry* 2005, 16, 1484-1487.

Zhang, S. Fabrication of Novel Biomaterials Through Molecular Self-Assembly. *Nature Biotechnology* **2003**, 21, 1171-1178.

Zhou, P.; Labuza, T.P. Effect of Water Content on Glass Transition and Protein Aggregation of Whey Protein Powders During Short-Term Storage. *Food Biophysics* **2007**, 2, 108–116.

Zydney, A.L. New Separations Using Membrane Filtration: New Opportunities for Whey Fractionation *International Dairy Journal* **1998**, 8, 243-250.

APPENDIX A

MAJOR WHEY PROTEIN STANDARDS

A.1. SDS-PAGE profiles of commercial standards of major whey proteins. Lane M: protein ladder, lane1: α-La, lane2: β-Lg and lane3: BSA

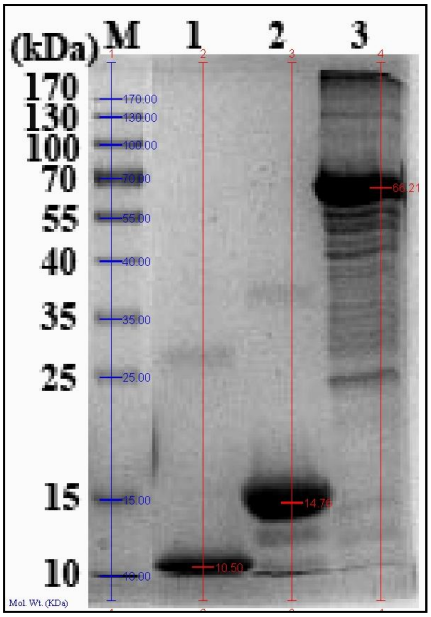

A.2. HPLC chromatograms of commercial standards of major whey proteins

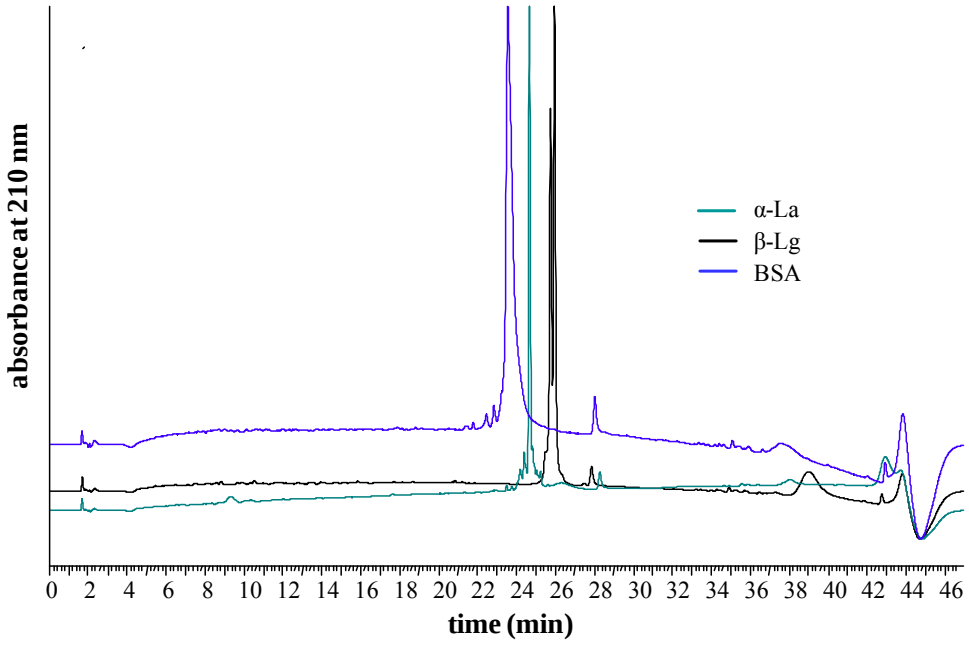

APPENDIX B

CALIBRATION CURVES

B.1. Calibration Curve for Lactose during HPLC analysis

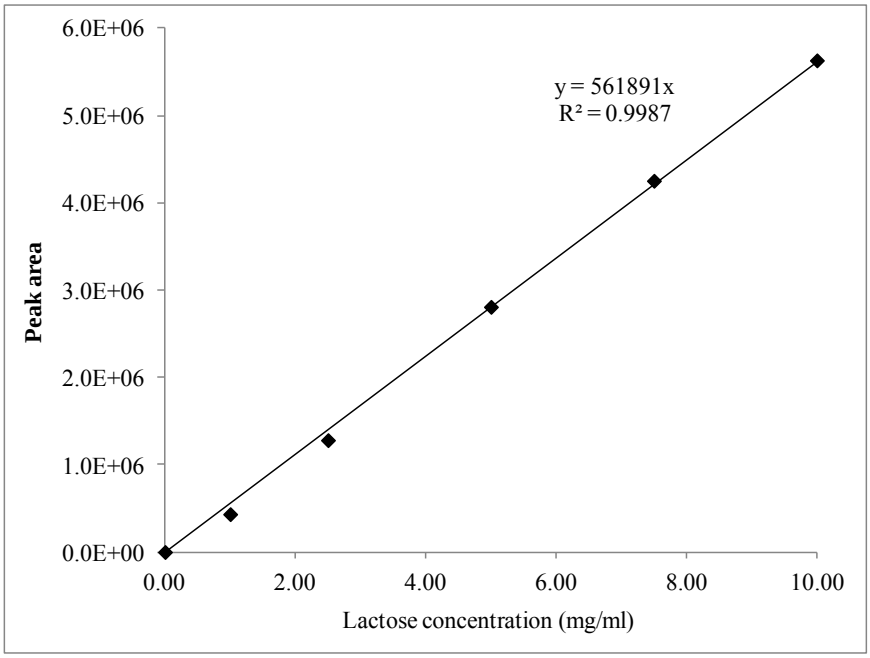

B.2. Calibration Curve for α-Lactalbumin during HPLC analysis

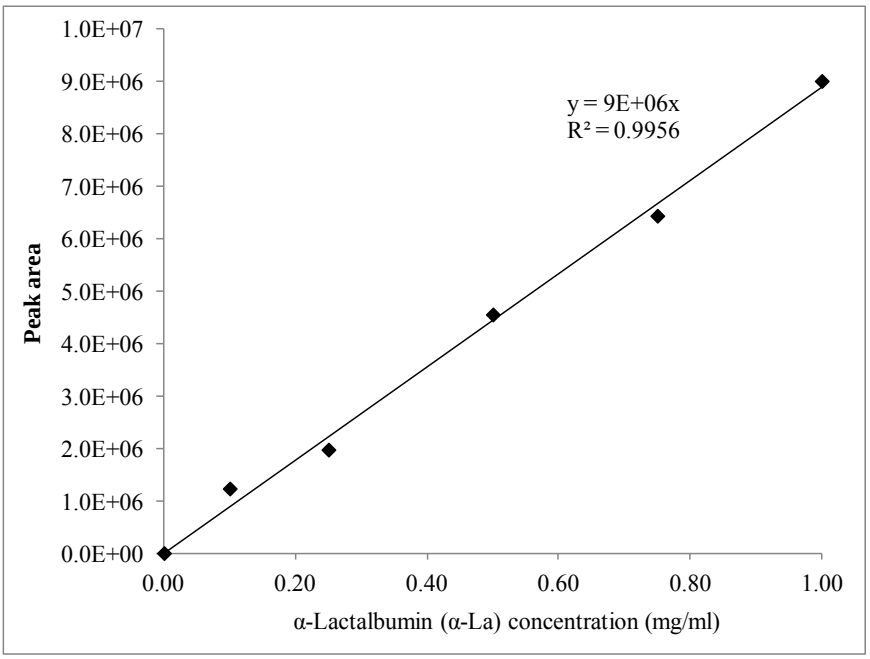

B.3. Calibration Curve for α-Lactalbumin during UV-Spectrophotometer analysis

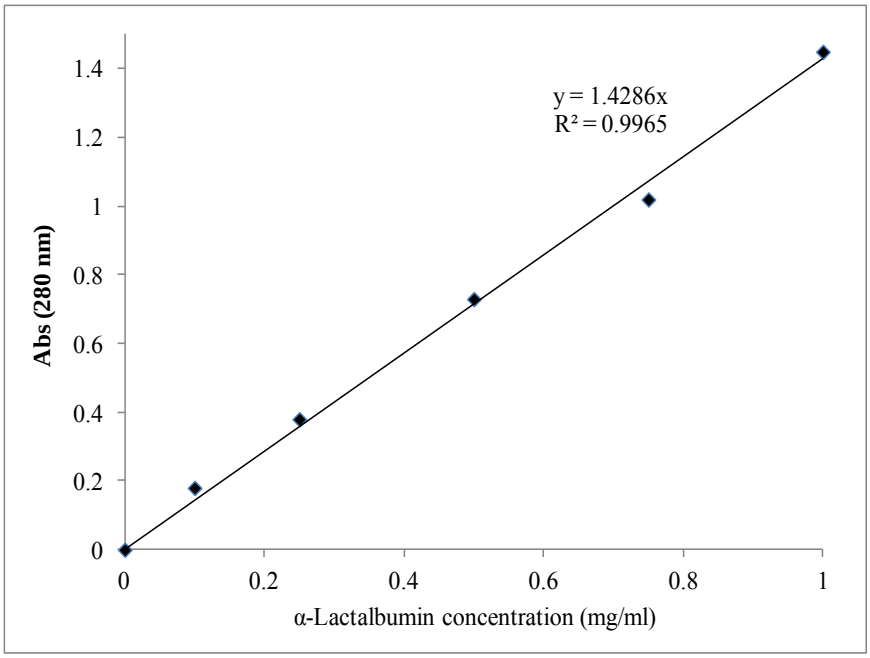

APPENDIX C

LACTOSE CHROMATOGRAMS

C1. Chromatogram of lactose in WPI, WPS, permeate (P) and retentate (R) fractions obtained during ultrafiltration

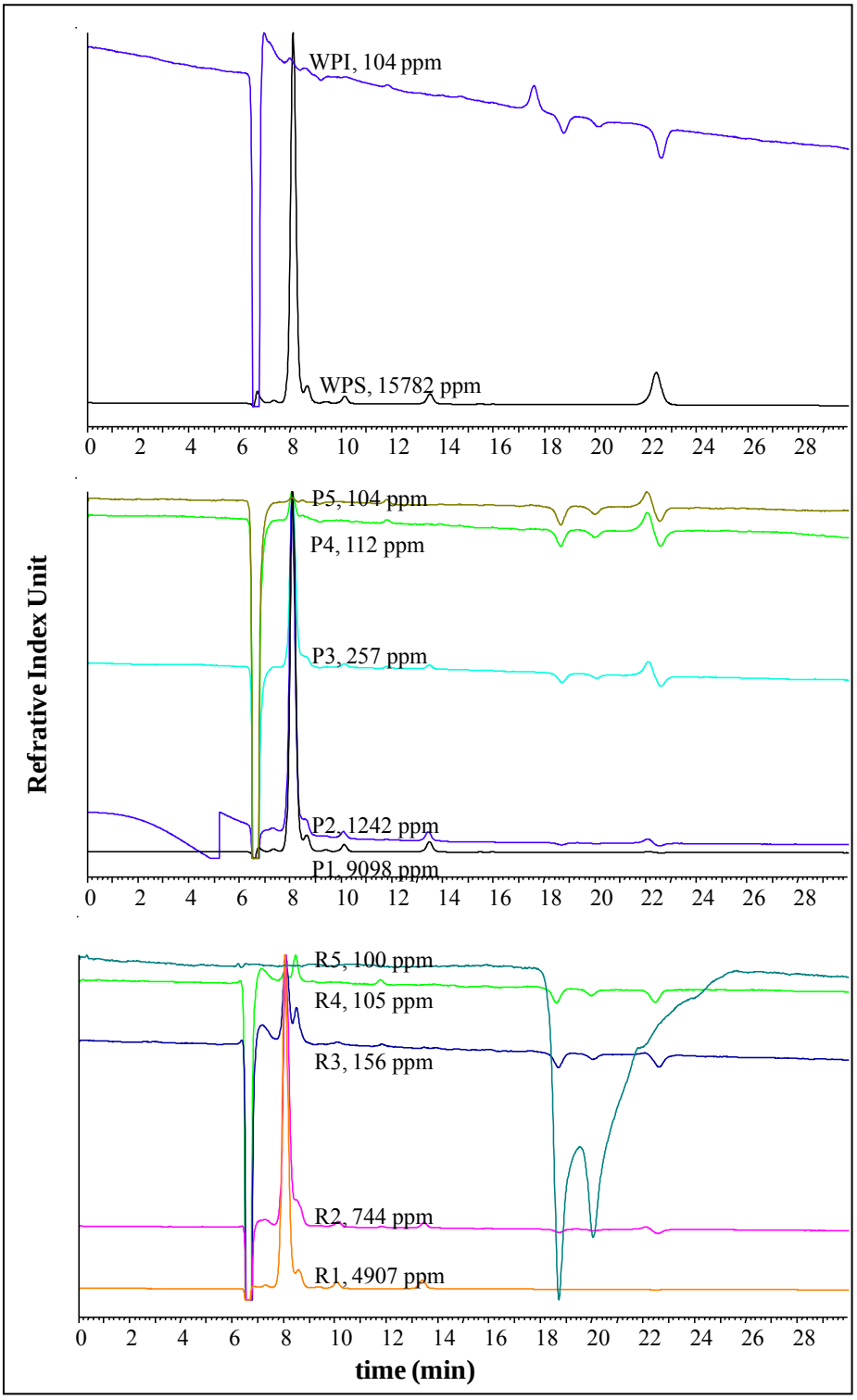

APPENDIX D

PURIFIED FRACTIONS BY CHROMATOGRAPHY

D1. SDS-PAGE profiles of whole whey protein fractions obtained by chromatography

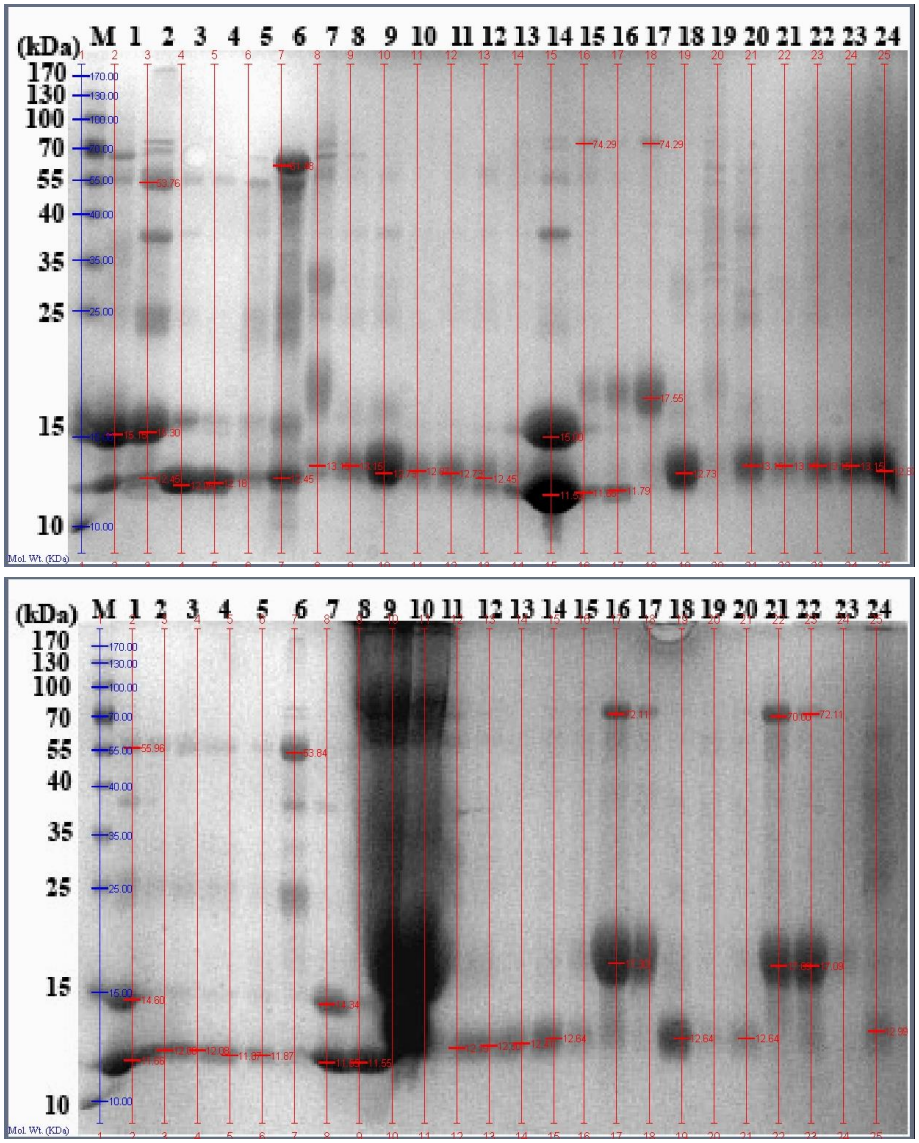

Gel1, laneM: protein ladder; lane1: WPI (1%); lane2 – lane4: Elution 1 fractions of WPI (set I); lane5 – lane6: Elution 2 fractions of WPI (set I); lane7: WPS (2.5%); lane8 – lane11: Elution 1 fractions of WPC (set I); lane12: Elution 2 fractions of WPC (set I); lane13 – lane18: SEC fractions of Elution 1 fractions of WPC (set II); lane19: SEC fractions of Elution 2 fraction of WPC (set II); lane 20 - lane22: Elution 1 fractions of WPC (set III); lane23 – lane24: SEC fractions of Elution 1 fractions of WPC (set III). **Gel2**, laneM: protein ladder; lane1-lane2: Elution 1 fractions of WPI (set II); lane3 – lane5: Elution2 fractions of WPI (set II); lane6 – lane8: SEC fractions of Elution 2 fractions of WPI (set II); lane9: WPC (10%, not filtered); lane10: WPC (10%, filtered); lane11-14: Elution 1 fractions of WPC (set VI); lane15-17: Elution 2 fractions of WPC (set VI); lane18 – lane22: SEC fractions of Elution 1 fractions of WPC (set VI); lane 23 – lane 24: SEC fractions of Elution 2 fractions of WPC (set VI).

APPENDIX E

RAW DATA FROM ENCAPSULATION EXPERIMENTS

E1. Analysis of α-LaNTs-ECg binding depending on pH

time	pH 4.0					pH 5.0					pH 7.0				
	Abs (275 nm)	ECg conc. (mg/ml)	volume (ml)	ECG amount (mg)	E* (%)	Abs (275 nm)	ECg conc. (mg/ml)	volume (ml)	ECG amount (mg)	E* (%)	Abs (275 nm)	ECg conc. (mg/ml)	volume (ml)	ECG amount (mg)	E* (%)
0 min	2.8827	0.0983	1	0.098		2.8879	0.0985	1	0.099		2.687	0.0917	1	0.092	
15min	0.4512	0.0154	0.925	0.014	***85.52***	0.368	0.0126	0.9	0.011	***88.53***	0.4031	0.0138	0.84	0.012	***87.4***
30min	0.8071	0.0275	0.9	0.025	***74.8***	0.8477	0.0289	0.925	0.027	***72.85***	0.889	0.0303	0.94	0.029	***68.9***
60min	2.2369	0.0763	0.89	0.068	***30.94***	1.8994	0.0648	0.875	0.057	***42.45***	2.0166	0.0688	0.86	0.059	***35.46***
3 h	2.2346	0.0762	0.825	0.063	***36.05***	2.0817	0.071	0.825	0.059	***40.53***	1.9025	0.0649	0.875	0.057	***38.05***
6 h	2.5497	0.087	0.865	0.075	***23.49***	2.4604	0.0839	0.91	0.076	***22.47***	2.8628	0.0977	0.89	0.087	***5.18***
24 h	0.0637	0.0022	0.85	0.002	***98.12***	0.1565	0.0053	0.9	0.005	***95.12***	0.1858	0.0063	0.85	0.005	***94.12***
48 h	0.8161	0.0278	0.85	0.024	***75.94***	0.8414	0.0287	0.9	0.026	***73.78***	0.7959	0.0272	0.875	0.024	***74.08***
72 h	0.1095	0.0037	0.925	0.003	***96.49***	0.0957	0.0033	0.89	0.003	***97.05***	0.1664	0.0057	0.95	0.005	***94.12***

*calculated efficiency

VITA

Özgür Tarhan was born on December 11, 1975 in Erzurum, Turkey. She graduated from Ankara High School in 1992. She entered the Food Engineering Department of Gaziantep University (Gaziantep, Turkey), in the fall of 1992. She graduated with a Bachelor of Science degree in Food Engineering, in February 1999. She worked in few companies with various responsibilities up to May 2000. She worked as Quality Control Engineer and then Plant Chief in Marta Kılıçlar Ltd. Şti. (Slaughterhouse) in Hendek, Adapazarı (Turkey) from May 2000 to September 2001. She entered the graduate school of İzmir Institute of Technology, İzmir, in September 2001. She received her Master of Science degree in Biotechnology, in October 2004. She is approved doctorate programme in Food Engineering Department of İzmir Institute of Technology, in September 2007. She has worked as the research assistant in Biotechnology Department between December 2001 and October 2007, and in Food Engineering Department after November 2007, in İzmir Institute of Technology. She is a citizen of Turkey and married with a son.